Sede amministrativa: **Università di Padova - Dipartimento di Biologia**

SCUOLA DI DOTTORATO DI RICERCA IN BIOSCIENZE E BIOTECNOLOGIE
INDIRIZZO: BIOCHIMICA E BIOFISICA
CICLO: XXV

Role of protein kinase CK2 in the targeting of LSD1 and regulation of chromatin condensation: implication of the C-terminal segment of CK2α

Direttore della Scuola: Prof. Giuseppe Zanotti

Coordinatore d'indirizzo: Prof. Maria Catia Sorgato

Supervisore: Prof. Lorenzo Alberto Pinna

Co-supervisore: Dott. Stefania Sarno

Dottorando: Roberto Costa

RIASSUNTO

La subunità CK2α contiene quattro motivi prolina diretti, localizzati al C-terminale, che sono fosforilati dalla Chinasi Ciclina Dipendente 1 (Cdk1). Queste fosforilazioni sono molto importanti per la regolazione di CK2, infatti, le cellule transientemente transfettate con un costrutto che mima costitutivamente la fosforilazione CK2αT344E/T360E/S362E/S370E (CK2α4E) mostrano come fenotipo una mitosi aberrante. I nostri dati confermano l'implicazione di CK2 nella regolazione mitotica e definiscono un preciso ruolo per CK2α fosforilata; infatti il mutante fosfo-mimetico CK2α4E è in grado di fosforilare in maniera preferenziale alcuni substrati. Uno di questi è la istone Demetilasi Lisina Specifica 1 (LSD1).

LSD1 è un importante attore dell'epigenetica. Esso reprime o attiva la trascrizione del gene bersaglio mediante la rimozione di gruppi metile dalla Lisina 4 o 9 dell'istone H3. La fosforilazione di LSD1 ricombinante umana è stata confermata *in vitro* e le costanti cinetiche sono state determinate. Tramite analisi di spettrometria di massa sono stati identificati i residui fosforilati: Serina131, Serina137 e Serina166. Tutti i fosfositi appartengono alla regione N-terminale di LSD1 (1-178), che non è osservabile nella struttura cristallografica (AOD 179-852) e che è già stata ipotizzata come regione regolatoria. Un'analisi bioinformatica del tipo "molecular modeling" suggerisce questa regione come metastabile ed evidenzia che la Ser131, Ser137 e la Ser166 sono esposte al solvente. Per confermare l'esistenza di un'interazione funzionale tra CK2 e LSD1 sono stati generati due vettori di transfezione (pTP6-Ko/Flag-LSD1), uno con la mutazione fosfo-difettiva Ser131Ala e l'altro con la mutazione fosfo-mimetica Ser131Glu. Questi costrutti hanno permesso di confermare il ruolo chiave esercitato dalla fosforilazione di LSD1 in cellule.

Mediante la tecnica "*quantitative Real time PCR"* alcuni mRNA modulati comunemente da LSD1 sono stati determinati, e dati riguardo l'attività dei mutanti di LSD1 sono stati raccolti. In particolare, la quantità di mRNA del fattore di trascrizione FoxA2 era ridotta dal mutante Ser131Glu, ma risultava inalterata in cellule che esprimevano il mutante Ser131Ala, in accordo con l'ipotesi che esista una relazione tra la fosforilazione della Ser131 e la trascrizione di FoxA2.

Inoltre, la transfezione di LSD1 "Flaggata" ha permesso di eseguire l'immunoprecipitazione del complesso di LSD1 in cellule HEK293T. Questa

procedura ha dimostrato che CK2α è un interattore di LSD1 in cellule; inoltre effettuando un saggio chinasico con [γ-^{33}P]ATP sul campione immunoprecipitato, e' stata rilevata la fosforilazione di LSD1 da parte di una chinasi presente nell'immunocomplesso. L'inibitore specifico di CK2, CX4945 (30 nM) riduceva la fosforilazione di LSD1 e confermava che CK2 è la chinasi responsabile di questo evento.

ABSTRACT

CK2α subunit contains four proline-directed phosphorylation sites on its C-terminal tail, which are phosphorylated in cell progressing through normal mitosis by Cyclin dependent kinase 1 (Cdk1). These phosphorylations play an important role in the regulation of CK2, considering that cell with transient expression of phospho-mimic mutant CK2αT344E/T360E/S362E/S370E (CK2α4E) show a defective mitosis.
Our data confirm the implication of CK2 in the mitotic regulation and disclose a precise role for the phosphorylated CK2α; indeed the phospho-mimic mutant CK2α4E preferentially phosphorylates few endogenous substrates in comparison to wild type. One of these is the Lysine Specific histone Demethylase 1 (LSD1).
LSD1, an important player of the epigenetic machinery, can either repress or activate target genes by catalyzing the demethylation at Lys4 or 9 of H3 histone. Phosphorylation of human LSD1 by CK2 has been confirmed *in vitro* and the kinetic constants have been determined. Furthermore, mass spectrometry analysis revealed that LSD1 is phosphorylated at several sites, Ser131, Ser137 and Ser166, in its N-terminal domain. This region of LSD1 (1-178) is not crystallographically aviable, in contrast to the AOD domains (179-852) and it has been supposed to play a regulatory function. The molecular modeling of this region suggests a metastable conformational state with Ser131, Ser137 and Ser166 exposed to the solvent. To confirm the existence of this functional interaction between LSD1 and CK2 *in vivo,* two transfection vectors (pTP6-Ko/Flag-LSD1) have been generated, expressing mutants of LSD1, a phospho-defective and a phospho-mimic mutant, Ser131Ala and Ser131Glu respectively. These tools have been exploited to confirm the key-role of Ser131 phosphorylation in the regulation of LSD1 in cells. The expressions of

several known LSD1 affected mRNAs were detected by Quantitative Real time PCR, disclosing correlation between LSD1 mutation and its biological activity. In particular, mRNA level and also protein expression of the transcription factor FoxA2 were decreased by the LSD1 Ser131Glu mutant, but remained unaltered when LSD1 Ser131Ala mutant was expressed, consistent with a relationship between Ser131 phosphorylation and FoxA2 transcription. Furthermore, the transfection of flagged LSD1 allowed the immunoprecipitation of the LSD1 complex in HEK293T cells. Our data disclose that CK2α is an interactor of LSD1 in cells. Performing kinase assay with [γ-^{33}P]ATP in IPs, the phosphorylation of LSD1 by a co-immunoprecipitated kinase was detected. The very specific CK2 inhibitor CX-4945 reduced the phosphorylation of LSD1 in IPs, confirming that CK2 is the kinase responsible for this phosphorylation.

Contents:

Introduction

1. Protein kinases

Protein phosphorylation is a common post-translational modification, and probably it involves about 50% of eukaryotic proteins, leading to a change in their own activities and biological functions.

The enzymes responsible for the catalysis of this event are referred to protein kinases.

Eukaryotes have more than 500 different protein kinases [1], each with specific substrates. This huge number of enzymes with a similar action reflects the importance of this modification and the specificity of signaling mediated by phosphorylation. In fact, many biochemical phenomena are finely tuned by phosphorylation (e.g. energy metabolism, transcription, cell survival, and cross-talk) [2].

Many human diseases are related with the altered expression or abnormal function of kinases, thus kinases and their substrates are often important drugable targets.

Protein kinases are enzymes able to catalyze the transfer of the terminal phosphate group (called γ-phosphate) of ATP and, more rarely, GTP to a nucleophilic residue. In principle all nucleophilic side chains could be phosphorylated, but some of them are not proved to be, and currently only serine, threonine, tyrosine and histidine appear the main players of this modification.

Protein kinases family is a monophyletic group of enzymes originated by a single ancestor protein, with a conserved domain of approximately 300 amino acids.

This conserved string of residues invariably codifies for a quite conserved

pocket able to host the phospho-donor (ATP or/and GTP), called catalytic site, and a variable phosphor-acceptor substrate binding zone, solvent exposed.

The modern classification of protein kinases family has been made by phylogenic comparison, allowing the identification of seven main groups (Fig. 1A) [3].

I. AGC kinases

Ser/Thr kinases with a basophilic consensus sequence. Member of this group are PKA and PKC.

II. CAMK kinases

Ser/Thr kinases regulated by Ca2+ /Calmodulin system.

III. CMGC kinases

A group including many proline direct kinases, such as CDKs and ERKs. CK2, the subject of this thesis is also part of the CMGC group.

IV. and V. TK and TKL kinases

A very large group, counting for Tyr directed (TK) or dual specificity kinases (TKL).

VI. STE kinases

Members of this cluster take part in the Mytogen Activated Pathways (MAP).

VII. CK1 kinases

Containing the “casein kinase I” subfamily.

Fig. 1A

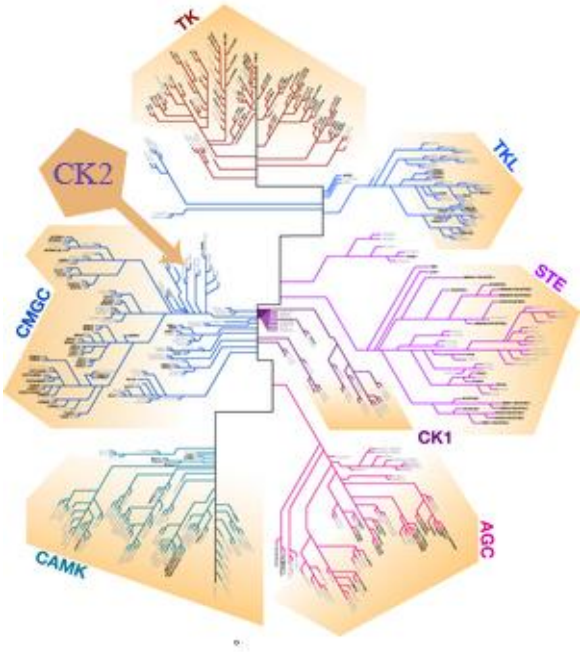

Fig.1A:
Radial phylogenetic tree of the protein-kinases family

By an unrooted phylogenetic tree, all the protein-kinases are reported. They form seven main groups.

As proposed in 1995 with the primary structure alignment of catalytic domains, it is possible to detect 12 typical "sub-domains" (I to XI and VI-b). There are only 12 "invariant" residues in protein kinases (Fig. 1B); most of them are implicated in the catalytic process and their substitutions are not allowed [3].

Fig. 1B:
Multi-alignment of kinases reveals the invariant residues.

A multi-alignment of CK2α, AMPK, CMGC has been performed by clustalX2 software. The twelve typical sub-domains can be observed. Furthermore in the pictures the invariable residues essential for the kinase activity are remarked in black.

```
   Domain                                                          I
                                                                  <---------
CK2alfa1a[Hom]          ---------------MSGPVPSRARVYTDVNTHRPREYWDYESHVVEWGNQDDYQLVRKL
AMP-Dep-KINASE-A        ------------------------------------------------MDQYEKVEKI
CMGC                    MLETSGDDLPVPNKVINYRIIATSRVHAYISKYIYPSFLSYSEFGLSFGVLSKYRVNKII

                                                                 ..*.  . :
```

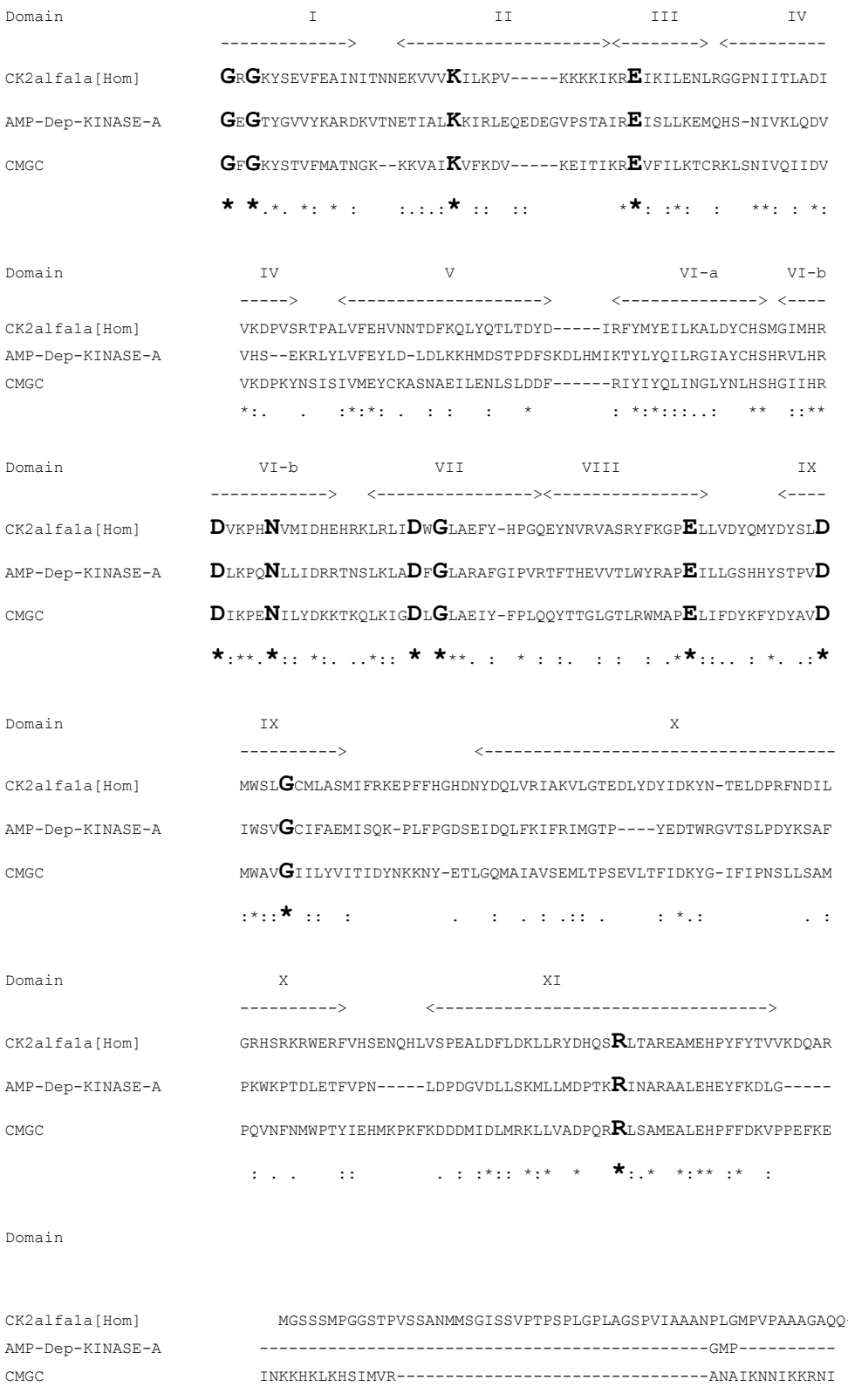
Domain I II III IV
CK2alfa1a[Hom]
AMP-Dep-KINASE-A
CMGC
Domain IV V VI-a VI-b
CK2alfa1a[Hom]
AMP-Dep-KINASE-A
CMGC
Domain VI-b VII VIII IX
CK2alfa1a[Hom]
AMP-Dep-KINASE-A
CMGC
Domain IX X
CK2alfa1a[Hom]
AMP-Dep-KINASE-A
CMGC
Domain X XI
CK2alfa1a[Hom]
AMP-Dep-KINASE-A
CMGC
Domain
CK2alfa1a[Hom]
AMP-Dep-KINASE-A
CMGC

2. The protein kinase CK2

CK2 is a pleiotropic Ser/Thr kinase with constitutive activity and more than three hundreds substrates are reported [4]. CK2 was the first of the protein kinase to be discovered, together CK1, in 1953 [5]. It catalyzes the phosphorylation of Ser/Thr residues, specified by an acidic consensus sequence and it is implicated in several important signaling pathways, such as "Wnt" or "Akt" cascades [6]. CK2 is commonly described *in vivo* as a tetramer (called holoenzyme) composed by two catalytic subunits (α) and two regulatory subunits (β). Although the catalytic α (or α') subunits of CK2 are constitutively active, β subunits stabilize the two catalytic subunits, and regulate their specific activity. Furthermore, the regulatory subunit β interferes with the recruitment of CK2 substrates, which can be classified by their preferential recognition either by CK2 tetramer (class 3 substrates), by the CK2 catalytic subunit (class 2 substrates), or by both of them (class 1 substrates) [7].

The phylogenetic analysis of the kinases discloses the presence of several conserved blocks [3], which can correlated to specific function. CK2 has these invariable blocks and many features of CK2 can be explained by these subdomains.

- The glycine rich loop: it is required for the binding of the phospho-donor molecule. Notably, in CK2 the ATP binding site is able to recognize also the GTP [8].
- N-terminus of CK2: this region is responsible for the constitutive activity of CK2, probably by "freezing" the activation loop in its open position to the consequently active conformation. In fact Δ2-12 and Δ2-30 deletion mutants bring to an inactive catalytic subunit, even if

its activity can be partially recovered adding the regulatory subunit β [9].

- Basic Stretch: CK2 has a huge positive area constituted mainly by two structural motifs, the basic stretch of the α-helix C (Lys74-Arg80) and the amino acidic triplet (Arg191, Arg195 and Lys198) in the P+1 loop. These regions are fundamental during the recognition of the acidic consensus motif typical of CK2 substrates, in particular at the positions n+3 and n+1 [10]. This motif is peculiar for CK2, indeed in Cyclin Dependent Kinase 2 (Cdk2) the sequence of ~KKKKKIKR~ (CK2) is replaced by the PSTAIRE helix, a motif required for the regulation of all the Cdks and for the binding of their substrates [11].
- Catalytic loop: the Asp156 (called catalytic aspartate) is connected to Asn161 by a short sequence. It comprises Lys158 that shields the negative charge of phosphoryl group during the reaction and the His160, which appears fundamental for the binding of the second negative determinants (n+2) of the consensus motif [12].
- Activation loop: many kinases need the rearrangement of this subdomain by phosphorylation or by interacting protein to exert full activity. CK2 does not need this step for its full activity, thanks to its N-terminal domain.

These regions define many features of CK2 and explain the molecular mechanism which favors the substrates with acidic residues near the phospho-acceptor site.

To understand the correct consensus sequence, a library of short peptides (substrates) was synthesized [13]. The research disclosed that in general serines are preferred over the threonines as phospho-acceptor amino acid, while exceptionally tyrosine can be phosphorylated. Furthermore, the minimal consensus of a generic CK2 substrate has a negatively charged

residue after the phospho-acceptor site at the position n+3 (Fig. 2).

Fig. 2:
Schematic representation of the minimum CK2 consensus sequence

Five amino acidic residues are reported, the minimal consensus of a generic CK2 substrate has a negatively charged residue after the phospho-acceptor site at the position +3.

Acidic determinants could be represented also by phosphorylated amino acids, generating hierarchical multi-phosphorylation events. Sometimes, the lacking of the preferred determinant at position n+3, CK2 can also phosphorylate sites specified by multiply negatively charged residues in the range n-4/+7. Furthermore, basic residues near the phospho-acceptor site and a proline at position n+1 negatively affect CK2 activity, while hydrophobic determinants are generally tolerated [14].

3. Druggability of CK2

CK2 is implicated in many neurodegenerative and inflammatory, diseases as well as viral affections and several types of tumors. For this reason CK2 has been indicated as a potential target for antiviral and antineoplastic drugs as well as for the treatment of neurodegenerative diseases; many ATP competitive inhibitors has been discovered until now with different chemical scaffolds (polyalogentated benzimidazole, cumarine, anthraquinones, flavones) [15, 16, 17, 18, 19].

On the other hand, a peculiar feature of CK2 is its insensitivity to

staurosporine, a promiscuous ATP-competitive inhibitor, due to the tight (narrow) pocket of CK2 respect to other kinases.

4. Functions and biological relevance of CK2

CK2 has more than three hundreds substrates reported, thus it is quite difficult to define a clear network of action for this enzyme. Generally, CK2 interferes in many pathways, generating a pro-survival response.

In normal cell, it exerts a crucial role in sustaining cell division and proliferation, but its deregulated activity is also strikingly dangerous. Indeed, CK2 is a common denominator of cancer cells as anti-apoptotic agent [6, 20].

As previously explained, the mechanism of action/regulation of CK2 is quite enigmatic. In the next section, some roles played by CK2 in three exemplificative biochemical pathways have been summarized.

- **Wnt signaling**.

The Wnt signaling pathway plays a significant role during embryogenesis, but it also exerts a very important action during the development of tumors, increasing cell-survival and counteracting apoptosis [21]. The final effector of Wnt pathway is β-catenin, a transcription factor able to modulate some important proteins and survival molecules.

When Wnt ligand is off, β-catenin is degraded and the pathway is interrupted. In contrast, the activation of the pathway by Wnt ligand blocks β-catenin degradation and allows the transcriptional modulation.

In addition to Wnt ligand, other mechanisms can modulate this pathway. In cancer cell, CK2 can take over the regulation of the Wnt pathway, generating a constitutive pro-survival stimulation. Indeed, CK2 is able to stabilize β-catenin, rescuing it from degradation [22].
Thus, stabilized β-catenin can move to the nucleus and mediate the stimulus.
Furthermore, other events mediated by CK2 have a role in this pathway. In fact, CK2 phosphorylates β-catenin, and at the same time the factor Dishvelled (DVI) [23]. Phosphorylated DVI further implements the β-catenin stability. Hence, CK2 modulates Wnt signaling by synergistic effects. These mechanisms of up-regulation signaling are good examples of CK2 pro-pathologic action. CK2 "elevation" in tumor cells drastically changes the Wnt network equilibrium by aberrant phosphorylation of many proteins, increasing the final effector of the pathway and by passing cellular check-points.

- **PI3K/Akt signaling.**

Akt is a very important protein kinase, involved in many cellular processes such as cell proliferation and development, and its activity is often increased in neoplastic cells, allowing the cellular abnormal proliferation.
It is demonstrated that CK2 up-regulates Akt by the phosphorylation at the residues Ser129 [24].
Furthermore, a synergistic effect able to up-regulate Akt pathway is carried out by the CK2 dependent phosphorylation of PTEN. Indeed, PTEN represses Akt by its catalytic action. Aberrant CK2 activity antagonizes PTEN and contributed to Akt hyper-activation [25].

- **NF-κB signaling.**

NF-κB is a transcription factor able to modulate cell proliferation, apoptosis and immune response. Aberrant activation of NF-κB leads to tumorigenesis by deregulation of cell cycle and by resistance to apoptosis. NF-κB is normally present in the cytoplasm, associated with IκB to form an inactive complex. The activation of NF-κB occurs by IκB-kinase (IKK), which phosphorylates IκB. Phosphorylated IκB is prematurely degraded, and then NF-κB raises its expression level and enters the nucleus, modulating the expression of several genes.

Also CK2 can phosphorylate IκB with the same effect of IKK [26], and furthermore CK2 can stabilize NF-κB by a directly phosphorylation [27].

CK2 phosphorylations act in a synergic way to increase NF-kB signaling.

These three examples suggest the presence of CK2 in a network of interaction involving many important pathways. Thus the definition “Master regulator kinase” has been already proposed for CK2 [28].

In the table 1, several examples of CK2 targets have been reported.

Tab.1:
A selection of CK2 substrates *in vivo* [4].

Signaling proteins	β-catenin, CDC-34, DARPP-32, Calmodulin, IRS-1, PP2Cα, PTEN, PKA RII, PKCIIβ.
Transcription or translation factor and DNA/RNA interacting proteins	TFIIIB-TBP, RNA Polymerases, TFIIIA, NF-κB, IκBα, IκBβ, DNA topoisomerase IIα, P53
Cytoskeleton and structural proteins	β-tubulin and spectrin
Metabolism enzymes	Acetyl CoA carboxilase and Ornithine decarboxilase

5. CK2 regulation: protein interaction, phosphorylation and the function of CK2α C-terminus

While the role of CK2 is clear, the mechanism which regulates the action of this protein-kinase is still quite enigmatic. Unlike other kinases, there is no evidence concerning an activation domain in CK2, thus other form of regulation have been hypothesized, for example a proposed mechanism is the regulation of CK2 by interacting proteins.

Consistent with this, many CK2 partners have been disclosed [29].

Furthermore, the interaction of the C-terminus segment of CK2α with some proteins is essential for the correct localization of CK2, in fact, the precise cellular localization of CK2 during the spindle formation is dependent on the

interacting protein peptidyl-prolyl cis/trans isomerase 1 (Pin1) [30] and on the phosphorylation of CK2α by the Cyclin dependent kinase1 (Cdk1) [30, 31].

Until 1995 the only feature disclosed about the C-terminus of CK2α was its instability, when the first observation of CK2 phosphorylation mediated by Cdk1 was published [31], raising interest on the C-terminal portion of CK2α and on the role that the phosphorylation of this domain could have on CK2 regulation.

Consistent with a regulation mediated by the C-terminal segment of CK2α, an isoform of CK2α commonly named as CK2α' has an alternative C-terminal sequence. Indeed, in human there are two catalytic subunits: α (391 AA) [NP_001886] and α' (350 AA) [NP_001887.1]. CK2α' and CK2α have high similarity within their catalytic domains, but CK2α' is by 40 amino acids shorter than CK2α. It can form a functional holoenzyme with CK2β ($\alpha'_2\beta_2$), which is reported *in vivo* and represent the main form of CK2 in particular tissues such as testicles [32].

CK2α and CK2α' have similar sequences (75% identity) while they have different functions, indeed in knock-out mice the lacking of CK2α cannot be compensated by the presence of CK2α'. Indeed, the disruption of the gene coding for the catalytic subunit α causes a lethal phenotype in *mus musculus* [33], while the knock-out of CK2α' gene determines viable phenotype. Although mice lacking of CK2α' are viable, they have a defective spermatogenesis and males being sterile [34].

Notably, CK2α' and CK2α are not present in all the organisms. For example, budding yeast but also plants and insects do not have the α' isoform, suggesting that in lower eukaryotes just a single CK2α isoform is required.

In 2009, the role of the C-terminal phosphorylation of CK2α was correlated to the mitosis [35], and more recently, it was reported that CK2α residues

Thr_p 344, Thr_p 360, Ser_p362 and Ser_p370 act as bait for peptidyl-prolyl cis/trans isomerase 1 (Pin1) *in vitro* and *in vivo* [36]. Furthermore the authors observed the complete segregation of CK2α mediated by Pin1 within the chromosomes to form mitotic spindle.

Interesting clues were provided by the experiment where the effects of the transient expression of phospho-mimicking CK2α mutant T344E-T360E-S362E-S370E (CK2α 4E) and of a not phosphorylable CK2α mutant T344A-T360A-S362A-S370A (CK2α 4A) were compared [35]. When CK2α4E promoter was activated, cells showed a defective reproduction with unbalanced chromosomic segregation and aberrant amplification of the centrosomes.

Taken together, these observations suggest that proper temporal regulation of CK2α phosphorylation is required for correct mitotic progression and highlight a role of CK2α C-terminal phosphorylation in the maintenance of spindle integrity and control of cell division [36].

In summary, CK2α C-terminus is related to mitotic events. The preferential expression of the CK2α' in tissue undergoing meiosis (e.g. testis) [32] is consistent with the hypothesis that CK2α' is important in cells having unconventional cell cycle (e.g. meiotic cell cycle and G0 quiescence). Notably, mice lacking CK2α' undergo defective spermatogenesis, which generates gametes with unbalanced epigenetic marks [34]. This data supports the view that CK2 is also involved in the epigenetic regulation.

6. CK2 is a player of the ATP-dependent chromatin-remodeling and histone-deacetylase activities complex NuRD

CK2 is abundant in the nucleus and it participates in many complexes, one of these is related to chromatin modification: the ATP-dependent chromatin-remodeling and histone-deacetylase activities complex (NuRD). This is a macro molecular aggregation of proteins, displaying both histone deacetylase and ATPase activities. It negatively modulates the transcription of the genes by removing acetyl groups bound to lysines of the histone proteins H3 and H4. This event generates a more stable interaction between DNA and nucleosome, blocking the recruitment of the RNA polymerase II.
CK2 is described as a player of this complex, exerting a fundamental role in its regulation *in vivo* [29]. Moreover, the treatment with CK2 inhibitors modulates NuRD complex activity suggesting that CK2 is related to the epigenetic machinery [37]. Increased binding of the transcriptional factor SDS3 to the promoter region after inhibition of CK2 further confirms this hypothesis *in vivo* [38]. CK2 is related in epigenetic at many levels. Transcriptional factors and HDAC2 are substrates of CK2, suggesting an important role mediated by CK2 in chromatin remodeling and quality control of gene transcription.

7. Histone proteins can control the genetic information

DNA is the most famous player of the genome, although it is not sufficient to store genetic information; indeed the basic unit of the chromatin is formed

by DNA and proteins. These units are termed "nucleosomes" (Fig. 3A) [39] and are the major components of chromatin and chromosomes.

Each nucleosome consists of an octameric particle of histone proteins (H2A, H2B, H3, H4 and their natural variants) that binds and wraps 146 base pairs of DNA (Fig. 3B) [40].

These structures represent a dynamic system in turbulent evolution. Hence chromatin fluctuates between its condensate form and its elongated form like a spring. Packaging of chromatin plays two fundamental roles: it preserves DNA from damage and prevents binding of effector proteins to DNA.

A proper management of condensation makes possible specific genetic programs instead of a random reading of the DNA.

Chromatin condensation regulates gene expression, cell proliferation, chromosome segregation and other essential events.

The histone protein modifications are essential signals for the cell, modulation of all these events. To note that, chromatin modulation is governed by covalent marks hitting the histone proteins and not directly DNA.

Consistent with this, a great amount of residues of histones are located in unfolded regions; N-terminal and C-terminal tails of histone proteins protrude from the nucleosomal surface, where they can be affected by numerous post-translational modifications (Fig. 4).

Fig. 3A:
Electron microscopy reveals the structure of the chromatin [40]

Chromatin appears as a chain of beads. Each bead is a nucleosome, a particles formed by proteins and DNA.

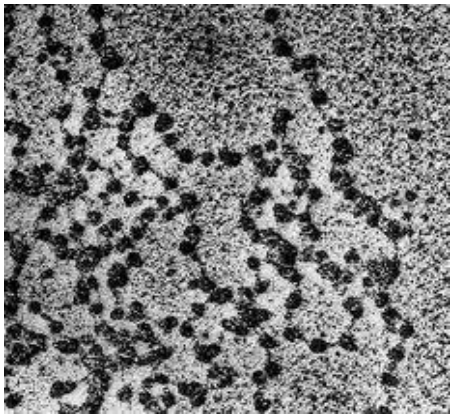

Fig. 3B:
Schematic representation of the crystallographic structure of nucleosomes and DNA

DNA and nucleosome form an ordered structure and each nucleosome binds 146 bp of DNA.

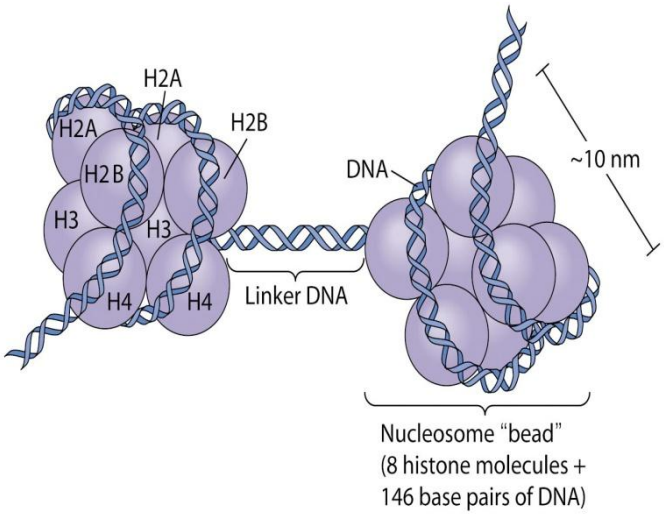

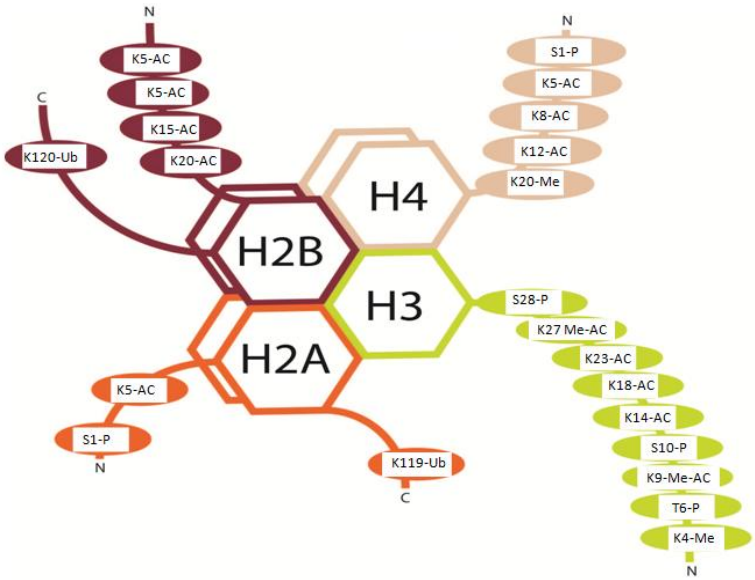

Fig. 4
Schematic representation of a nucleosome and its possible modifications

N-terminal and C-terminal segments of the histone proteins (H2A, H2B, H3 and H4) protrude from the surface and become the target of many enzymes. About twenty modifications have been reported, and each of these has a biological effect.

Histones (especially H3 and H4) can be specifically modified by a set of enzymes:

1. Protein kinases and protein phosphatases can add or remove

phosphates to serines and threonines.

2. Lysine methyl-transferases (HMTs), lysine demethylases (HDMs), lysine acetyl-transferases (HATs) and lysine deacetylases (HDACs) can modify the nucleosomes, creating methyl and acetyl docking sites.
3. Also other events can happen such as lysine ubiquitination, lysine biotinylation, lysine sumoylation, arginine methylation, glutamic acid ADP-ribosylation, and furthermore glutamic acid δ-polimerization.

All these modifications together generate a whole signal (sum of many messengers), modulating the genome reading, and furthermore all the events occurred to chromatin.

Indeed, histone post-translational modifications allow DNA-Histone stabilization and destabilization, but also the recruitment of specific protein complexes [41].

Histones are a remarkable example of combinatorial and hierarchical regulation. Many stimuli converge into a global signal, which defines the chromatin region responsible for a specific biological function, suggesting how to process the genetic code.

Without histone modifications an essential counterpart of the genetic code would lost; the genetic code would becomes cryptic and equivocal by the lacking of "reading schemes".

On the other hand, DNA can be decrypted simply by the analysis of histone modifications, for example defining coding sequence and non-coding region [42, 43].

7A. Histone acetylation

Acetylations of histones have a positive effect on the transcription, preventing a stable interaction between DNA and chromatin scaffold (e.g. histones and other proteins). This allows at transcription factors to gain

access to promoters region, leading to the transcription of the genetic code in mRNAs, and then to the translation into proteins [44, 45].

The acetyl groups are bound to lysines present on the histone tails of H3 and H4 by histone acetyltransferases (HATs), using Acetyl-CoA as donor [41].

Acetylation neutralize the positive charge of the lysine, preventing its interaction with the negative charge of the DNA by a merely electrostatic mechanism.

Acetylations can be quickly reverted in a dynamic process, repressing or allowing gene transcription.

To ensure a fine regulation of acetylations, specific enzymes are required. The units responsible for removing acetyl groups from lysines are called histone deacetylases (HDACs). Notably, HDACs and HATs can be found in the same complex, in conjunction with other enzymes able to modify histones [46], but even now, the modulation of these multi-protein complexes with many catalytic functions is quite enigmatic.

7B. Histone methylation

Histone methylation occurs both at lysines, where the amino group of the side chain become methylated, and at arginines, where methyl groups are covalently bound to the guanidinium group.

Lysines are methylated by histone methyltransferases (HMTs), while arginines by protein arginine methyltransferases (PRMTs) [47]. PRMTs and HMTs are strictly site specific and act on distinct arginine and lysine residues. Methyl groups have specific functions and specific regulatory pathways, controlling these signals

Methyl lysines could be mono-, di-, tri- methylated and the saturation of the individual residue is also finely tuned by many enzymes, suggesting specific functions for each variably methylated form.

7C. Methylation of histones has specific features distinguishing this epigenetic mark from acetylation

Methylations of histone proteins do not neutralize the charge of lysine and arginine residues, thus do not significantly affect the interaction between DNA and the histone proteins. In contrast, methylated residues become binding sites for specialized domain able to recognize the methylated histone tails: Chromo-domain and Tudor-domain are two examples of these binding partners of methylated lysines [44, 48].

The specificity of an interactor for a single modification distinguishes the biological functions associated to each modified residues (e.g. H3K4me3 vs. H3K9me3). Unfortunately, the large amount of residues undergoing methylation impedes the understanding of the role of each individual modification.

Another element, which distinguishes methylation and acetylation, is the half life of the mark. For a long time, histone methylation was considered to be a stable mark and no lysine specific demethylases were known. Thus lysine methylation was thought to be a signal responsible for the propagation of epigenetic information over many generations and it was thought that un-methylated lysine were generated only by neo-synthesis.

This view has been corrected and put in a new perspective by the recent identification of several demethylases [49, 50]. However, the half-life of histone methylation is significantly longer in comparison to other post-translational modifications (e.g. acetylation) [51].

8. Functions of methylated sites

Histone methylation sites generate a wide pool of different biological signals; however it is difficult to assign a precise function for each modification.
Below are reported several examples with known function of modifications involving histone H3.

- H3K9me1 (Histone protein H3, lysine 9, mono-methylated) is generated by specific methyltransferases [52] and it is enriched in the promoter and 5' UTR with decreasing levels in coding regions of active genes and minimal enrichment in non-genic regions [53, 54]. This sharply contrasts with H3K9me3, which is found in non-genic regions, repressed promoters and coding regions of some inactive genes [55].

- H3K9me2 domains are strongly correlated with binding of Lamin B1. Mapping of Lamin B1 interacting domains demonstrates that inactive genes are preferentially located at the nuclear periphery in association with the nuclear lamina [56]. The genomic blocks associated with the lamina change during differentiation, underscoring the dynamics of the interaction. The Lamin B1 associated regions are depleted of H3K4me3 and RNA polymerase II [56]. Taken together, these data suggest that H3K9me2 domains are critical determinants of higher order chromosome structure and nuclear architecture.

- H3K9me3 has been thought to occur at heterochromatin regions and at repressed promoters. Indeed, studies concerning specific genes or

looking at the entire genome have clearly demonstrated that this modification is connected to non-coding regions [57, 58]; however the exact role that this mark performs on coding regions is still unknown and it also emphasizes the necessity to better understand the importance of its localization.

Interestingly, H3K9me3 is depleted at telomeres, but not at sub-telomeric regions, suggesting that telomeres and subtelomeric regions are structurally distinct and different from other non-genic regions.

One might speculate that the combined localization and activity of KMTs and KDMs are responsible for establishing, maintaining and restricting these domains [55]. Furthermore an additional speculation might be related to requirement of a more specific tuning of KDMs and KMTs by other signaling pathways (e.g. protein-kinases and phosphatases), generating additional steps in this regulation.

- H3K4me3 signal typically shows peak levels at the 5′ UTR of actively transcribed genes [59], and shows strong positive correlations with transcription rates, activated RNA polymerase II occupancy, and histone acetylation levels [60]. The H3K4me3 marks function as the exclusive docking signal for plant homeo domain (PHD) finger proteins and other proteins involved in the recruitment of chromatin remodeling complexes, thus providing its own layer of transcriptional regulation [60, 61]. Consistent with this, the H3K4me3 signal is extremely weak, or even non-detectable, at regulatory sequences of the β-globin genes and other loci that remain silent in Central Nervous System (CNS) cells [62, 63, 64].

- H3K4me2: In yeast, the role of H3K4me2 is related to the early

transcription process acting in concern to histones deacetylation [65]. If H3K4me2 plays a central role in transcription initiation, it will be of great interest to understand whether H3K4me2 is the subsequent result of H3K4me3 demethylation or to the addiction of methyl groups to H3K4 and H3K4me1.

Understanding this regulation will provide fundamental insights on how promoter fidelity is dynamically controlled.

Furthermore, the recent discovery of cryptic transcript emerging from bidirectional promoters in budding yeast and mammalian cells generates the question whether directional deposition of H3K4me2 also plays a role in controlling transcriptional orientation when a promoter is activated [66]. Indeed, it is interesting to observe that H3K4me3 deposition overlap with the promoter, while H3K4me2 encompasses the promoter region and the early coding sequence, suggesting a role in the ORF orientation (Fig. 5). A useful complement to the "opening" marks (H3K4me3 and me2) is provided by tri- and di-methylated forms of histone H3 lysines 9 and 27 [67], which define inactive or repressed gene and promoters.

Fig. 5:
Representation of the gene Var of *Saccharomyces Cerevisiae*, during the transcription and the silencing [68]**.**

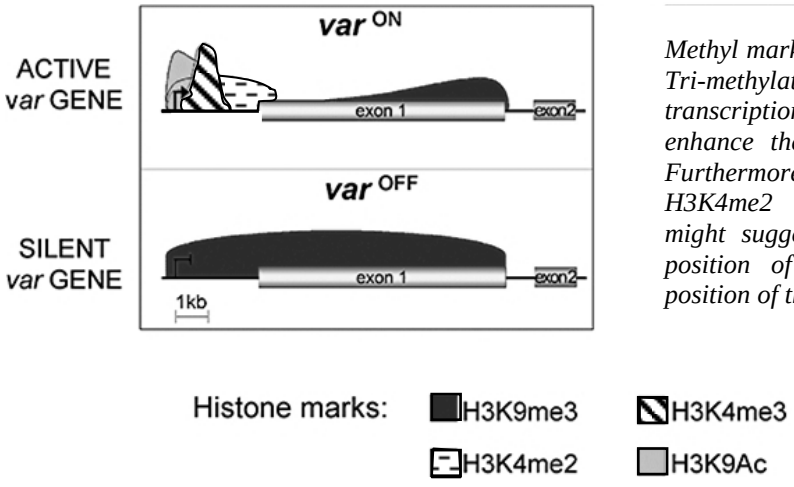

Methyl marks define the fate of the gene. Tri-methylated H3K9 represses the transcription, while Lys4 methylations enhance the activity of the promoter. Furthermore, directionality of the H3K4me2 and H3K4me3 deposition might suggest to the RNA Pol II the position of the gene respect to the position of the promoter.

The distinction between H3K4me2 and H3K4me3 remains difficult but H3K4me3 is one of the most significant modifications present at the subtelomeric regions in human CD4+ T cells supposed to be transcriptionally silent [66].

In summary, H3K4me2 is present only in euchromatin, while H3K4me3 is present in euchromatin and subtelomeric regions, thus H3K4me2 and me3 usually carry signal "active transcription" but also other messages, probably in concert to acetylation and methylation at other residues.

The additional findings of complexes able to modify many residues of the histone proteins suggest that a single action modulates at the same time Lys4, Lys9 and Lys27 methylation. This conclusion is further confirmed by the recent discovery of the Lysine Specific histone Demethylase 1, the first H3K4 demethylase identified [49]. Remarkably, LSD1 can also demethylate H3K9me2 and H3K9me1. Although the regulation of this ability remains unclear, unique mechanism able to modulate alone the methylated Lys4 and Lys9, which are opposite in functions, seems predictable [72].

Furthermore, the action played by LSD1 during the mitosis and the finding of its hyperphosphorylation, might link CK2 and LSD1, opening new insight in LSD1 regulation. The observations that LSD1 overexpression leads to unbalanced chromosomic segregation [69] and that unbalanced levels of di-methylated lysine 4 on Histone H3 generates aberrant chromosomes segregation [70], further suggests a relation with CK2. Thus the phosphorylation of LSD1 could be a rational explanation of the Lys4 and Lys9 demethylase activity of just a single enzyme.

9. Lysine Specific histone Demethylase 1 (LSD1)

LSD1 is a lysine specific histone demethylase, belonging to the FAD-dependent amine oxidase super-family, which uses folate as final acceptor of the removed methyl group.

LSD1 is an enzyme of 94 KDa, consisting of an N-terminal SWIRM domain and a C-terminal amine oxidase domain (AOD). The active site cavity of LSD1 is located within the AOD and comprises about 50 invariants residues, creating a substantially larger catalytic pocket in comparison to other FAD-dependent amine oxidases. The stable inhibition of LSD1 through FAD dependent cross-linker permits to understand the structure of LSD1 bound to an H3 peptide by crystallization [49], providing structural evidence for the reaction mechanism by which LSD1 demethylates H3K4. The crystal structure reveals electron density corresponding to the first seven residues of the 21-aminoacid peptide; the 2–6 residues of H3 adopt three consecutive γ-turns assuming an unusual serpentine shape that fits tightly into the active site, forming numerous sequence-specific interactions with LSD1. The structure also suggests how the ε-N-methylamine moiety of H3K4 would protrude against the isoalloxazine ring of FAD in the context of a productive enzyme–substrate complex, while it shows that the N-terminus of H3 engages a small anionic pocket present in the active site [49]. This suggests that the specificity of LSD1 for preferential H3K4 methylation arises from the stringent steric constraint that allows three residues of the N terminal segment of the histone protein H3 to fit within the enzyme pocket. Interestingly, the substrate specificity of LSD1 can be modulated by association with different regulatory proteins. For example, Metzger and colleagues disclosed that LSD1 can work as an H3K9 demethylase in the

presence of the androgen receptor (AR) [72]. The mechanism of this change in specificity remained elusive until the discovery that, during AR-dependent transcription, the phosphorylation of H3 at threonine 6 by PKCb1 prevents LSD1 from demethylating H3K4 due to steric constrains [73]; however how methylated H3K9 can fit in the same catalytic site as H3K4 remains elusive.

Anyway, the crystallographic data provided a clear-cut explanation for why phosphorylation of histone H3T6 by PKCb1 leads to the inaccessibility of methylated H3K4 to the enzyme [72, 73, 74].

Concerning Lys4 and Lys9 demethylation, it may be surprising the lack of a second enzyme responsible for those two signals. In particular, the cross-talk between these two post-translational modifications (Lys4 and Lys9) catalyzed by a single enzyme appears paradoxal, because these residues have apparently opposite physiological functions. In fact, Lysine 4 is generally related to active transcription, while Lysine 9 is generally related to gene repression.

These controversial aspects suggest that LSD1 may display antagonistic functions, and its regulation may influence the recognition of Lys4 or Lys9.

This regulatory effect could lead to use one enzyme to regulate two opposite signals. Consistent with this, where H3K4me3, me2 and me1 stimuli are strong H3K9me3, me2 and me1 are weak.

Remarkably, LSD1 is found in the HDAC containing CoREST complex [75, 76, 77], suggesting that this complex may represent a global system able to modulate methylation and acetylation at the same time.

Indeed, HDAC inhibition enhances histone acetylation but also increases Lys4 methylation [75].

Current problems and aims of this thesis

Until 1995 the only feature disclosed about the C-terminus of CK2α was its instability. The troubles encountered to obtain the full length form of CK2 prevented for a long time the understanding of the function of the C-terminal.

In the 1995 the C-terminal phosphorylation of CK2α was reported and recently, a precise link between CK2 C-terminal sequence and chromosomes stability was discovered.

These two findings are raising the interest on this domain of CK2α, suggesting that the C-terminal domain has regulatory function.

Starting from these observations, we shed light on the role played by this domain of CK2α.

In this thesis, we disclose several biological events occurring to the cells after the phosphorylation of the C-terminal segment of CK2α and describe a new signaling pathway related to the phosphorylation of the catalytic subunit.

Results and Discussion

10. Phylogenic analysis of CK2α paralogous proteins

CK2α and CK2β proteins have fundament functions and can be observed in all the species from *Homo sapiens* to plants and unicellular fungi.

The CK2β is always observable in these organisms within a large amount of conserved residues.

Also CK2α is invariably conserved in all species which have CK2β, suggesting the essential duality of these proteins.

To note that, CK2α subunit can be coded by two genes in many species; two isoforms with homology and with a conserved catalytic domain.

In human for example, the catalytic subunit α of CK2 is represented by two different genes: CK2α is placed on chromosome 20 and CK2α' is placed on chromosome 1.

The catalytic domain of CK2α' is almost identical to CK2α, having similar catalytic function. The main difference is found in the two C-terminal domains, unrelated to each other.

This particular evolution of CK2α and CK2α' suggests divergent functions due to the C-terminus. This conclusion is also supported by tissue specific expression of CK2α' (e.g. testicles) [32]. A third catalytic subunit of CK2 was annotated in databank as CK2α", a splicing variant of CK2α detected in neoplastic cell line Huh7 [78]. Notably, CK2α" has an almost identical sequence to CK2α from amino acids 1 to 353, but after amino acid 353 protein sequences are totally different.

These three isoforms of CK2α are compatible with two hypotheses about their evolution:

Hypothesis 1: The C-terminal sequence of CK2α has not a physiological function, thus the evolution can act on it without any selection. These three sequences could diverge during the evolution, in contrast to the catalytic domains, which have a much stronger constrain and are almost identical in three isoforms.

Hypothesis 2: The C-terminal domains of the three CK2α subunits have distinct roles. They can respond to specific messengers and signaling pathways, acting as regulators and modulating the CK2 activity *in vivo* by a still unknown mechanism. Owing to this, CK2α, CK2α' and CK2α" are isoforms having their own biological functions.

The neighbor joining phylogenetic tree (Fig. 6A) formed by nineteen proteins "representative" of almost all the species belonging to the CK2α family, suggests that the three C-terminal segments of the catalytic subunits have functions and discards the idea of random evolution in this portions of the proteins.

Indeed "human like" CK2α C-terminus is significantly conserved in CK2α proteins of all vertebrates (subclade 1). Hence, a strong selection plays against C-terminal mutated organisms, crystallizing the evolution of the sequence (Fig. 6A).

Furthermore, in the phylogenetic tree, CK2α' forms a specific group (subclade 2). This data suggests a strong evolutive pressure, conserving the two isoforms with distinct biological functions. In fact, if CK2α and CK2α' have identical functions, the C-terminals of the two enzymes should be random and could not form specific subclades; moreover several organisms should lose these segments without functions.

The conclusion of distinct biological functions is consistent with the experiments of knock down of CK2α or CK2α' in mice, where they generates different phenotypes.

Fig. 6A:
Phylogenetic tree of 19 CK2α sequences of different species.
In the tree the evolutive history of the catalytic subunit CK2α is reported. The catalytic core is highly conserved from plant to human, while two minor subclades appear in vertebrates. CK2α in these species is represented by two isoforms in contrast to the other organisms (e.g. invertebrates have one isoform and a single gene). CK2α and CK2α' of vertebrates have additional segments located to the C-terminus, not present in insects, plants and fungi; CK2α of vertebrates has 57 conserved residues, while CK2α' has 16 non-homologous residues.

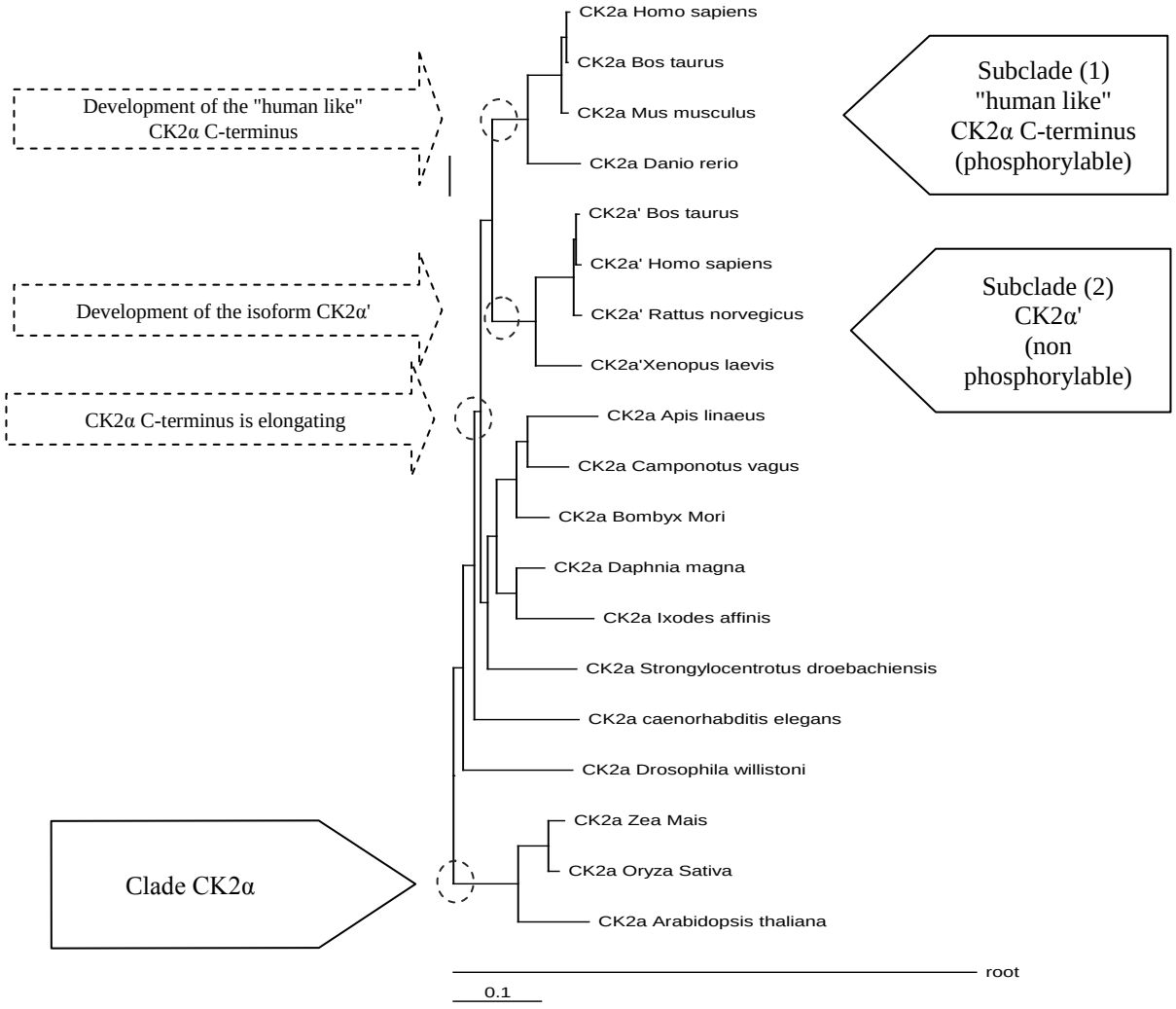

Fig. 6B:
Multialignment of CK2α homologous sequences reveals that the phosphoresidues are developed later than the catalytic domain.
In the multialignment the evolutive history of the protein CK2α is reported. The catalytic core is highly conserved from plant to human, while an additional segment located to the C-terminus can be observed in several organisms. The Cdk1 directed sites are located in this portion of CK2α, we can speculate that this domain has regulative functions, indeed the phylogenetic analysis suggests this portion of protein present only high evolved species, while simpler organisms don't have the phosphorylation sites.

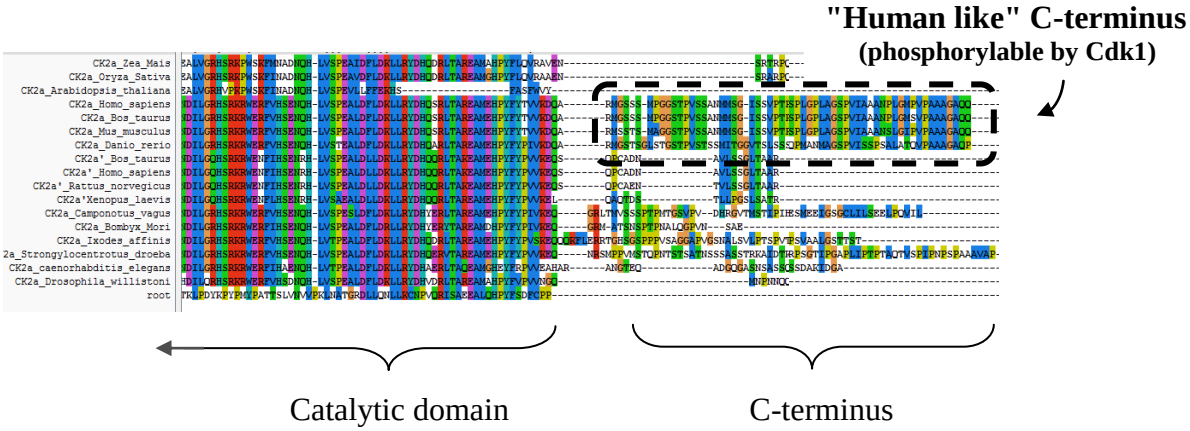

The additional observation that ancestral organisms have shorter sequences (within the catalytic domain and without any form of C-terminus), discloses that "human like" C-terminal segment is not essential in the catalytic mechanism, but opens a new insight about a putative regulation in vertebrates.

Taken together, these data support the hypothesis for the acquisition of a regulative function by this region, forming binding sites for interacting proteins and/or targeting CK2 towards favorable substrates.

In fact, the C-terminal region of the human CK2α is phosphorylated during mitosis [31] and this event leads to a re-localization of CK2 in the nucleus [36], while CK2α' has not the phospho acceptor residues, and is not involved in mitotic events.

As shown, many organisms have not this region and their CK2α cannot be phosphorylated (Fig.6B). The development of the "human like" CK2α C-terminus generates the basis for a new form of regulation in human and in

other vertebrates, but not in plant, fungi and invertebrates.

To note that CK2α' has developed in organisms which have the phosphorylable CK2α, suggesting that a non-phosphorylable enzyme is essential for these organisms, besides the phosphorylable one.

Human isoforms of CK2 α

Three isoforms of CK2α have been annotated in databanks: CK2α, CK2α', CK2α".

The main differences among the three isoforms are length and sequence of the C-terminal segment. This supports the hypothesis that this structural elements act as docking site for interactors.

Consistent with this function, peptidyl-prolyl cis/trans isomerase 1 (PIN1) binds to CK2α through by its phosphoresidues located in the C-terminal segment [30, 36].

In figure 7 are schematically represented the three isoforms to outline the main difference and the putative docking sites.

Fig. 7:
Schematic representation of the three isoforms of human CK2α

In the picture, a similar catalytic core (AA 1-334) is linked to three alternative segments. Currently, no regulatory functions are associated to the C-terminal portion of CK2α, but the phosphorylation of α isoform and development of α' in vertebrates might sustain this hypothesis. The additional finding of the third isoform (α") discovered in neo-plastic cells further supports this idea.

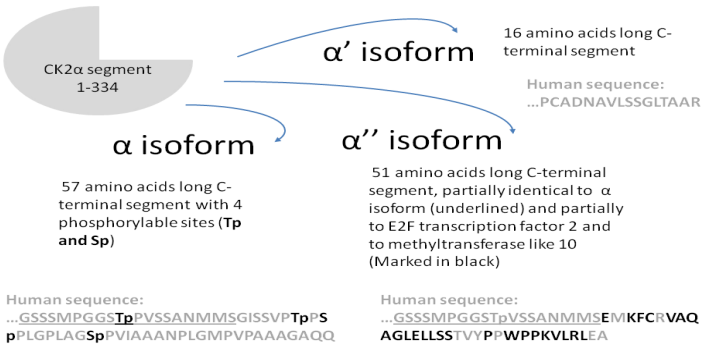

11. Possible role of CK2α C-terminal as regulator of the catalytic activity

The specific activities of CK2α-wt, CK2α-4E and CK2α-Δ1-336, purified to homogeneity (supplementary materials S1), were determined using the synthetic peptide RRRADDSDDDDD as a phospho acceptor substrate.

In table 2 and in figure 8, the means of the values of specific activities of the three forms of the catalytic subunits CK2α are reported. The mutants help to understand if the C-terminal segment plays a role during the catalysis. In particular the mutant CK2α-4E mimics the effect of the phosphorylation of CK2α, while the truncated form Δ1-336 gives information about the role of the whole C-terminal segment.

Our data suggests that the mutant CK2α-Δ1-336 has a higher specific activity than CK2α-wt ($p<0.05$), reflecting a possible down-regulatory role of the C-terminal tail.

In contrast, the specific activity of CK2α-4E (a mutant of CK2α able to mime the phosphorylation of the Thr344, Thr360, Ser362, and Ser370) is quite comparable to that of CK2α-wt.

Tab. 2 and Fig. 8:
Evaluation of the specific activity of CK2wt, CK2α-Δ1-336 (no C-terminus), CK2α-4E (phospho mimetic C-terminus).

Specific Activities	**CK2α-wt**	**CK2α-4E**	**CK2α-Δ1-336**
Mean (pmol/mg*min)	587,4 (#)	710,8	1000,2 (#)
Confidence (CF:95%)	±157,2	±135,1	±188,8

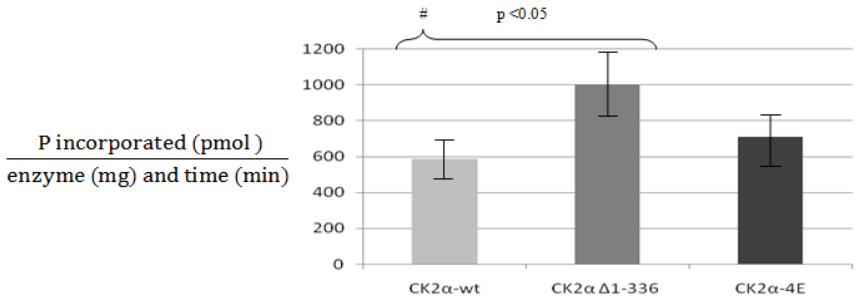

To sum up, the lack of the C-terminal segment of CK2α leads to a significant increase of CK2 activity.

However, the presence of truncated forms (Δ1-336 or similar) have not been demonstrated *in cell*, thus our finding is interesting in term of structural and functional biology, but probably it is not related to any mechanism of regulation *in vivo*.

The additional finding that CK2α-4E (mimicking the C-terminal tetra-phosphorylation) has similar specific activity to CK2α-wt, suggests that CK2 activity is not modulated by the C-terminal phosphorylation. This data suggests that the real function of this segment of CK2α is related to other events.

12. Autophosphorylation of the catalytic subunits CK2α-wt, CK2α-4E and CK2α-Δ1-336

Autophosphorylation of CK2α is often reported in the literature, although no one has disclosed any clear function for this event.

The autophosphorylation of the mutants CK2α-4E and CK2α-Δ1-336 in comparison to CK2α-wt was analyzed. The experiment shows an increased autophosphorylation of CK2α-4E in comparison to CK2α-wt.

However, the autophosphorylation of the catalytic subunits (in absence to CK2β) is inhibited in presence of 50 and 100 mM NaCl (Fig. 9A), suggesting that the phosphorylation could be negligible in a physiological conditions.

In the presence of CK2β, CK2α-4E auto-phosphorylation remains detectable up to 200 mM NaCl, while the other CK2α forms don't undergo autophosphorylation under these conditions. Thus, the autophosphorylation of CK2α-4E acquires a physiological relevance in presence of CK2β (Fig. 9B) and in presence of polycations (supplementary materials S2).

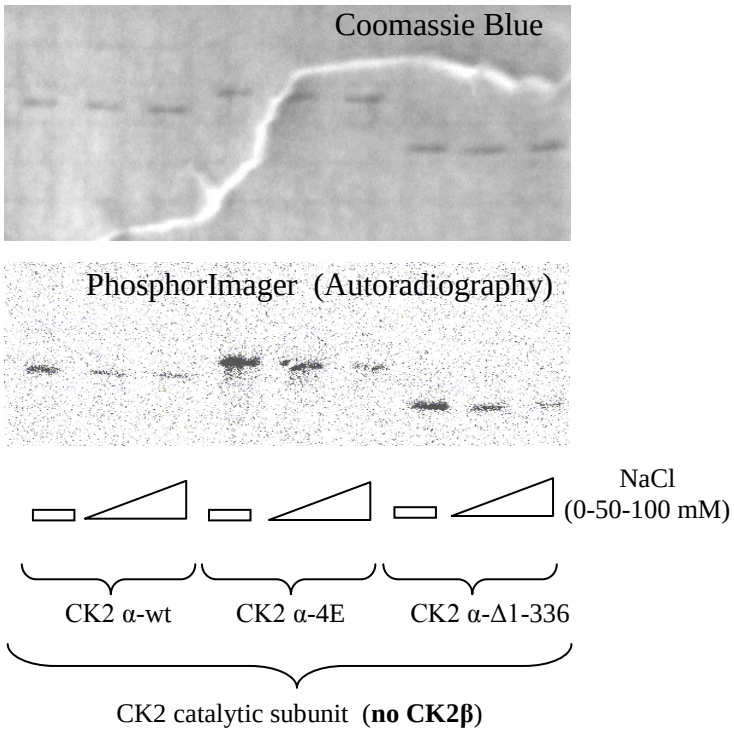

Fig. 9A
Autophosphorylation of CK2 catalytic subunits (CK2α-wt, CK2α-4E and CK2α-Δ1-336)
In these two pictures, a coomassie stained SDS-PAGE suggests similar amounts of enzymes, while the autoradiographic pattern shows that CK2α-4E is more autophosphorylated than CK2α-wt.

Fig. 9B:
Autophosphorylation of CK2 holoenzymes
In the picture, the autoradiographic pattern discloses that CK2α-4E autophosphorylation is resistant to a 200 mM NaCl buffer. The presence of the β subunit does not alter CK2α-4E autophosphorylation while completely abolish autophosphorylations in CK2α-wt and CK2α-Δ-1-336.

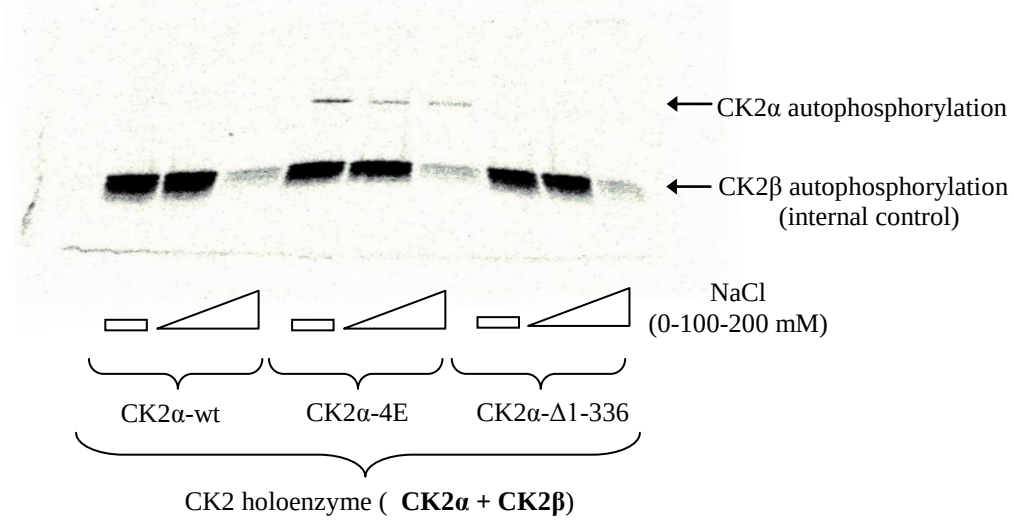

The autophosphorylation of the regulatory subunit CK2β is also reported (Fig. 9B). This data suggests a specific event related to CK2α-4E autophosphorylation, indeed the P^{33} incorporation in the regulatory

subunit CK2β is comparable between the different holoenzymes (CK2α-wt, CK2α-4E and CK2α-Δ1-336), while the autophosphorylations of the catalytic subunits show a different trend. Our hypothesis is that the four amino acidic substitutions in CK2α-4E sustain Ser357 as new autophosphorylation site. In particular, the replacement of Thr360 and Ser362 with glutamic acids can support the phosphorylation of Ser357 as acidic determinants in position n+3 and n+5, respectively.

This data supports a hierarchical autophosphorylation occurring after the intervention of the Cyclin directed kinase 1 (Cdk1), increasing the amount of phosphates linked to the C-terminus of CK2α.

It is also interesting to observe the molecular weight exhibited by the CK2α-4E on SDS-PAGE. The four mutations (Serines to Glutamic acids) don’t modify significantly the MW of the protein, but in contrast CK2α-4E mutant has a slower migration of about 5KDa; the four mutations may alter the structure of the C-terminal segment, which may interfere with the binding of the SDS.

This structural alteration of CK2α-4E might suggest a role as bait for interactors and substrates related to the C-terminal phosphorylation of CK2. Indeed, the altered binding of SDS might reveal an altered affinity for different ligands (e.g. CK2 substrates or interactors).

As useful complement, some experiments were performed to detect an alteration in the catalytic activity of the enzyme CK2α-4E, CK2α-wt or CK2α-Δ1-336 after autophosphorylation, but the results don't show significant modulation of the specific activity (data not shown). Data like this supports the idea of a role as bait for interactors and substrates and not as regulatory domain.

13. Bidimensional electrophoretic analysis of cellular extracts phosphorylated by CK2 α-wt and CK2α-4E

A 2D separation of total soluble cellular extracts derived from human neuroblastoma cells (SK-N-BE) phosphorylated either by CK2α4E or by CK2αwt was performed. After the separation stage, the two patterns of radio labeled proteins showed significant differences mainly in "spot 6" (Fig. 10). "Gel spot 6" was manually excised for protein identification by MALDI-TOF-TOF. Five proteins with putative phosphorylatable sites for CK2 have been identified (Fig. 10).

Fig.10: Experimental scheme
In the scheme, all the steps of the experiment are proposed. Step1, the phosphorylation in vitro; in step 2, bidimensional separation; in step 3 analysis of the radio labeled spots; in step 4: identification of the proteins by mass spectrometry.

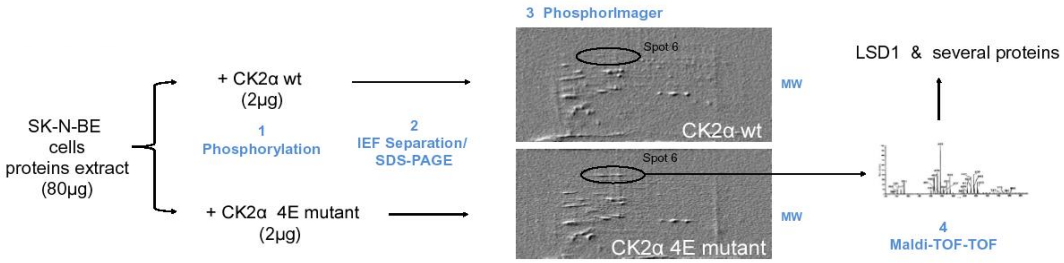

Fig. 11: Bidimensional PAGE autoradiographic profiles

In the picture, three panels show the phosphorylation profiles of the CK2α wild type and mutant 4E, and the negative control. The same cellular extract phosphorylated in vitro in the three condition reveals few significant difference due to the mutant CK2α 4E able to mime the phosphorylation of the Thr344, Thr360, Ser362, Ser370. In particular the spot 6 is significantly elevated by the CK2 mutant.

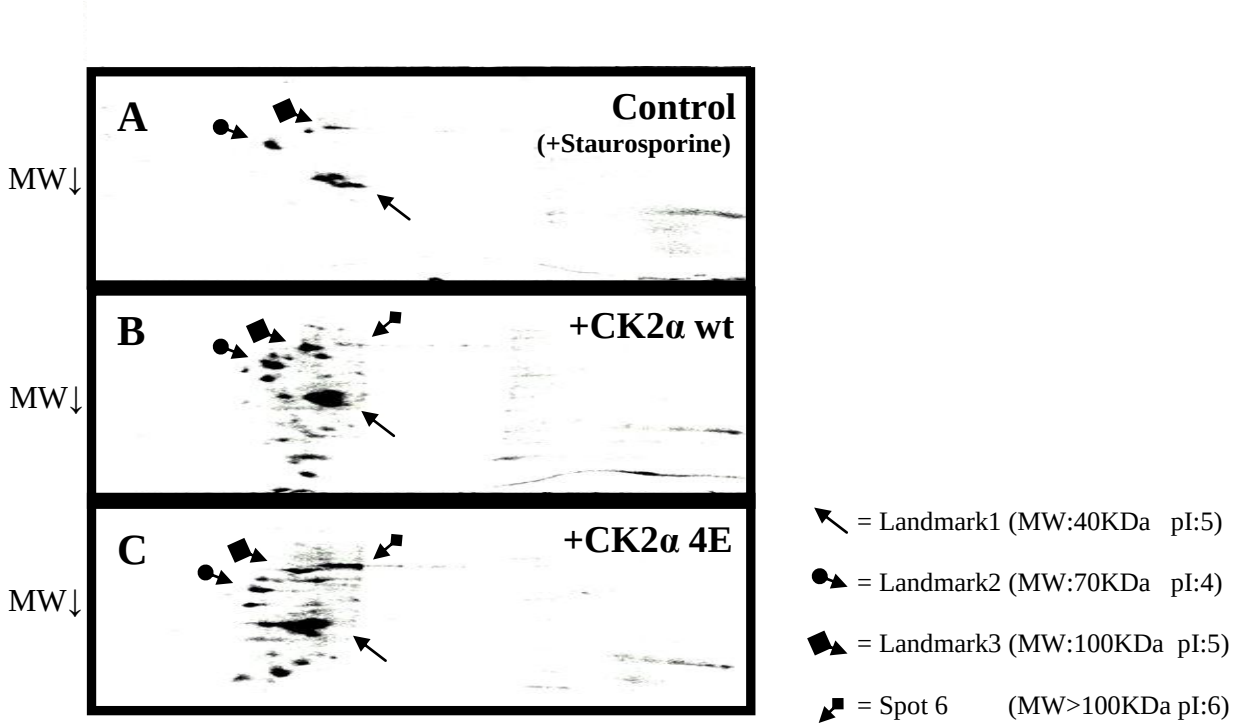

These pictures represent three 2D profiles (1 control and 2 samples) (Fig. 11). In the panel A, the phosphorylation of cellular proteins in presence of staurosporine is reported. This compound is a potent but non-specific ATP competitive kinase inhibitor [71]; CK2 is able to resist to staurosporine (Ki>1μM) instead of many other kinases (Ki=1-100 nM), thus all the kinase activity showed in the picture is due to this enzyme.

The whole cellular extract from neuroblastoma cells is phosphorylated by CK2 catalytic subunit α (1,1 μM) and by CK2α 4E mutant, see panels B and C respectively.

Staurosporine in the samples correlates the phosphorylation pattern to CK2 alone.

The large amount of radio-labeled spots generated by CK2 wt and mutant 4E, respectively panels B and C (Fig. 11) confirms the extraordinary pleiotropism of this enzyme and its role in a large number of biological processes.

Furthermore, the focusing of all the substrates of CK2 in the acidic portion of the IEF Run reveals that main CK2 substrates have an acidic isoelectric point (pI), thus in addition to the local consensus also the global charge is important.

The similarity of the phosphorylation patterns of CK2α-wt and CK2α 4E confirms the similar values of specific activities of the two forms of CK2α measured in the chapter 11. In fact, many spots are identical or have negligible alterations in the two panels and only a single spot ("the spot 6") has a strong fluctuation (CK2α-wt vs. CK2α 4E), suggesting the preferential recognition by CK2α 4E mutant.

The two dimensional electrophoresis run has been repeated three times with independent samples. The "Spot 6" appeared in the presence of CK2 mutant 4E and it was mild or negligible with CK2α wt.

In summary, there are many similarities in the phosphorylation patterns (B vs. C), but also few local differences ("Spot 6"), suggesting the specific recognition of few proteins due to the "4E" mutations.

Starting from the mass spectrometry data (supplementary materials S3), five proteins have been identified as CK2α-4E putative substrates in the "Spot 6" (Tab. 3), but it is probable that some of these proteins are merely contaminant (excided in the same band of the CK2 substrate).

Tab. 3

Mass spectrometry identifies five proteins phosphorylated in the sample named "spot 6". For each protein, several hypothetical sites have been proposed, which fulfill the minimal CK2 consensus (T/S-X-X-D/E), but only the phospho-peptides proposed for LSD1 (also denoted by the acronym KDM1A) have already been annotated in vivo (^=[79])

Cod.	Name	Score	Molar Weight	Match	Hypothesized sites by CK2 acidic consensus
GANAB HUMAN	Neutral alpha-glucosidase AB	816	107375	46	1-S<u>S</u>^{244}SADPEGHFET
HGS HUMAN	Hepatocyte growth factor-regulated tyrosine kinase substrate	511	86848	21	1-Q<u>S</u>^{272}EAEEKERLRQ
KDM1A HUMAN	Lysine-specific histone demethylase 1A	314	93484	13	1-<u>S</u>^{131}EDEYY<u>S</u>^{137}EEE(^) 2-<u>S</u>^{166}EPEEPSGVEG(^)
HS74L HUMAN	Heat shock 70 kDa protein 4L	251	95705	8	1-R<u>S</u>^{74}FDDPIVQTERI 2-<u>S</u>^{409}FEDG<u>S</u>^{414}GECEVF 3-<u>S</u>^{832}SGEMEVD
OGDHL HUMAN	2-oxoglutarate dehydrogenase-like, mitochondrial	99	115474	4	1-S<u>S</u>^{50}YMEEMYFA 2-TVT^{536}LQEFEEEIA 3-M<u>S</u>^{789}NDDSDAYPA 4-S<u>S</u>^{904}QDLEEKVA

We focused our attention on Lysine Specific histone Demethylase 1 (LSD1), an enzyme involved in the modification of the histone proteins and in chromatin regulation. Indeed these arguments support LSD1 as a new CK2 substrate:

1. Dephoure and colleagues described LSD1 phosphorylation in cell (without identifying the kinase responsible). Consistent with our hypothesis, they identified the phosphorylated residues as Ser131, Ser137 and Ser166 [79]. To note that, these residues have putative consensus motifs for CK2.
2. LSD1 is related to mitosis [69], as well as CK2.

LSD1 catalyzes the removal of one or two methyl groups from methyl lysine 4 and 9 of histone H3 [49, 72].

Shuang and colleagues reported that LSD1 is required during the mitotic

phase and its breakdown leads to chromosomic instability [69], a similar phenotype has been observed in HeLa cells expressing the mutant CK2α-4E [35]. The more recent finding that unbalanced levels of Histone H3 di-methylated lysine 4 has been correlated to defective incorporation of the centromeric protein CENP-A in kinetochore and then to an aberrant chromosomes segregation due to a defective mitotic spindle [70], fits with our hypothesis and further confirms the relation CK2/LSD1.

In summary, LSD1 clearly appears a possible link between CK2 and the chromosome instability; many independent observations support a network involving CK2α phosphorylation by Cdk1 and LSD1 phosphorylation by CK2. The misregulation of this pathway might lead to chromosome instability by a defective formation of the mitotic spindle.

14. CK2α-4E phosphorylates the recombinant LSD1, but also CK2α-wt is able to recognize LSD1 *in vitro*

The LSD1 phosphorylation is confirmed *in vitro* (Fig.12B). The minimum observable quantity of phosphorylated LSD1 by autoradiography is 50 ng (26 nM), suggesting LSD1 as a very good CK2 substrate.

Surprisingly, also CK2α-wt is able to phosphorylate the recombinant LSD1; indeed the phosphorylation appears similar to CK2α-4E (Fig. 12A and 12B).

In the graph.1 are reported the DLU values measured in the kinetic experiments, which refer the amount of radio labeled phosphates incorporated in the full length band of LSD1.

In the table 4, the values of the kinetic constant (Km and Vmax) of CK2α-wt and CK2α-4E are reported.

Fig. 12A and 12B:
Phosphorylation of recombinant LSD1 by CK2α-wt and CK2α-4E
LSD1 is phosphorylated performing a kinetic analysis; eight concentration points are tested (0-531 nM).

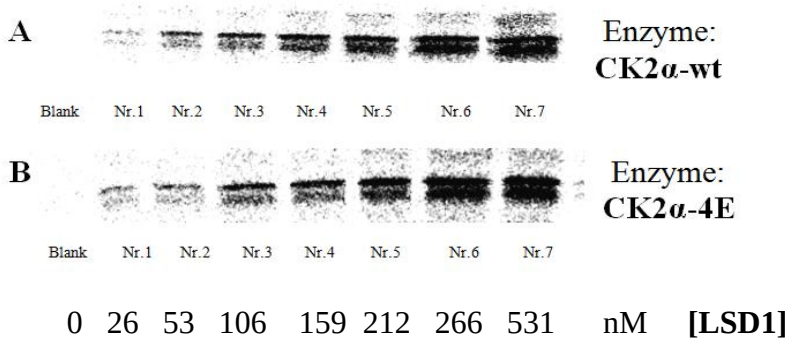

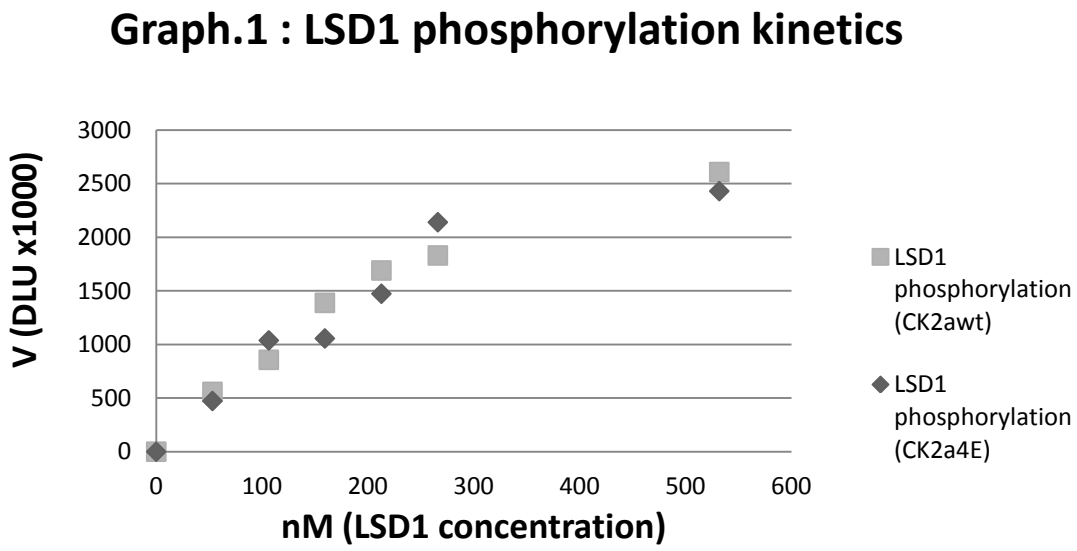

Tab 4:
DLU Values Plotting, Km and Vmax of the reactions
The signals of the autoradiographic profiles are converted by OptiQuant software (Perkin Elmer) in values of Density Light Units (DLU). DLU values of the two kinetics are plotted by Prism 5 (Graphpad Software); Km and Vmax are estimated by nonlinear regression.

Enzyme	Km Value	Vmax	Confidence (R^2)
CK2α-wt	393.0 nM	7,9 x10^6 DLU/mg x min	0.981
CK2α-4E	367.9 nM	7,9 x10^6 DLU/mg x min	0.968

The values of Km and Vmax for the LSD1 phosphorylations are very similar

and a significant difference between the two enzymes is not present. The nanomolar range of the Km value suggests that LSD1 phosphorylation *in vivo* could be very effective, as well as *in vitro*. Consistent with this, LSD1 phosphorylation has been already reported in cell by several independent authors [69, 79].

As useful complement, the autoradiography of the LSD1 phosphorylation reveals three mayor bands in the lane (data not shown). The upper one is the full-length protein of 94 KDa (observable in the Fig. 12A and 12B), while the other two bands (40 KDa and 25 KDa) are phosphorylated fragments of LSD1.

Repetitions of the experiment suggested a spontaneous degradation related to the freeze and thaw of LSD1 solution. These fragments appear spontaneously after the FPLC purification and increased with time (supplementary materials S4). WBs disclose the presence of the N-terminal region in all the fragments and the absence of the C-terminus (data not shown), confirming the phosphorylation at the N-terminal portion of LSD1.

Moreover, full-length band is split in two bands with very similar MWs (Fig.12A and 12B). The complete separation of the two bands requires an SDS-PAGE with low acrylamide concentration (<8%), thus sometimes the two bands can appear as a single signal using gel with higher acrylamide concentration (e.g. Fig. 13).

15. Characterization of LSD1 phosphorylation *in vitro* and the effect of CK2β

The mechanism which favors the LSD1 phosphorylation by CK2α-4E in cellular extract has not been disclosed yet, indeed the Km values measured

are very similar, suggesting that an indirect mechanism enhances LSD1 phosphorylation in cellular extract.

Additional experiments of phosphorylation by CK2α-wt, CK2α phospho-mimetic mutant 4E and CK2α C-terminal truncated Δ1-336 in the absence and in presence of the regulatory subunit CK2β were performed.

Again no differences have been detected using as enzyme: either CK2α-4E, or CK2α-wt, or CK2α-Δ1-336 (Fig. 13A and Tab. 5A). Indeed, all the forms of CK2α in the presence of CK2β equally phosphorylate LSD1 (Fig. 13B and Tab. 5B), while the α-casein phosphorylation used for the comparison of the three CK2 forms confirms the similar specific activities of the 3 enzymes.

In summary, the stimulation of CK2β increases the amount of phosphates incorporated, but the C-terminal segments of CK2α (wt, 4E in comparison to Δ1-336) don't alter LSD1 phosphorylation.

It seems predictable that the difference observed in 2D separations depends by interactors able to recruit CK2α-4E and/or to block CK2α-wt.

These interactors are absent in the *in vitro* assay and their lacking allow a generalized phosphorylation of LSD1.

Fig. 13A:
LSD1 phosphorylation by the CK2α subunits and CK2 holoenzymes (autoradiography)

LSD1 is phosphorylated by the catalytic subunits CK2α-4E, CK2α-wt and CK2α-Δ1-336, and by holoenzymes (α2β2). CK2β stimulates the phosphorylation, while no difference are reported about the action of C-terminal segments of CK2α (wt and mutants).

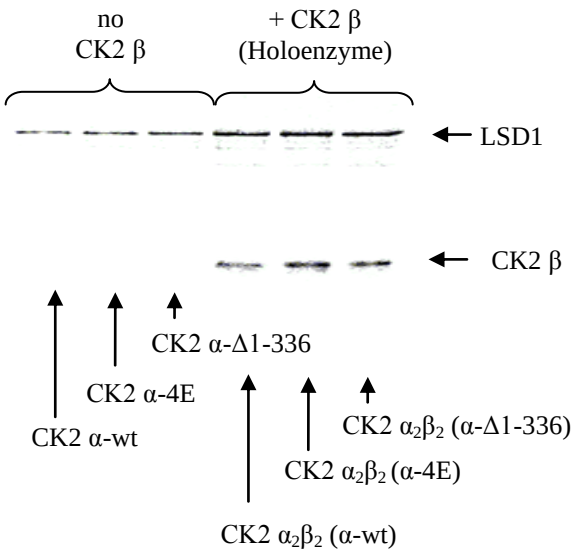

Tab. 5A:

DLU values are extrapolated by the fig.5a. The three forms of CK2α phosphorylates LSD1in a similar manner.

LSD1 phosphorylation by the CK2 α-wt CK2 α-4E CK2 α-Δ1-336

	CK2 α-wt	CK2 α-4E	CK2 α-Δ1-336
Substrate: LSD1	0.58 x10^6 DLU	0.68 x10^6 DLU	0.77 x10^6 DLU
Substrate: LSD1 (CK2β effect)	1.28 x10^6 DLU	1.38 x10^6 DLU	1.48 x10^6 DLU
Effect of CK2β	+124 %	+101 %	+91 %

Fig. 13B and Tab. 5B
Specific activity controls of CK2α-4E, CK2α-wt and CK2α-Δ1-336

The three forms of CK2 tested are analyzed against α-casein to ensure a similar value of specific activity.

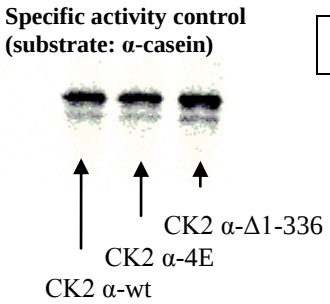

	CK2 α-wt	CK2 α-4E	CK2 α-Δ1-336
Substrate: α-Casein	2.7x10^6 DLU	2.5 x10^6 DLU	3.0 x10^6 DLU
Ratio	90%	83%	100

16. LSD1 phosphorylation occurs at physiological ionic strength

LSD1 phosphorylation by CK2 ($\alpha_2\beta_2$) in performed in different conditions of ionic strength. Data suggests that the phosphorylation could be very effective in a physiologically buffer; the best condition tested is 130 mM NaCl (Fig. 14 and Graph. 2).

The inhibitory effect by high saline buffer (>130 mM NaCl) reflects the susceptibility of CK2 to ionic strength and doesn't seem related to any particular interference in relation to the interaction CK2/LSD1. Consistent with this α and β caseins phosphorylations are affected in a similar way (data not shown).

Fig. 14 and Graph.2
Effect of ionic strength on LSD1 phosphorylation by CK2 holoenzyme

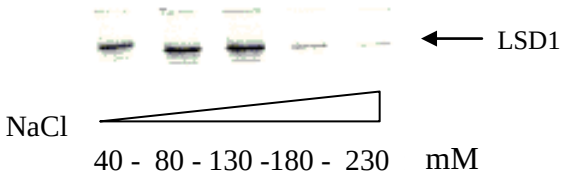

LSD1 is phosphorylated by the CK2 holoenzyme; a gradient of saline concentrations is tested. The phosphorylation is dependent to ionic strength, as well as almost all the CK2 substrates, and the best condition tested is 130 mM NaCl.

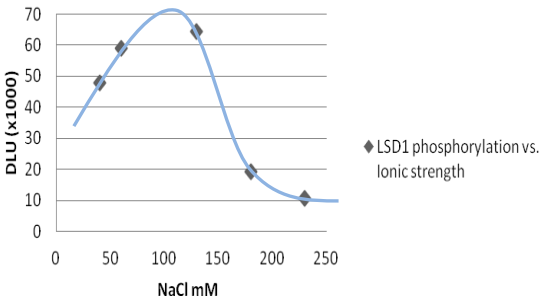

In the graphic are reported the values of DLU measured by the figure 14, the estimations represent the amount of phosphates incorporated into LSD1 after 10 minutes of reaction.

17. Polycations and histone proteins modulate CK2 and repress LSD1 phosphorylation

In figure 15, the phosphorylations of β-casein and LSD1 by CK2 are increased in presence of CK2β. In figure 16 and in the table 6, β-casein phosphorylation by the CK2 holoenzyme is positively modulated by poly-L-lysine, while LSD1 is inhibited by the same compound.

These data suggest that LSD1 is a class I substrate, recognized by both the holoenzyme and the catalytic subunit α [7].

Fig. 15:
Effect of CK2β subunit on LSD1 phosphorylation by CK2 holoenzymes (autoradiography)

LSD1 and β-casein phosphorylations by CK2 are analyzed. LSD1 phosphorylation is stimulated by the presence of CK2β, as well as, β-casein.

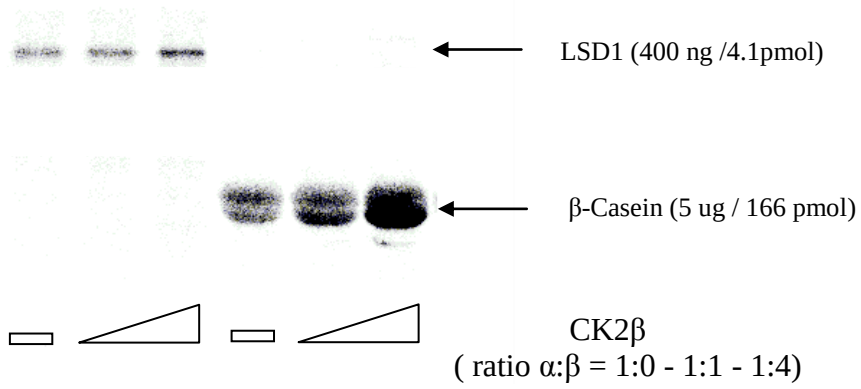

Fig. 16 and Tab.6:
The effect of poly-L-lysine on the LSD1 phosphorylation
LSD1 is phosphorylated by the CK2 holoenzyme; the effect of a gradient of poly-L-lysine (0-3μM) is tested. The phosphorylation of β-casein is increased, while LSD1 phosphorylation is dramatically affected by polycations.
In the table are reported the values of DLU measured by the Fig.16, the estimations represent the amount of phosphates incorporated into LSD1 after 10 minutes of reaction. The phosphorylation of LSD1 is affected by poly-L-lysine.

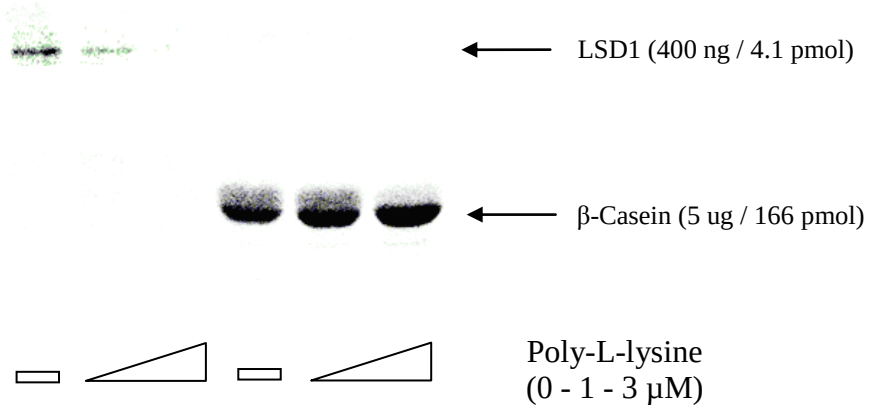

	Poly-l-Lysine 0 μM	**Poly-l-Lysine 1 μM**	**Poly-l-Lysine 3 μM**
LSD1 phosphorylation	100%	55%	33%
β-casein phosphorylation	100%	131%	180%

Natural counterparts of poly-L-Lysine are polyamines and monoamines (e.g. spermines, spermidines and serotonin), but also positively charged proteins (e.g. histone proteins).

The role of these proteins such as LSD1 phosphorylation regulators appears predictable, indeed LSD1 is commonly bound to histone proteins *in vivo*. Histones are the substrates of LSD1, but in our case are also regulatory elements.

In our experiments (Fig. 17 and Tab. 7), LSD1 phosphorylation was strongly reduced in presence of 0.6 - 1.2 µg/µl of histone sub-fraction lysine rich f1 (a mixture of histone proteins enriched of the H1 subunit). H1 is particularly abundant in condensed chromatin and in low transcribed region, where the histone proteins acquire their higher positive charge.

Fig. 17 and Tab. 7
The effect of histone proteins on the LSD1 phosphorylation
Histone proteins are common interactors of LSD1, in the picture LSD1 is phosphorylated by the CK2 holoenzyme in three condition (histone proteins 0 - 0.6 - 1.2 µg/µl*). The phosphorylation of β-casein is stimulated by these proteins, while LSD1 phosphorylation is dramatically affected by polycations. In the table 7 are reported the values of DLU measured by the fig.17, the estimations represent the amount of phosphates incorporated into LSD1 after 10 minutes of reaction.*

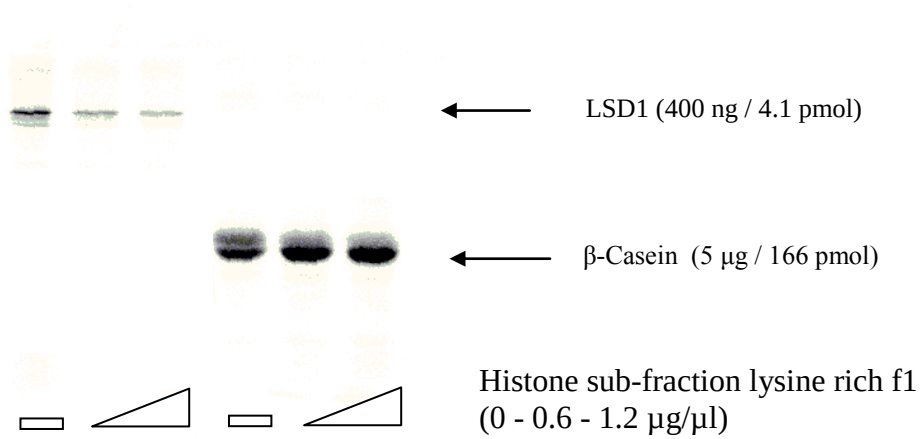

	Histone subfraction 0.0 µg/µl	**Histone subfraction 0.6 µg/µl**	**Histone subfraction 1.2 µg/µl**
LSD1 phosphorylation	100%	46%	34%
β-casein phosphorylation	100%	151%	150%

In vitro many clues of a strong modulation of CK2 by polyamines and histone proteins have been already proposed [80], but currently no data

have been published to demonstrate the physiologic occurrence of this modulation.

LSD1 is commonly bound to histone proteins and may be an excellent example of CK2 substrate regulated by polycations *in vivo*.

Hereby we hypothesize that the histone proteins charge modulates CK2 action and then the LSD1 phosphorylation. Indeed, histone proteins are very close to CK2 during the LSD1 phosphorylation and a direct interaction seems predictable.

The additional findings that the positive charges of histone proteins can be altered by several post-translational modifications (e.g. histone acetylations) suggest that these events might indirectly modulate LSD1 phosphorylation by CK2.

In summary, CK2 is able to phosphorylate LSD1 when it is located to a specific portion of DNA. These loci are characterized by a low positive charge and the hyperacetylation of the histone proteins; for these reasons CK2 might generate an essential complement for the gene regulation and might explain many controversial observations about LSD1 (e.g. the demethylation of the Lys9 instead the Lys4).

In our model shown in figure 18A, CK2 preferentially phosphorylates LSD1 near active genes, leading to a subsequent modulation of the methylation. On the other hand, CK2 fails to phosphorylate LSD1 when it binds heterochromatin (high positively charged histones and poor in term of acetylations).

To note that, LSD1 phosphorylation may alter the epigenetic marks, but at the same time epigenetic marks alter the CK2 activity, thus a feedback mechanism is generated (Fig.18B).

Fig. 18A
CK2 recognizes preferentially LSD1 in hyperacetylated loci
Actively transcribed genes are marked by hyperacetylated histones, which are characterized by a low positive charge; in this loci CK2 is not repressed and LSD1 phosphorylation is allowed.

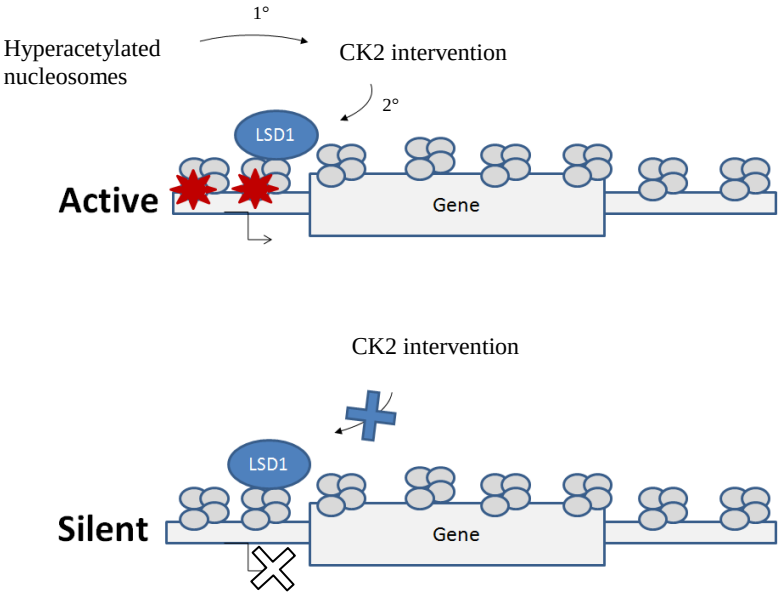

Fig. 18B
CK2 modulation by histone proteins and LSD1 modulation by CK2 might form a circular feedback mechanism.

The positive charges of histone proteins are greatly dependent to the modifications on the protruding tails, in particular by acetylations. Hereby, we hypothesized a feed-back mechanism able to modulate LSD1 phosphorylation by the modulation of CK2. Indeed CK2 is strongly affected by histone proteins during the phosphorylation of LSD1

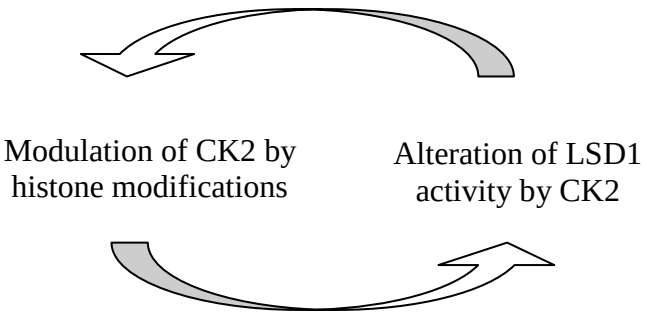

The action *in vivo* of poly-L-lysine, spermines and histone proteins on CK2 is still matter of debate. LSD1 is a very particular example of CK2 substrate,

and might be physiologically regulate by histone proteins, indeed histones can directly interact with CK2 during the recruitment of LSD1.

18. Phosphorylation of LSD1 *in vivo*

LSD1 is hyper-phosphorylated in nocodazole-synchronized cells, and it is required for a proper chromosomal segregation during mitosis [69].

We have confirmed the conclusion about the hyper-phosphorylation of LSD1, but furthermore we suggest that LSD1 phosphorylation is widespread in the whole cell cycle in our cellular model (SK-N-BE).

Calf Intestinal Phosphatase (CIP) de-phosphorylates LSD1 in a cellular extract as shown in Fig. 19A. LSD1 incubated with CIP has an altered mobility in SDS-PAGE. The shifting is very little but detectable and reproducible.

The molecular weight of LSD1 in SK-N-BE cells is due to presence of phosphorylated residues and it can be reduced by de-phosphorylation.

In our experiment, it is very interesting the observation of the phosphorylation in the whole cell cycle in SK-N-BE cells. Indeed, Shaung and colleagues [69] got great emphasis to the LSD1 phosphorylation occurring in the M phase in HeLa cells, correlating it to the increased amount of LSD1 during mitotic events.

In contrast our data with SK-N-BE cells do not show any altered migration of LSD1 attributable to the pro-mitotic phosphorylation (Fig. 19B).

Although, additional experimentation is required, it seems that LSD1 is constitutively phosphorylated in SK-N-BE cells.

Fig. 19
LSD1 is commonly phosphorylated in human neuroblastoma SKNBE cell
In the picture A, SKNBE cell proteins extracts (20µg) were incubated in ice, at 30°C, and in presence of phosphatase CIP at 30°C for 1h. After the incubation of the samples have been subjected to SDSPAGE and blotted onto PVDF membranes. Molecular weight of LSD1 has been revealed by a C-terminal antibody. Consistent with the experiments of Shuang and colleagues [62], the molecular weight of LSD1 is reduced by the action of phosphatase.
In the picture B, the nocodazole treatment of SKNBE cells does not induce an altered migration of LSD1 in contrast to the reported experiment.

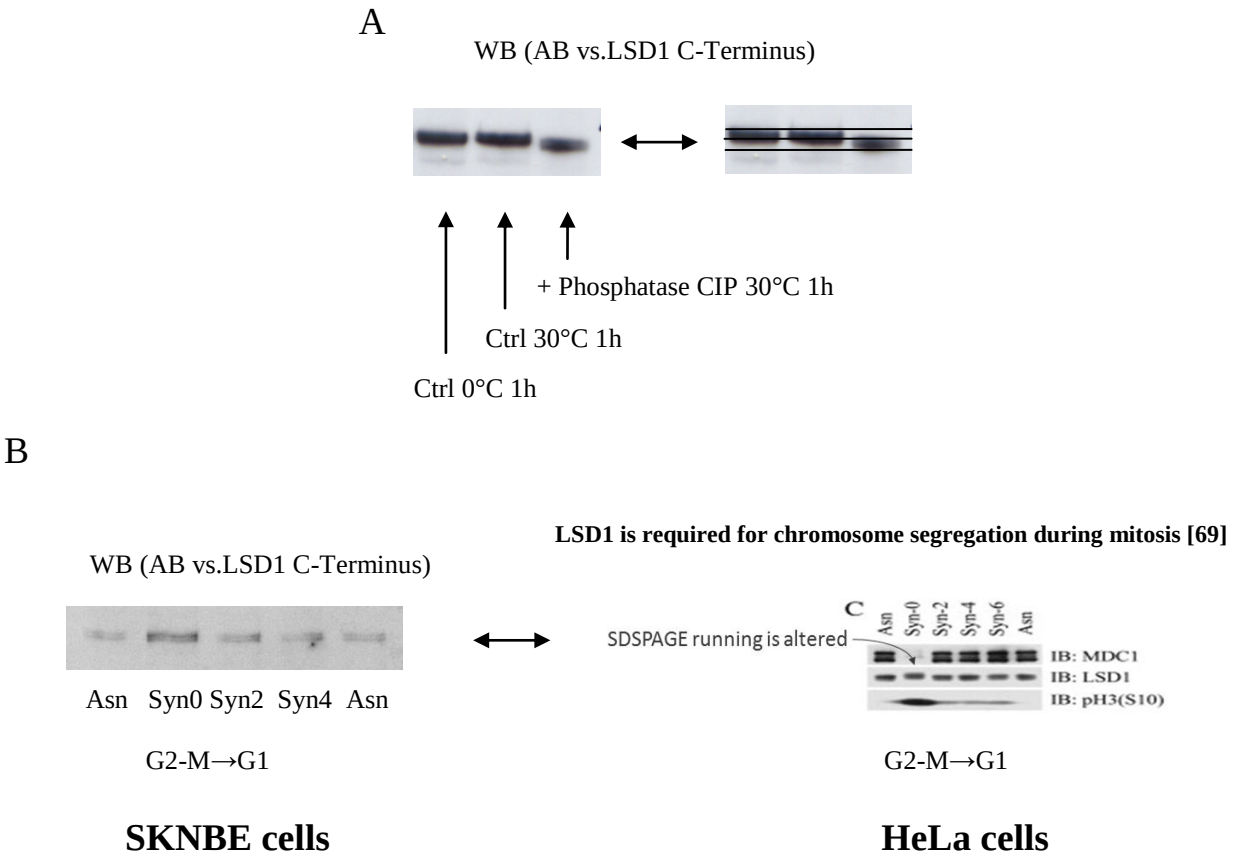

This finding suggests that LSD1 phosphorylation plays a role during the whole cell cycle, supporting cell survival in SK-N-BE tumor cells.

In a non tumor cell (e.g. Fibroblasts) and in tumor cell without the constitutive phosphorylation of LSD1 (e.g. HeLa cells), LSD1 has two levels of regulation: the first one is related to the mitotic phase, it needs the complete saturation of the phospho-acceptor sites and it is associated to a

stronger modulation of LSD1 [69], while the second one is associated to a smooth modulation of LSD1 and it is related to the whole cell cycle.

19. LSD1 phosphosites identification by mass spectrometry

In the sequence of LSD1 (O60341 KDM1A_HUMAN) there are at least 4 putative sites fulfilling the consensus of CK2 (Fig. 20A). Three of these residues (Ser131, Ser137 and Ser166) have been already reported to be phosphorylated in cells [79], but no data about the kinase responsible are available.

In order to identify the residues which are phosphorylated *in vitro* by CK2α4E, LSD1 was incubated with ATP *in vitro*. The exhaustive phosphorylation has been performed by the incubation of 50 pmol of LSD1 [0,5 μM] in presence of 10 pmol of CK2α4E [0,1 μM] and 10 nmol of ATP [100μM] for 40 minutes at 30°C.

Phosphorylated LSD1 was excised from SDS-PAGE, subjected to tryptic digestion, purified by TiO_2 affinity chromatography and analysed by MS (LTQ Orbitrap XL Termofisher scientific).

Two sites are detected: Ser131 and Ser166 (Fig. 20B and 20C).

Manual refinement analysis discloses also Ser137 as phospho-residues in a di-phosphorylated peptide, containing both Ser131 and Ser137 (Fig. 20C).

The re-fragmentation analysis doesn't describe Ser137 such as a single phospho-residue, it might suggest the opening of this sub-domain after the first phosphorylation (Ser131), leading the exposure of the Ser137 to CK2 in a hierarchical process.

Although we cannot exclude that other kinases phosphorylate LSD1, our data provide the clear-cut demonstration that LSD1 is a new substrate of

CK2 *in vitro* and *in vivo*.

Fig.20
Mass spectrometry reveals several phosphorylated peptides

In the picture A, the four putative CK2 directed sites are reported, while in the picture B the three sites detected by mass spectrometry are reported.
In the picture C, manual spectrometry reveals a di-phosphorylated peptide Ser131 and Ser137 and a mono phosphorylated peptide Ser166.

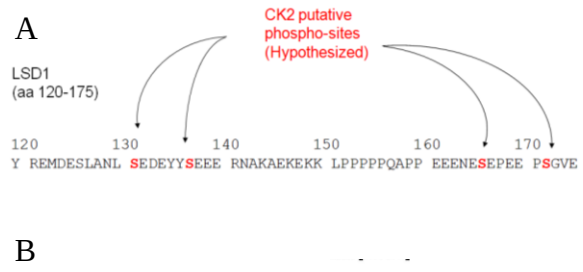

LSD1 phospho-sites identified by mass spectrometry

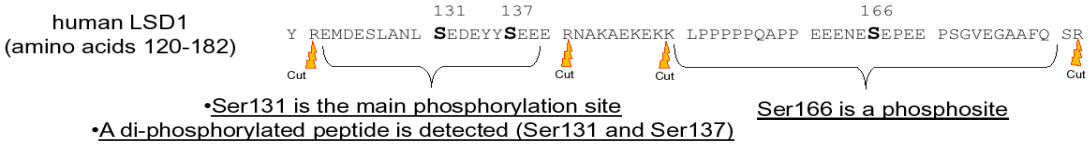

•Ser131 is the main phosphorylation site
•A di-phosphorylated peptide is detected (Ser131 and Ser137)

Ser166 is a phosphosite

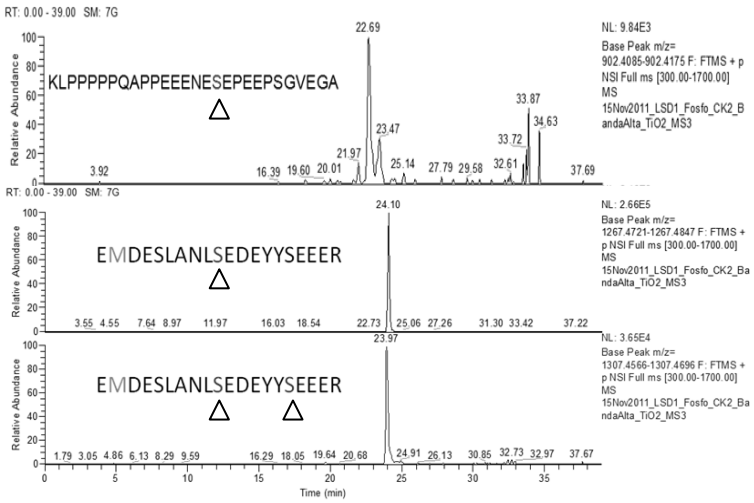

20. Mutagenesis of the vector pTP6_Ko-FLAG/LSD1wt

Mass spectrometry demonstrates the phosphorylation of Ser131, Ser137 and Ser166 by CK2. Molecular modeling of this region suggests a metastable structured domain with Ser131, Ser137 and Ser166 exposed to the solvent. The additional analysis of Protein-Protein Docking complex between LSD1 and CK2α, obtained using Zdock software, followed by 100 ns of Molecular Dynamic (NAMD) further suggests the ability of these peptides (and in particular the Ser131) to enter in the catalytic site of CK2 (data not shown).

To shed light on the role of the LSD1 phosphorylation, we planned to mutagenize the two Ser residues (Ser131 and Ser137), while the Ser166 mutagenesis was immediately excluded for reasons of time.

Starting from the mammalian vector pTP6_Ko-FLAG/LSD1wt (Fig.21), I tried many times to perform the mutations, using the Quick-Change Mutagenesis Kit, but no colonies were obtained by this strategy.

To bypass the problem, an alternative method has been developed (Fig. 22) and two Ser131 mutants have been obtained (S131E and S131A).

Ser131 is the most abundant phosphoresidues detected by mass spectrometry and the crucial site in the Molecular Docking Analysis. Thus, it might have a role in LSD1 regulation alone.

Hence, S131A and S131E mutants are essential tools to understand the effects of the LSD1 phosphorylation, a phospho-defective and a phospho-mimic mutant respectively. The study of transfected cells with the mutant forms of LSD1 can provide evidences about the function of Ser131 phosphorylation in cell and in general suggest a role for the phosphorylation of LSD1 by CK2.

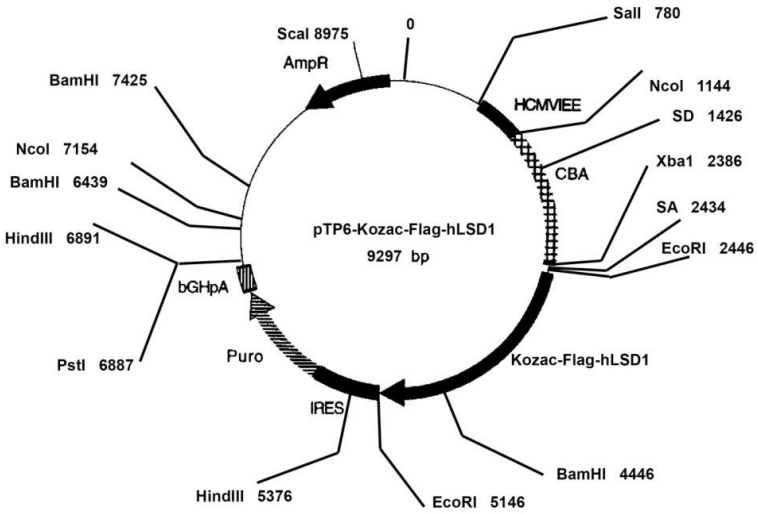

Fig. 21
pTP6-Kozac-Flag-human LSD1

In the picture is reported the vector pTP6-Kozac-Flag-human LSD1 used for transfecting HEK293T cells.

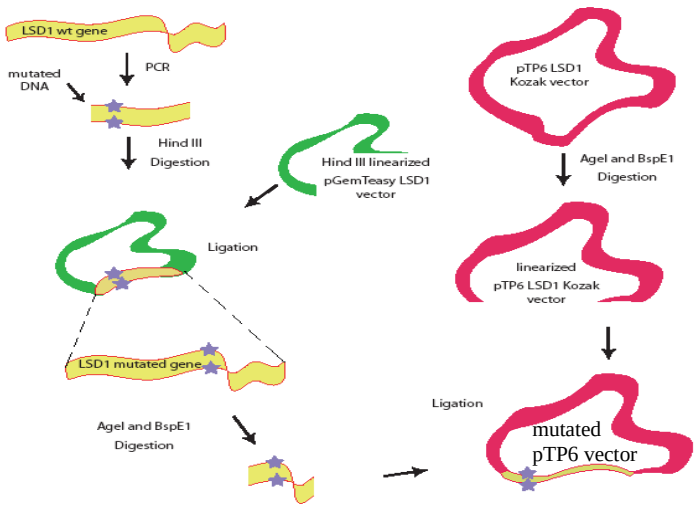

Fig. 22
Scheme of the mutagenesis

A mutated PCR product of 820 nt has been obtained by PCR with the primers Ser131Glu1°for (or Ser131Ala1°for) and LSD1exon8rev. A 73nt fragment HindIII- (Ser131mutated)-HindIII has been excided from the PCR product and ligated into a cloning vector pGEMt-easy-LSD1wt linearized by the same restriction enzyme. The orientation of the insertion has been verified by sequencing.

The mutated fragment BspE1-AGEI has been excided by pGEMt-easy-LSD1wt and ligated into a pTP6_Ko-FLAG/LSD1 vector linearized by the same enzymes.
The insertion has been verified by EcoR1 digestion, obtaining data about the full length gene. Finally, the genes have been sequenced to exclude unexpected mutations.

21. Transfections of LSD1 wt and LSD1 mutants in HEK293T cells

The major aim of this piece of work is to demonstrate that cells transfected with LSD1 mutants have a different phenotype respect to the wt one. The first step to achieve this target is to generate stable and transient transfection of HEK293T cells (Fig. 23).

Transfections with the pTP6-Ko-LSD1 wt and mutants were performed and stably transfected cell lines expressing LSD1 and Puromycin *N*-acetyl-transferase have been achieved (Fig. 24).

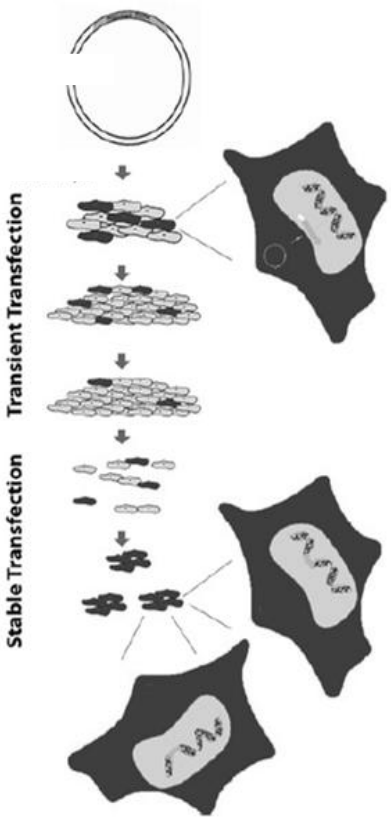

Fig. 23
Scheme of stable and transient transfection protocol

A linearized plasmid was transfected by lipofectamines for 24h. Transient expression of was reported for 7-10 days by anti flag AB and anti Pan LSD1.
From the day 10, 3 selection treatments with puromycin (1- 3 -10 ug/ml) were performed. Cells adhesion after the puromycin treatments disclosed the selection and non transfected cells were lost together the exhausted media
All the survived cells were positive to the construct and expressed LSD1 at high level.

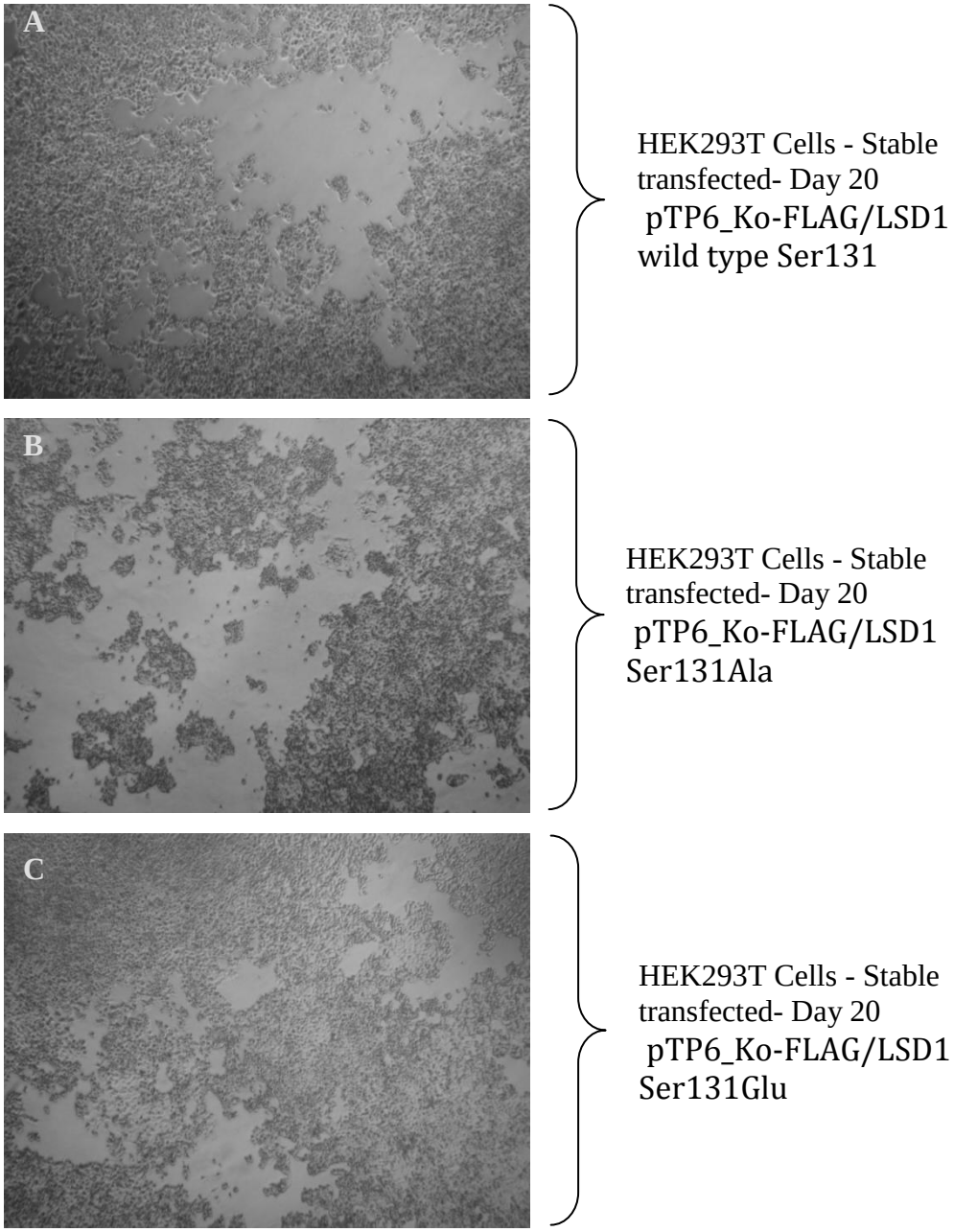

Fig. 24
pTP6_Ko-FLAG/LSD1 transfected HEK293T clones.

Three clones of cells HEK293T, transfected by lypofection, expressing LSD1 wt (A), LSD1 Ser131Ala (B) and LSD1 Ser131Glu (C) are shown. All the three clones were viable. Each picture was collected by a 10X objective.

Transfected cells expressing LSD1 wt and mutants are viable. Now, a catastrophic phenotype mediated by the misregulation of LSD1 Ser131 phosphorylation can be excluded and it seems predictable that the phenotype

may be the abnormal modulation of several mRNAs, or the alteration of the LSD1 complex.

22. Analysis of LSD1 expression in transfected cells

LSD1-FLAG protein expressions have been analyzed at different times by WB (day 2, 10, 20 and 40). Each line (Wt, Ser131Glu, and Ser131Ala) showed a stable expression of the exogenous proteins, although a gradual loss of expression was evident 40 days after the transfection.

Anyway, LSD1 was strongly expressed for many days, probably 10-100 fold higher than the endogenous form. As expected, the exogenous LSD1 forms (detected by a Flag specific antibody) were present only in transfected lines, while the pan LSD1 WB indicates dramatic increase in LSD1 cellular concentration, detecting the endogenous LSD1 and the transfected one (Fig. 25A and 25B).

All the forms of LSD1 (wt, Ser131Ala, Ser131Glu) codified for a stable protein and no evidence of toxicity was detected.

Fig. 25
Analysis of the expression of transfected LSD1 in HEK293T cells.
A: Two WBs are reported. The lower one reports the amount of B-actin, and is used as standard, while the other WB reports the amount of the transfected LSD1 by a C-terminal epitope (present also in the endogenous LSD1). Each sample was subjected in two lanes; 5 and 10 µg were used.
B: The transfected LSD1 is detected by an antibody raised against the Flag N-terminal peptide.

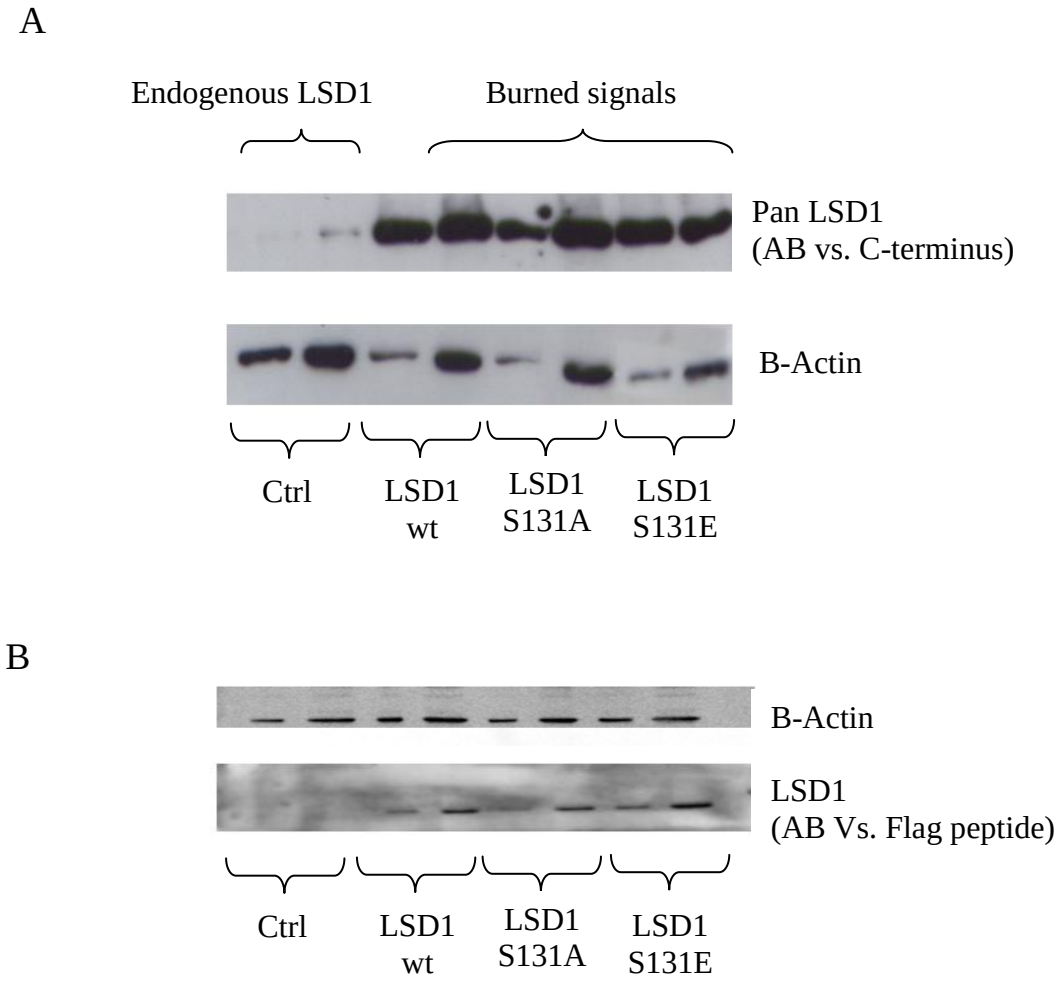

23. Nuclear localization of the LSD1 mutants

The subcellular fractionation (Nucleus vs. Cytoplasm) suggests the ability of the mutated proteins as well as the transfected LSD1 wt to have access in the nucleus (Fig. 26). Thus, both mutants of Ser131 don't affect the nuclear import and the protein solubility.

Consistent with this, a large amount of flagged LSD1 are usually recovered by cellular lysis (in comparison to the amount of LSD1 recovered by control cells), suggesting the good solubility of the protein and the absence of inclusion bodies.

Fig. 26
LSD1 mutants Ser131Ala and Ser131Glu are localized in the nucleus.

In these pictures, WBs report the mobility of LSD1 and the intake in the nucleus. The lower one reports that the majority of LSD1is in the nucleus as well as β-Lamin, a nuclear protein.

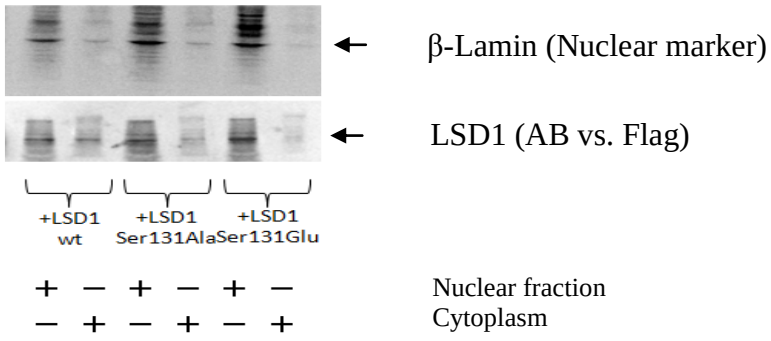

24. LSD1 overexpression alters mRNAs level of several genes, while the mutation Ser131Ala impairs the modulation of FoxA2

LSD1 activity has a great impact on gene transcription, indeed LSD1 silencing down-regulates the transcription of many genes [82]. In particular, FoxA2, EOMES, BMP2, HNF4, Sox17, Pax6 and many other mRNAs are important targets of the LSD1 action.

To understand if phosphorylation of LSD1 by CK2 can play a role in altering the expression of different genes, stable transfected lines (LSD1-wt, LSD1-Ser131Ala, and LSD1-Ser131Glu) and control line (non-transfected) have been analyzed by Real time PCR.

The primers were designed to detect three mRNAs modulated by LSD1 (Pax6, FoxA2 and BMP2), two LSD1 interacting proteins (Rcor2 and ZNF198), GAPDH and CK2β as control (Tab. 9).

mRNAs of each stable transfected clones and of control line were extracted, reverse-transcribed and amplified with specific probes.

Each signal is standardized by the values of GAPDH (*housekeeping gene*) allowing a relative quantification of each mRNA. Similarly, the relative quantifications are divided to the amount in control cell allowing a direct comparison of the effects of the transfection in each condition.

Real-time PCR discloses a big interference due to the transfection on the mRNA transcription (Tab. 10 and Graph. 3); several mRNAs are positively stimulated. For example, all the forms of LSD1 increase significantly ZNF198 (Zinc finger MYM-type protein 2) in comparison the control. This observation suggests that all the three enzymes are biologically active; indeed the alterations are similar in each transfected line.

BMP2 (Bone morphogenetic protein 2) is increased by the transfection of

LSD1wt in comparison to the control, but moreover LSD1 Ser131Ala seems particularly able to increase this mRNA. Consistent with this BMP2 is commonly modulated by LSD1 activity [82].

To note that, LSD1 Ser131Ala mutation significantly increases also Corest2 and FoxA2 mRNA level in comparison to the mutant Ser131Glu and the wild type LSD1.

In particular, FoxA2 (Forkhead box protein A2) appears as a good example of this effect; in the table 10 its transcription is significantly reduced in cell expressing LSD1 wt and LSD1 Ser131Glu, but not in cells expressing LSD1 Ser131Ala, suggesting that the mutation impairs the modulation of FoxA2 mRNA.

Tab. 9

mRNAs detected by Real-time PCR.

mRNA	Note
CK2β	CK2 subunit and internal control
GAPDH	Housekeeping gene
BMP2	transcriptional factor
FoxA2	transcriptional factor
ZNF198	transcriptional factor and LSD1 interactor
Corest2	LSD1 interactor
Pax6	transcriptional factor

Tab. 10

Relative quantification of the mRNAs in HEK293T cells transfected by LSD1 wt LSD1 Ser131Ala and LSD1 Ser131Glu in comparison to control cells (=1).

Values are means of 6 experiments. GAPDH values were fixed at 1 (100%) in each cell of this table to get comparable results, furthermore also mRNAs of non transfected HEK293T cells were fixed at 1 to get comparable data in each column (= at least p<0.05) .*

mRNA	Ctrl	LSD1 WT (fold change)		LSD1 Ser131Ala (fold change)		LSD1 Ser131Glu (fold change)	
CK2β	1	0,88	-12%	1,05	+5%	0,98	-2%
Corest2	1	0,8	-20%	1,21	+21%*	0,72	-28%*
Pax6	1	0,63	-37%	0,84	-16%	0,87	-13%
FoxA2	1	0,52	-48%*	1,28	+28%	0,56	-44%*
ZNF198	1	1,48	+48%*	2	+100%*	1,51	+51%*
Bmp2	1	1,77	+77%*	2,51	+151%*	1,96	+96%*

Graph. 3
Relative quantification of the mRNAs in HEK293T cells transfected by LSD1 wt LSD1 Ser131Ala and LSD1 Ser131Glu in comparison to control cells (100%).

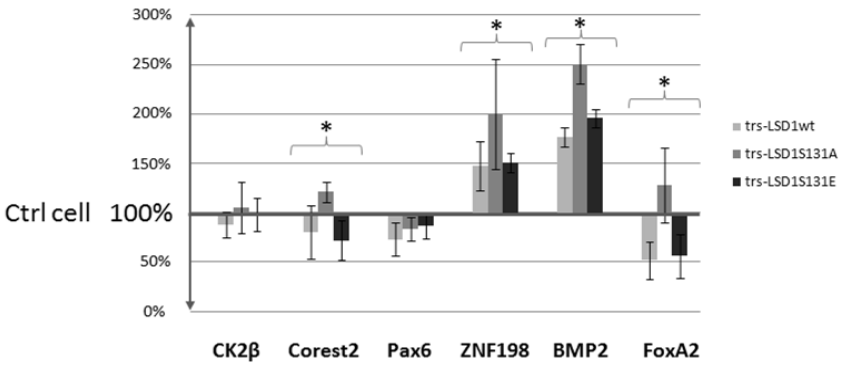

LSD1 Ser131Ala significantly enhances the transcription of several mRNAs in comparison to the other two transfected lines.

Currently, it is not clear if these increments lead to an abnormal modulation for the cell, indeed the fold-changes are not so important, but it suggests that the LSD1 Ser131 phosphorylation is involved in the modulation of several mRNAs, opening a new insight in the action of LSD1.

25. FoxA2 protein expression is reduced by LSD1 Ser131Glu mutant in comparison to LSD1 Ser131Ala

Quantitative Real-time PCR revealed that FoxA2 mRNA level is significantly reduced in cells overexpressing LSD1 and LSD1 Ser131Glu, but not affected by the mutant LSD1 Ser131Ala.

According to the quantification of the mRNAs, FoxA2 protein is reduced in cells overexpressing LSD1wt and LSD1 Ser131Glu in comparison to non transfected cells and cells expressing the mutant Ser131Ala (Fig. 27).

As reference many proteins are also checked. CK2α and α' seems unaffected by LSD1 over-expression, as well as β-actin and β-lamin.

Fig. 27
Analysis of protein expression in transfected cells.
WBs report the amount of several proteins in transfected cells. FoxA2 protein is reduced in cells overexpressing LSD1wt and LSD1 Ser131Glu in comparison to non transfected cells and cells expressing the mutant Ser131Ala. However, the other proteins are generally unaffected by LSD1 overexpression.

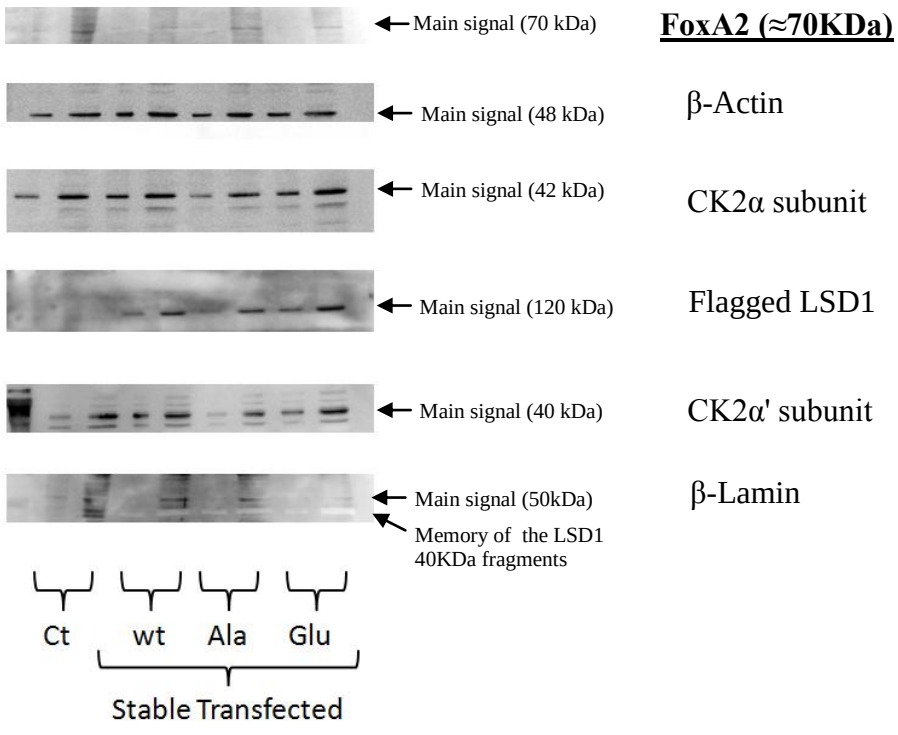

25A ZNF198 protein is elevated in LSD1 transfected cell lines

The result about ZNF198 mRNA has been verified by WB. To understand this event many other players of the CoREST complex have been analyzed. In figure 28, ZNF198, LSD1 Corest1 and HDAC2 are elevated in term of protein level in comparison to the lanes of control cells (non transfected).

All the players of the CoREST complex are increased. Now it seems predictable that this is an indirect effect of the increasing of LSD1. Indeed, the complex formation is an essential step to have a functional LSD1.

We conclude that the increase of a single protein of this complex leads to the incrementation of several interacting proteins (Fig. 29).

As useful complement, ZNF198 protein is equally elevated by both of the LSD1 mutants. The increase in mRNA concentration, showed by the mutant Ser131Ala in comparison to the Ser131Glu mutant, was due to the error bar. (see graph.3 - pag.67).

Fig. 28
Analysis of the expression of several LSD1 interacting proteins in transfected cells.

WBs report the amount of several proteins in transfected cells. ZNF198 is increased in term of mRNA, but also in term of protein. Many interactors of LSD1 are increased, suggesting the general increase of the proteins of the LSD1 complexes.

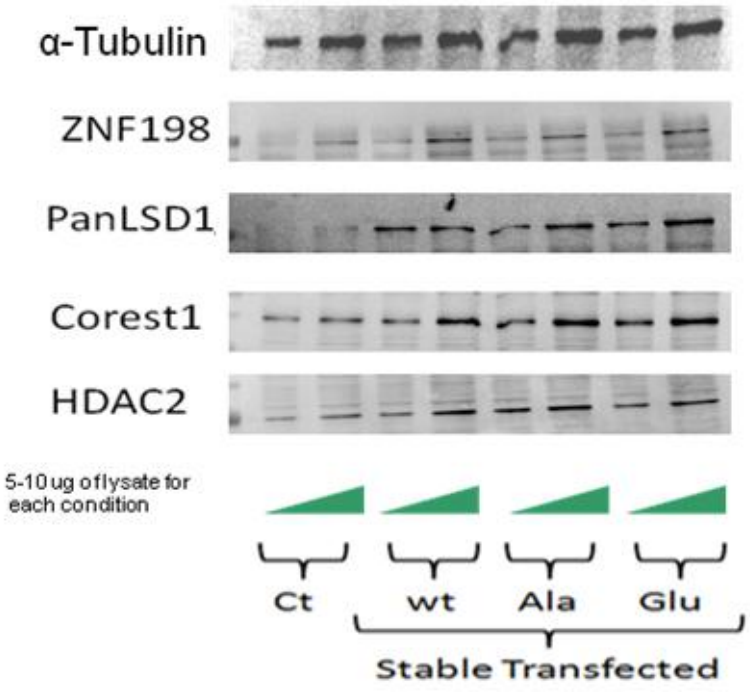

Fig. 29
General increase of LSD1 complex proteins as a consequence of LSD1 increment

In the picture are summarized the results of the WBs of the Fig.28, suggesting the general elevation of the proteins of this complex.

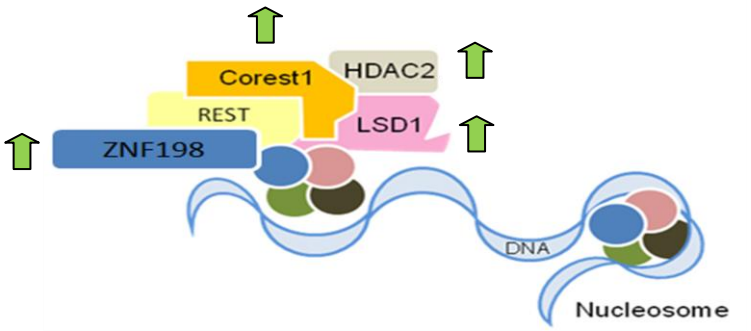

26. LSD1 complex immunoprecipitation

The kinetics of phosphorylation of LSD1 by CK2 (α-wt and α-4E mutant) didn't suggest any advantage for the mutant CK2α-4E in comparison to CK2α-wt, while the 2D experiments specifically associate LSD1 phosphorylation only to CK2 phospho mimetic mutant 4E.

To explain the preferential phosphorylation of LSD1 by the mutant CK2α4E a hypothesis of a direct interaction between LSD1 and CK2 has been formulated, involving the C-terminal domain of CK2α. Consistent with this, experiments of confocal microscopy disclose that phosphorylated CK2 overlaps the DAPI staining signal, localizing this form of CK2α near the chromatin, and thus suggesting a direct interaction of CK2 with DNA and DNA/proteins complexes during the mitosis [36].

To test a direct interaction between LSD1 and CK2 *in vivo*, we performed immunoprecipitation of LSD1 and data about the IPs complexes have been collected.

In IPs of lysates of HEK293T cells transfected with pTP6_Ko-FLAG/LSD1 vectors (Wt, Ser131Ala, Ser131Glu) (Fig. 30), a large amount of flagged LSD1 is immunoprecipitated; the interactive protein Corest1 is co-immunoprecipitated in equimolar ratio and HDAC2 is also present.

Furthermore, a small amount of CK2α is also co-immunoprecipitated. The interaction is almost undetectable in comparison with Corest1 and HDAC2 but the signal is clearly significant considering the negative control (lane IP- of Fig. 30).

Fig. 30
LSD1 complexes immunoprecipitation reveals the presence of CK2.

WBs disclose the immunoprecipitation of several players of the LSD1 complexes. A little signal about the presence of CK2 in the complex is detected. The lacking of β-actin in IPs and the burned signals in the lanes of the surnatants (flash signal detected) confirm the proper washing and the trueness of the CK2 signals.

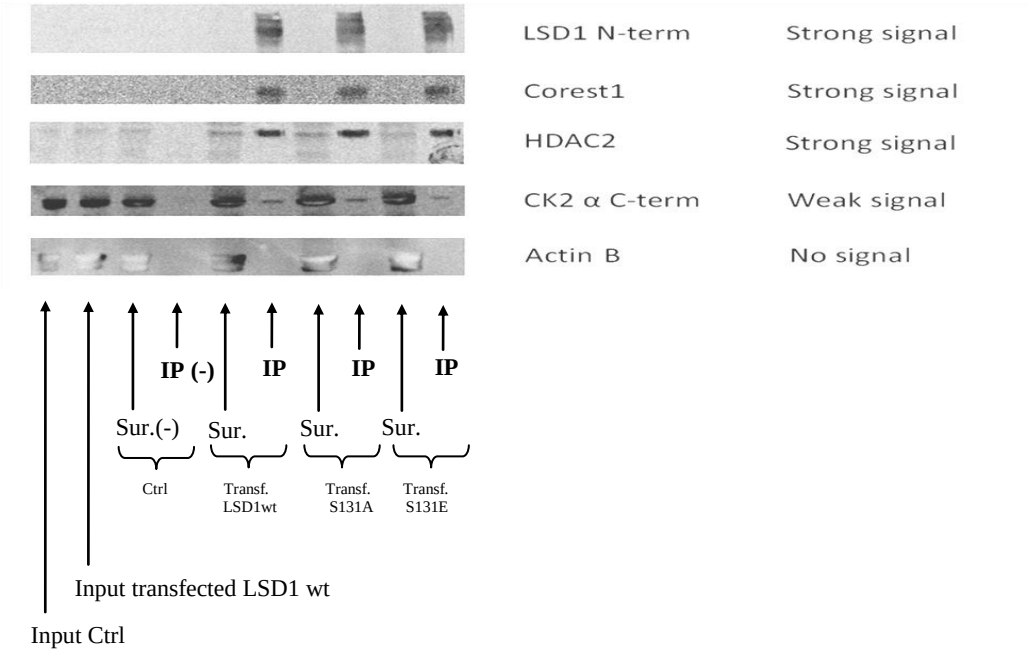

The CK2 signal becomes detectable if a large amount of LSD1 is immunoprecipitated and anyway the CK2α signal in the IP lane appears lower than its response in the surnatant (10 μg of cellular lysate), suggesting that only a minor fraction of CK2 is bound to LSD1 in a non-equimolar ratio.

We can conclude that CK2 is not a stable component of this complex, and the action of CK2 may be related to its kinase activity.

To note that, the mutated LSD1 proteins (Ser131Ala and Ser131Glu) do not significantly modify the interactions of Corest1 and HDAC2, suggesting that the binding of several important players of this complex are not regulated by Ser131 phosphorylation.

However, we cannot exclude that LSD1 phosphorylation of Ser131 plays a role as bait for other proteins not included in the test, indeed LSD1 complexes contain many proteins and just a little portion of these are checked at date (Fig. 31).

Although, we disclose that CK2 binds this complex, the identity of the protein which is responsible for this binding remains elusive.

The unumbigous identification of this protein might help to explain how the phosphorylated CK2α is recruted by the complex.

Indeed, in our hypothesys the phosphorylated C-terminal of CK2α plays an essential role in this biological process, managing the phosphorylation of LSD1.

Fig. 31
Model of the interaction between CK2 and LSD1 complex
A: Many players of this complex perform their own role by a physical interaction as well as CK2, but in contrast for this enzyme the binding seems instable. In fact, only a small amount of CK2 is co-immunoprecipitated in comparison to LSD1, Corest1 and HDAC2 (Fig.30).
B: The LSD1 mutants Ser131Ala and Ser131Glu form a complex similar to the wild type one, but many players of this complex have not been analyzed [72, 85, 86].

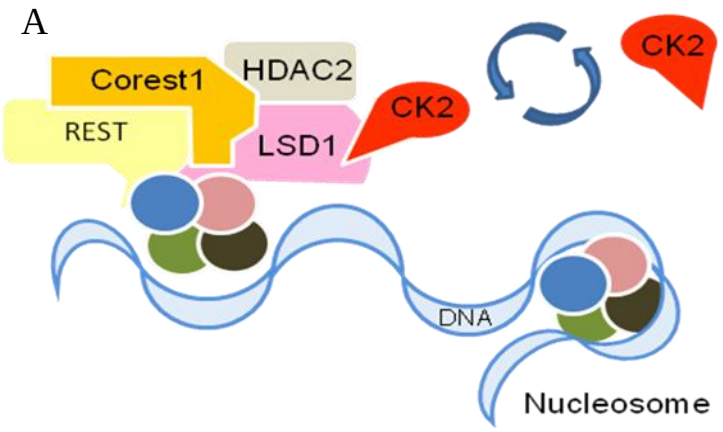

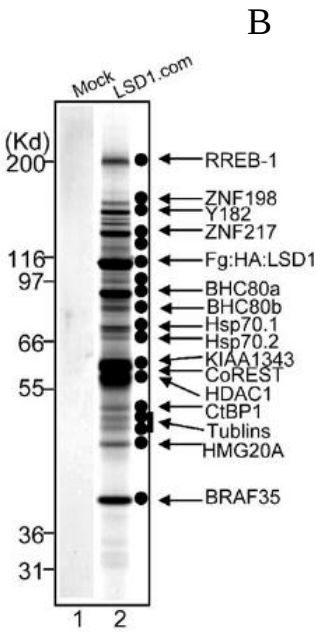

Regulation of LSD1 histone demethylase activity by its associated factors [86]
Identification of LSD1-associated proteins. The LSD1-associated factors were purified using tandem tag affinity purification (Shi et al.,2003), separated on a 4%–12% gradient SDS NUPAGE gel, and visualized by silver staining. The identities of these proteins were revealed by MS/MS and indicated on the right. [86]

26A. Phosphorylation of the immunoprecipitated complex by co-immunoprecipitated CK2

The endogenous CK2, immunoprecipitated by the flagged LSD1 is still enzymatically active, indeed radio-labeled ATP addiction to the immunoprecipitated pellet marks a single bands at about 120 KDa (Fig. 32A). WB identifies the phosphorylated band as LSD1, but also an additional lower band, suggesting that the phosphorylation induces an quite altered migration in SDS-PAGE, which is detectable in this experimental condition (SDS PAGE with 6,5% of acrylamide) (Fig. 32A).

The inhibition of the phosphorylation due to the CX4945 (30 nM), a selective inhibitor of CK2, confirms that this phosphorylation is due to CK2 (Fig. 32B) and confirms the WB results (Fig.30).

In the complex LSD1 appears as the main target of CK2, but many radio labeled bands are also identified, thus we cannot exclude that other proteins of this complex can be CK2 substrates (Fig.32B).

Fig. 32
LSD1 complex phosphorylation by a co-immunoprecipitated kinase.
A: IPs, resuspended in 50 mM Tris-HCl pH 8.0, 12 mM MgCl2, 20 μM [γ-33P]ATP (2000 cpm/pmol) in a total volume of 20 μl and incubated for 15' at 30°C are phosphorylated by an endogenous kinase. WB reveals the identity of the main phosphorylated bands as LSD1.
Furthermore WB analysis reveals that LSD1 are split in two bands. The upper one corresponds to a phosphorylated form of LSD1, while the lower one is the non-phosphorylated protein.
B: LSD1 complex phosphorylation is inhibited by the CK2 inhibitor Cx4945. In the picture, IPs are phosphorylated by an endogenous kinase. The compound Cx4945 (30 nM) reduces the phosphorylation, confirming that the co-immunoprecipitated kinase is CK2. NB: In this experiment the phosphorylated band seems a doublet, but is an effect due to an unusual degradation of this sample.

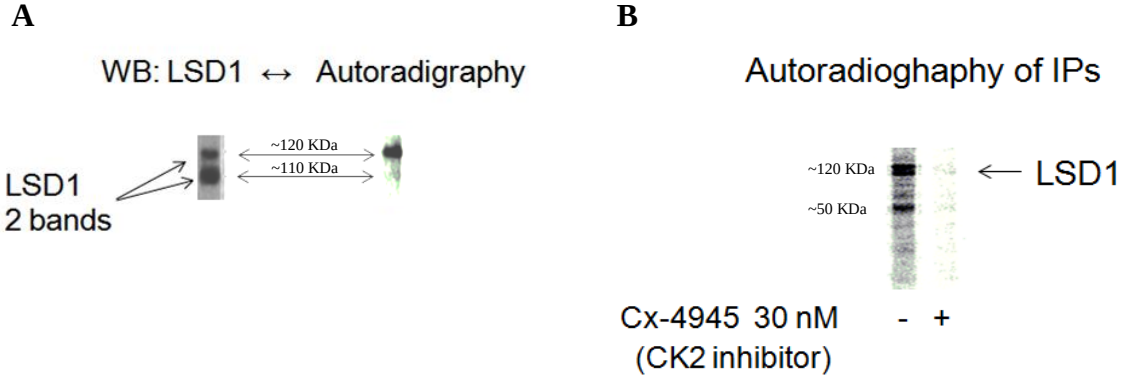

27. Co-occurrence of the LSD1 sub-domain 1-178 and CK2 C-terminus in chordata.

27A. Temporal evolution of LSD1, an additional domain is developed by chordata at the N-terminal segment.

Similar to CK2α, LSD1 has an unfolded segment. This latter however is N-terminal, while the one is C-terminal. Many hypotheses have been formulated regarding the role for this domain of LSD1, suggesting regulatory functions (e.g. sumoylation at a KxE motif [81]). The N-J phylogenetic tree reported below (Fig. 33) shows the temporal evolution of the Amine Oxidase catalytic Domain (AOD) and the "human like" N-terminal domain. LSD1 N-terminal domain appeared later than the AOD domain in the evolution, suggesting an auxiliary role for this portion of LSD1. However, it is invariably conserved in all the chordata and moreover in several deuterostomes, suggesting that this portion of LSD1 is very important for these organisms and its evolution now is "crystallized". Furthermore, it is very interesting that the CK2 consensus motifs are invariably conserved in these organisms.

Our data suggest the conservation of the AOD (AA 178-852 of sequence **O60341** KDM1A_HUMAN) in all the species analyzed. Notably, LSD1 homologues are found also in fungi and plants.

Consistent with the idea of a unique clade collecting all the LSD1 sequences; LSD4 and Juji2A (two lysine specific demethylase; isozymes of LSD1) belong to a separate clade, as well as the root protein (Fig.33).

27B. LSD1 acquires a regulatory domain in its N-terminus in chordata

Chordata (like *Homo sapiens*) show an additional domain at the N-terminus, which contains the three CK2 phosphorylation sites, generating the basis for a new regulatory network (Fig. 34).

Remarkably, we reported (Fig.6B and Fig35) a similar evolution for the Cdk1 directed phosphosites on the CK2α C-terminal sequence. Indeed, the phospho acceptor sites were developed starting from the insects, and reached the "human like sequence" only in vertebrates.

We hypothesize that CK2α C-terminus and LSD1 N-terminus domains appeared in the evolution starting from shorter enzymes (with only the catalytic domains), correlating these two enzymes into a common regulation strategy. Consistent with this, our experiments provide data about a functional relation between CK2 and LSD1, suggesting a preferential recognition of LSD1 by the phosphorylated CK2.

These phosphorylated segments of LSD1 and CK2α are not essential for the catalytic events [49 and Chapter 11], suggesting that their functions are auxiliary for the cell and probably regulatory.

We hypothesize that these two motifs allow an interaction between CK2 and LSD1 and play key role their recruitment *in vivo* in chordata (Fig. 35).

Ancient organisms don't have this regulatory network, simply by the lacking of phospho-acceptor residues (Fig. 36).

In chordata and in several deuterostomes, CK2 gains the C-terminus and the ability of co-localize to the mitotic spindle [36] and readily LSD1 gains the phosphorylable serines. Intriguingly, only these organisms showed to have bait/prey sequences, hence we can speculate that C-terminus region of CK2α is present to respond to a more complex mitosis and in general to a more complex cellular regulation. Furthermore, we speculate that other proteins are able to recognize the CK2α C-terminus, as well as LSD1, forming

"CK2α C-terminus specific" signaling cascades.

Fig. 33

Phylogenetic tree of the 22 LSD1 paralogous sequences.

In the tree is reported the evolutive history of the protein LSD1. The catalytic core is highly conserved from plant to human, while an auxiliary N-terminal segment appears with the evolution of the chordata. The internal controls: LSD4 and Juji2A (two lysine specific demethylase; isozymes of LSD1) belonged to a separate clade, as well as the root protein, suggesting that the other sequences clusterize together in a group of paralogous proteins.

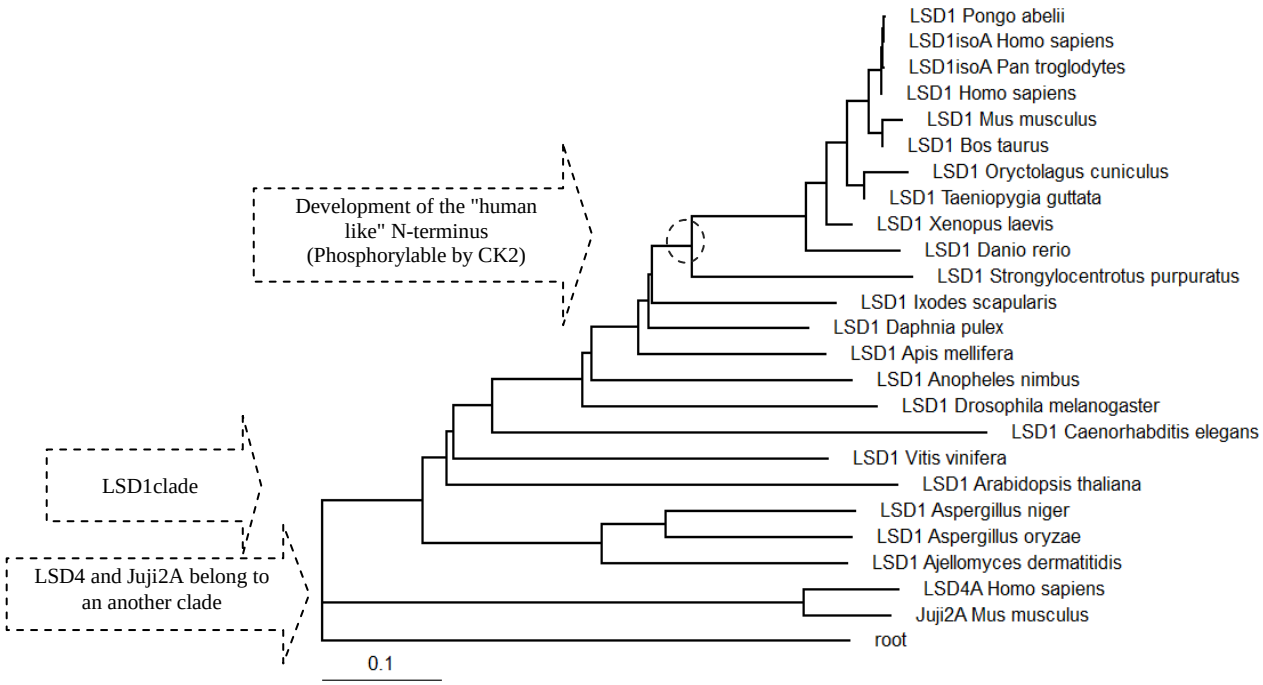

Fig. 34

Multialignment of LSD1 paralogous sequences reveals that the phosphoresidues lately appear in the evolution of LSD1

(Focus on amino acids 120-260 of the human LSD1 O60341-KDM1A_HUMAN)

In the picture, a little group of organisms have the consensus motifs for CK2 and phospho acceptor residues, while many proteins, having the AOD domain, don't show this portion of sequence.

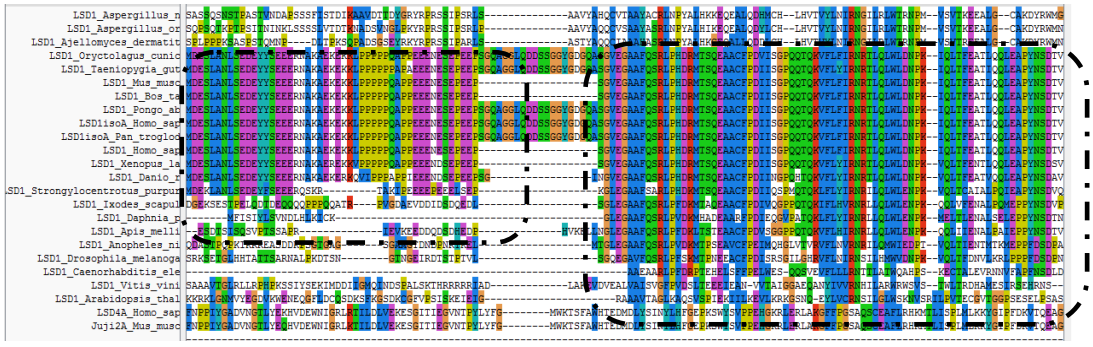

LSD1 N-terminus **Amine oxidase domain (AOD) →**

Fig. 35

Evolution of N-terminal domain of LSD1 suggests an acquired regulation through phosphorylation, while a similar evolution of the CK2α C-terminus suggests its involvement in this event, suggesting the existence of a new regulatory pathway.

A: The relationship, linking the evolution of the N-terminal segment of LSD1 and the C-terminus of CK2α, is proposed. Indeed, organisms which have a phosphorylable CK2α invariably have an LSD1 protein with CK2 consensus motifs, such as showed in the multialignments (B and C).

A

LSD1	Non-chordata	> Chordata
Amine Oxidase Domain	Conserved	Conserved
N-terminal domain 1-177	Absent	Invariably conserved
CK2 phosphorylation consensus motifs	Absent	Invariably conserved
CK2α		
CK2α Kinase Domain	Conserved	Conserved
C-terminal segment 331-392	Absent	Invariably conserved
Cdk1 phosphorylation consensus motifs	Absent	Invariably conserved

B

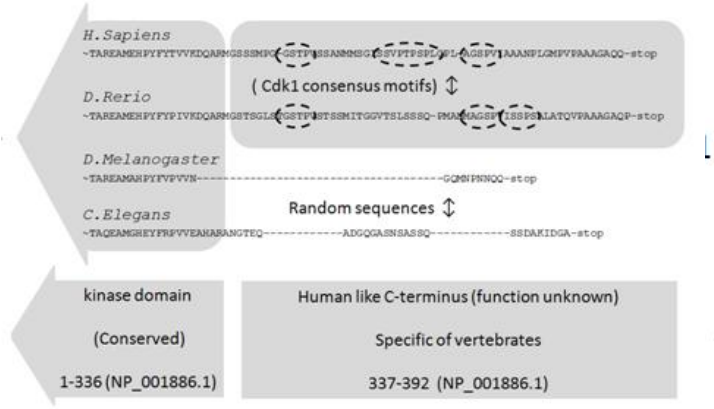

C

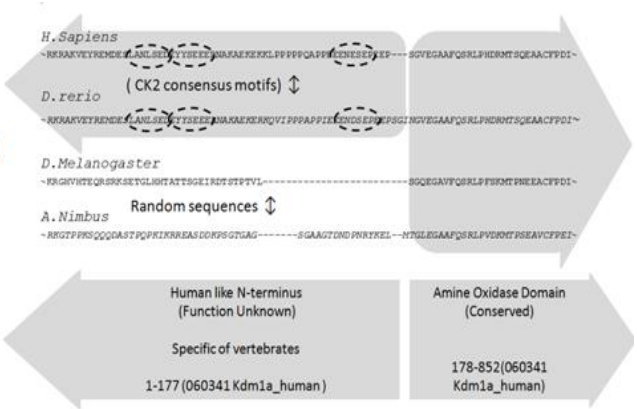

CK2α *LSD1*

Fig. 36

A regulatory pathway involving the CK2 phosphorylation and the phosphorylation of LSD1 is present in chordata but not in ancient organisms.

The data of the Fig.35 are summarized. Only a little group of Animalia, have phosphorylable CK2, phosphorylable LSD1 and the hypothesized pathway.

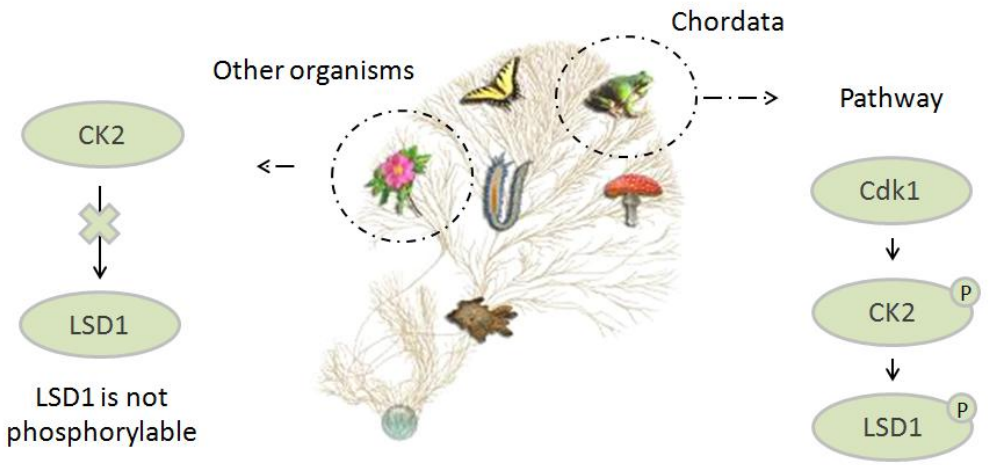

Conclusions

28. CK2α and LSD1 phosphorylations are involved in mitosis

CK2α subunit contains four proline-directed phosphorylation sites located on the C-terminal tail, which are phosphorylated in cell progressing through normal mitosis by Cyclin dependent kinase 1 (Cdk1). These phosphorylations play an important role in regulating the function of CK2, considering that cell lines with transient expression of phospho-mimic mutant CK2αT344E/T360E/S362E/S370E (CK2α4E) show "mitotic catastrophe" [35, 36].

Our data confirm this view and disclose the preferential phosphorylation of a few endogenous substrates by CK2α4E in comparison to wild type. One of these is the Lysine Specific histone Demethylase 1 (LSD1). CK2α4E is able to mime the phosphorylation of CK2α, suggesting that LSD1 is preferentially recognized by the phosphorylated form of CK2α, generating an essential step for a proper mitosis. LSD1, an important player of the epigenetic machinery, can either repress or activate target genes by catalyzing the demethylation at Lys 4 and 9 of H3 histone [56, 72], modulating gene transcription and forming functional centrosomes [69, 73]. LSD1 phosphorylation regulates the activity of LSD1, favoring the formation of "a proper" epigenetic status in the cell. Indeed, LSD1 misregulation or the misregulation of the phosphorylation of CK2 lead to chromosomic instability [35, 69, 70], through the formation of a defective mitotic spindle. We propose a new signaling cascade composed by Cdk1, CK2 and LSD1, controlling methyl marks on the histone protein H3 (Fig. 37). Moreover, the detection of CK2 in LSD1 complex suggests a new role

of CK2 as transcriptional modulator and as requirement for a proper mitosis.

Mass spectrometry analysis reveals that LSD1 is phosphorylated at Ser131, Ser137 and Ser166, in the N-terminal domain. This region of LSD1 (1-178) is not crystallographically aviable, in contrast to the AOD domains (179-852).

Molecular modeling of this region suggests a metastable structured domain, thus CK2 phosphorylation might alter this structure, allowing the fine regulation of LSD1.

Fig. 37
The regulatory pathway involving CK2, Cdk1 and LSD1.

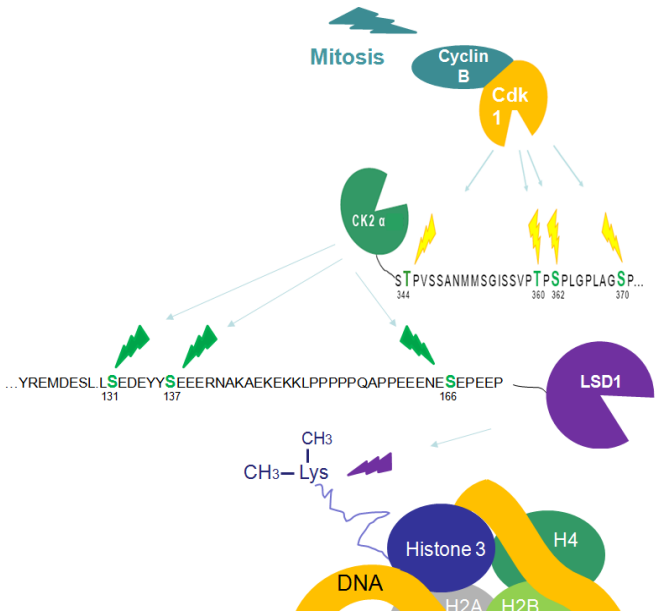

To note that only high eukaryotes like chordata have this pathway; indeed, non-chordata, plants and fungi do not have the phosphorylable domains in CK2α and in LSD1, in contrast to the catalytic domains which are invariably conserved. Taken together, these data suggest that high eukaryotes have acquired a new regulatory pathway, responding to a more complex mitosis and in general to a more complex cellular regulation.

29. LSD1 Ser 131 phosphorylation modulates the transcription

The existence *in vivo* of a functional interaction between LSD1 and CK2 is confirmed by the transfection of two mutants of LSD1, Ser131Ala and Ser131Glu, a phospho-defective and a phosphomimic mutant respectively. The expression of these mutated forms of LSD1 in HEK293T cells has allowed to confirm the key-role of Ser131 phosphorylation as regulator for LSD1 in cells.

In particular, mRNA level and the protein expression of the transcriptional factor FoxA2 is affected by the LSD1 Ser131Glu mutation, but remained unaltered when LSD1 Ser131Ala mutant is expressed, consistent with a relationship between Ser131 phosphorylation and FoxA2 transcription. This regulation is gene-specific, indeed Pax6, a common target of LSD1, does not show a similar effect.

Our data suggest that LSD1 Ser131Glu, but not the LSD1 Ser131Ala is able to repress the FoxA2 promoter in a specific manner.

Currently, data about the methylation of the histone proteins near the FoxA2 promoter are lacking, but several peculiar alterations seem predictable.

The modulation of FoxA2 corroborates the hypothesis that LSD1 phosphorylation is important during whole cell cycle (Fig. 38). In our hypothesis, a massive phosphorylation of LSD1 generates the modulation required during the mitosis, while a lower level of phosphorylation occurs in other events. Consistent with this, in addition to the Ser131 also the Ser137 and the Ser166 are phosphorylated during the mitosis, thus we hypothesize that Ser131 phosphorylation effect will be enhanced in a synergistic way by the N-terminal tri-phosphorylation, allowing a pro-mitotic regulation.

Fig. 38 Scheme of action of LSD1 phosphorylation

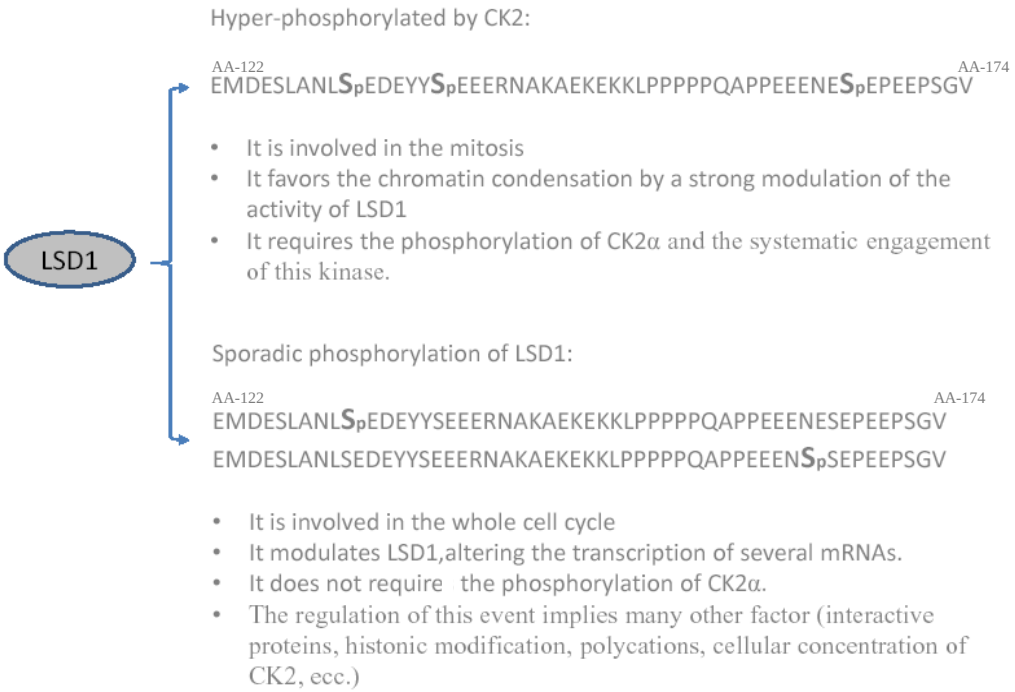

Consistently, a small amount of CK2 co-immunoprecitates during the whole cell cycle and the Ser131 phosphorylation is just sufficient to generate a phenotype.

LSD1 phosphorylation may explain many paradoxal features of this protein. Indeed, no molecular mechanism accounts for selective demethylation of H3 Lys4 or Lys9 by LSD1, two events displaying opposite biological functions [72] and the phosphorylation may provide an elegant explanation of this apparent contradiction.

As useful complement of this hypothesis, we reported the inhibition of the LSD1 phosphorylation by polycations and by the histone subfraction f1, suggesting that CK2 phosphorylates LSD1 when is located in actively transcribed region of the chromatin. In this portion of the chromatin, the

histone proteins are generally neutralized by acetylations and CK2 is not repressed. On the other hand, CK2 fails the recognition of LSD1 when it binds heterochromatin, generating an essential complement for the gene regulation.

In according to the modulation of FoxA2 by LSD1 Ser131 phosphorylation, also other mRNAs are modulated; indeed mRNAs of Corest2 and BMP2 are significantly increased by the LSD1 mutant Ser131Ala in comparison to the wt one, suggesting that LSD1 Ser131Ala is defective during the repression of the FoxA2, Corest2 and BMP2 genes.

30. LSD1 phosphorylation might be involved in the apoptosis, allowing chromatin condensation

To note that, phosphorylation of LSD1 by CK2 may be involved in another event unrelated to the mitosis, in fact in the supplementary materials S5, we describe the phosphorylation of CK2 by the pro-apoptotic kinase HIPK2 (homeo-domain interacting protein kinase 2).

This suggests that CK2α phosphorylation may have a role in the apoptotic events. In effect an essential step of the apoptosis is the chromatin condensation in the peculiar half-moon appearance. CK2 and LSD1 may have a role in this event for many aspects similar to the mitosis.

Materials and Methods

31. Phylogenetic analysis

The phylogenesis of the proteins has been performed by N-J clusterization. ClustalX2 and TreeView have been used.

The input sequences were collected by random sampling of sequences representative of almost all the species (databases: UniprotKB\Swissbank), excluding almost all hypothetical sequences of proteins (non reported in vivo).

Proteins which belong the CK2α multialignment:

NP_777060.2	NP_031814.2
NP_001886.1	NP_777061.1
NP_001100879.1	NP_001085109.1
NP_001002164.1	NP_001887.1
NP_001036956.1	NP_492811.1
NP_524918	NP_001105486.1
XP_623397	NP_179890.1
EFX82799	BAB21589
XP_785475.3	EFN62439.1
X	XP_002407929.1

Proteins, which belong the LSD1 multialignment:

NP_055828	BAC97980.1
XP_002716073.1	XP_002811361.1
XP_001272154.1	NP_001229924.1
XP_001984247.1	NP_193364.5
EFR26969.1	ABO32368.1
XP_002265069.1	XP_002646136.1
XP_612243.4	XP_002194853.1
XP_001122201.2	EFX90178.1
EGE77622.1	NP_055478.2
XP_002410496.1	XP_003724297.1
NP_001009999.1	XP_001816769.1
JAA05976.1	NP_759014.2

32. Bacterial cultures and recombinant protein purifications

Liquid bacterial cultures were performed at 37°C for the routinely uses in LB medium (10 g/l NaCl, 10 g/l Tryptone, 5 g/l Yeast extract).

Solid bacterial cultures were performed in LB medium / agar 15 g/L.

Bacterial selection was performed by the addiction of ampicillin 100 ug/ml to the medium, in according to the resistance gene carried by the plasmid.

Recombinant proteins inductions were performed by the addiction of IPTG 0.5 mM (Inalco cod.17581400) at 30°C for 4h in LB medium. Induction started at cellular 0.6 OD at 600 nm. In contrast, LSD1 expression was performed by the addiction of IPTG 0.2 mM (Inalco cod.17581400) at 37°C for 6h in LB medium.

Bacterial cell lysis was performed by sonication (PBI Sonic ruptor 400) (pulse 15" at 40% of power), 60" of incubation in ice between the pulses prevents over-heating. Six times were occurred to obtain a clear extract.
The lysis buffer was 50 mM Tris HCl pH 8.5, 7 mM B-Mercaptoethanol, protease inhibitor Cocktail- EDTA free Roche mini was added (1 pill / 40 ml of buffer).

Purification of recombinant proteins:

CK2α-wt

This protein was purified by GE-heparin Hi-trap column, collecting all cationic proteins in a gradient buffer 300mM Tris HCl pH 8.5, 0-1 M NaCl. A second step, size exclusion G75 column GE-superdex-buffer 50 mM Tris HCl pH 7.5, 0.3 M NaCl, allowed the collection of the CK2α protein at homogeneity.

CK2α-Δ1-336

This protein was purified by GE-heparin Hi-trap column, collecting all cationic proteins in a gradient buffer 50 mM Tris HCl pH 8.5, 0-1 M NaCl. This step allowed the collection of the CK2α-Δ1-336 protein with high grade of purification.

CK2 β

CK2β was purified by phosphocellulose column collecting by affinity, ATP binding proteins. A gradiented buffer 50 mM Tris HCl pH 8.5, 0-1.5 M NaCl released CK2β. A second step, size exclusion G75 column GE-superdex-buffer 50 mM Tris HCl pH 7.5, 0.3 M NaCl, allowed the collection of the CK2β protein at homogeneity.

LSD1 (Plasmid was kindly provided by Shi Y.)

His-tagged LSD1 was purified by nickel affinity column (GE-his Trap) collecting histidine rich proteins. A second step, size exclusion G200 column GE-superdex-buffer Tris HCl pH 7.5, 0.3 M NaCl, allowed the collection of the LSD1 protein with 90% of purity.

33. Protein *in vitro* phosphorylation and kinase autophosphorylation

33A. Phosphorylation of synthetic peptide CK2-tide

The synthetic peptide RRRADDSDDDDD was kindly provided by Dr. Oriano Marin. The lyophilized powder was resuspended in water and neutralized at pH 7 by 0.5 M NH_3.

The reaction is performed in buffer 50 mM Tris HCl pH 7.5, peptidic substrate 0.1 mM. 1 pmol of CK2α proteins were added to obtain an observable phosphorylation at 30°C for 10'.

The reaction (27µl for tube) was started by 3µl of radio labeled [γ-^{33}P]ATP (1000 cpm/pmol) 0.66 mM.

The reaction was stopped by spotting on a phosphocellulose paper P81 (2cm x 2cm), the synthetic peptide was immobilized by affinity on the paper and radio labeled ATP was removed by washing.

Each spotted paper was measured by scintillation (Packard 1500 tricarb liquid scintillator analyzer). Each sample was repeated twice.

33B. CK2 auto-phosphorylation

The reaction is performed in buffer Tris HCl pH 7.5 50 mM,

2 pmol of CK2α proteins (and eventually 2-4 pmol of CK2β) were added to obtain an observable phosphorylation at 30°C for 10'. 50-100-200 mM NaCl could be added in according to the specific application. The reaction (17µl for tube) was started by 3µl of radio labeled [γ-^{33}P]ATP (1000 cpm/pmol) 0.66 mM.

The reaction was stopped by the addiction of 10 µl of Laemmli buffer, and then was immediately subjected to SDS-Page 15%. The gel trapped the proteins, while the mix and the radio labeled ATP were discarded in running buffer. The dehydrated gel with radio labeled spots were imaged by a Cyclone phosphorImager system (Molecular Dynamics) and analyzed by OptiQuant software (Perkin Elmer).

34. Human cells cultures

The human neuroblastoma cell line SK-N-BE (SKNBE) and human embryonic kidney 293 transfectable cells (HEK293T) were cultured at 37°C with 5% CO_2, in DMEM (Sigma Aldrich D5671) supplemented with 10% heat inactivated FBS (Sigma Aldrich F6178) and 1% PSG (Sigma Aldrich D6784).

The cryopreservation of these cells was performed in liquid nitrogen and/or in freezer -86°C. The freezing medium was a mixture of 80% DMEM medium, 10% heat inactivated FBS and 10% DMSO.

35. Phosphorylation of cellular extracts in vitro

SKNBE cells were cultured to reach 70–80% confluency and then lysed in a MAPK buffer containing 50 mM Tris, 150 mM NaCl, 0.5% Triton X-100 with a cocktail of anti-proteases (Roche, Mannheim, Germany) and anti-phosphatases (Sigma). After protein quantification, lysates corresponding to 80 μg were incubated with radio labeled [γ-^{33}P]ATP (2000 cpm/pmol) 20 μM, 12 mM $MgCl_2$, 45 mM NaCl. After 5' of incubation at 30°C, the reaction was stopped by 4 volume of 99% ice-cold acetone.

36. Separation by bi-dimensional gel electrophoresis of cellular extracts

The phosphorylated reactions (stopped by 80% ice-cold acetone) were collected by precipitation at −80°C o/n, and spun down at 13000×g, 4°C for 30', the supernatant was removed and the pellet was air dried. The pellet was then resuspended in a buffer containing 7 M urea, 2 M thiourea, 3% 3-[(3-cholamidopropyl)dimethylammonio]-1-propanesulfonate, 1% ampholyte (3–10), and 40 mM Tris. Samples were reduced with 65 mM DTT for 1 h and then alkylated by 60 mM acrylamide for 1h. Isoelectrofocusing was performed on ReadyStrip IPG strips, 3-10NL. For the second dimension, the strips were equilibrated in 375 mM Tris (pH 8.8), 6 M urea, 20% glycerol and 2% sodium dodecyl sulphate for 30'. The strips were then run on 12% SDS-PAGE gels. Radioactive spots were imaged by a Cyclone PhosphorImager system (Molecular Dynamics) and analyzed by OptiQuant software (Perkin Elmer). After the detection, the spot were excided and

analyzed by MALDI TOF-TOF.

37. Phosphorylation of the recombinant LSD1 by CK2 *in vitro*

The reaction was performed in buffer 50 mM Tris HCl pH 7.5, 1 pmol of CK2α proteins were added to obtain an observable phosphorylation at 30°C for 10', eventually NaCl 40-230 mM could be added in according to the specific application.

The reaction usually contains 400 ng of LSD1 (≈ 4.1 pmol), while for kinetic analysis, LSD1 phosphorylation was performed at concentrations between 0 and 531.9 nM (0-1000 ng).

The effect of CK2β on the LSD1 phosphorylation was checked by the addition of CK2 β (2-4-8 pmol), while the effect of the polycations was checked either by the presence of poly-L-lysine 0-1-3 μM (Sigma Aldrich p8920) or by the addition of the calf histone sub-fraction lysine rich f1 (Sigma-Aldrich H1255) at the final volumes 0.6 and 1.2 μg/μl.

The reaction (17 μl for tube) was started by 3μl of radio labeled [γ-^{33}P]ATP (1000 cpm/pmol) 0.66 mM.

The reaction was stopped by the addiction of 10 μl of Laemmli buffer, and then was immediately subjected to SDS-PAGE 10-15%. The gel trapped the proteins, while the mix and the radio labeled ATP were discarded in running buffer. The dehydrated gel with radio labeled spots were imaged by a Cyclone phosphorImager system (Molecular Dynamics) and analyzed by OptiQuant software (Perkin Elmer).

38. Lysis of cells (WB and IP)

Cells recovery of SKNBE from culture flask was performed by Trypsin/EDTA (Sigma Aldrich T3924) and centrifugation, while HEK293T recovery by simple agitation and centrifugation. Cells were washed by PBS buffer 1 time.

Cellular pellets were lysated by RIPA Buffer (PBS buffer 1X, 0.5% Na-Deoxicolate, 1% NP40, 0.1% SDS and protease inhibitor Cocktail - EDTA free (Roche Cat. No 11873580001).

The cells were harvested in ice for 30' and cells lysis has been ensured by pipetting. Finally, the lysates were centrifuged (18000×g, 20' at 4 °C) to separate cellular debris from the "crude extract".

39. Proteins determinations by Bradford assay

900 µl of Bradford reagent (100 mg Coomassie G250, 50 ml Ethanol, 100 ml phosphoric acid 85%, 850 ml H_20) was added to 100 µl of H_2O and sample.

A standard calibration curve with BSA (bovine serum albumin) at known concentrations was prepared.

Absorbance was detected by spectrophotometer (GE Genequant100) at 595 nm and linear regression detects sample concentration.

40. SDS-PAGE and Western blotting

SDS-PAGE

A discontinuous gel, consisting of a stacking and a running gel, was prepared to separate protein in a solid phase.

Running Gel Composition: 6-15% Acrylamide (in according to the

application),

H_2O, 300 mM Tris HCl pH 8.8, 0.1% SDS, 0.05% APS (ammonium persulphate), 12 ul TEMED (N,N,N',N'-tetra-methylen-di-amine).

Stacking Gel Composition 4% Acrylamide, H_2O, 125 mM Tris HCl pH 6.8, 0.1% SDS, 0.05% APS (ammonium persulphate), and 12 µl TEMED.

The samples, consisting of phosphorylated reactions, recombinant proteins or 1- 20 µg of cellular lysates, were diluted in Laemmli buffer 3X (185 mM Tris/HCl pH 6.8, 6% SDS, 30% glycerol, 15% 2-mercaptoethanol, 0.01% pironin y).

The electrophoresis was performed in 25 mM Tris/HCl, 19.2 mM glycine, 0.1% SDS, at constant amperage of 25 mA.

After running, proteins were stained by Commassie R/Ethanol/Acetic acid or transferred onto PVDF membrane.

Western Blotting (WB)

1-20 µg of proteins were transferred to a PVDF membrane Immobilon-P (Millipore IPVH00010) at 60V, for 30-90' in cold buffer (CAPs 2.02 g/L, methanol 1%, NaOH pH 10, 4-8°C).

In order to saturate non specific binding sites, the membrane was incubated in methanol 99% for 30" and dried for 2-4 h a r.t. Dried membrane was washed in H_2O for 5' and then for 30' in TBS-1% BSA (50 mM Tris/HCl, 0.15 M NaCl, pH 7.5, 1% BSA).

The membrane ready for the immuno-staining was incubated from 2 hours to O/N with the primary antibodies, appropriately diluted in TBS 1% BSA (see below). Several antibodies require over-night incubation.

The membranes were washed 3 times for 10' in TBS. Then, the membrane was incubated for 20' in presence of the secondary antibody conjugated with peroxides HRP (Perkin Elmer NEF812001EA; anti-mouse or anti-rabbit) diluted (1/4000) in TBS 1% BSA.

Following the final wash, the membranes were incubated in luminol/H_2O_2 for several seconds and the detection of the antibody complex was performed by the Kodak Image Station 4000MM-Pro.

The following primary antibodies were used:

Code	Company	Target	Dilution
X	House made	CK2α	1/1000
A300215	Bethyl	Pan-LSD1	1/9000
F3165	Sigma-Aldrich	Flag-LSD1	1/5000
A301710	Bethyl	ZNF198	1/1000
07455	Millipore	Corest1	1/1000
s9959	Santa Cruz	HDAC2	1/1000
S8035	Santa Cruz	Tubulin-α	1/5000
C0603	Santa Cruz	B-Actin	1/5000
Ab10474	Abcam	CK2α'	1/1000
AF2400	R&D systems	FoxA2	1/1000
F0208	Santa Cruz	B-Lamin	1/1000

41. Dephosphorylation of LSD1 by calf intestinal phosphatase

Lysates of Neuroblastoma SKNBE Cells (10 μg) was de-phosphorylated by 100 U of Calf Intestinal Phosphatase (CIP) for 1h at 30°C and immunoblotted. For a direct comparison, an equal amount of lysate was treated in absence of the CIP enzyme for 1h at 30°C and furthermore an another sample was incubated in ice.

SDS-PAGE and WB have been performed and the molecular weight was detected by an antibody. Notably, a low concentration SDS-PAGE gel has been used (polyacrylamide 6%), resolving proteins with high molecular weights.

42. Mutagenesis of pTP6_Ko-FLAG/LSD1wt to Ser131Ala and Ser131Glu

pTP6_Ko-FLAG/LSD1wt kindly provided by Dr. A. Adamo of the CMRB institute of Barcelona.

Mutagenic primers Ala131for, Ala131Rev, Ala137for, Ala137Rev were purchased by Sigma Aldrich and mutagenic primers Glu131for, Glu131Rev, Glu137for, Glu137Rev were purchased by Invitrogen Custom synthesis.

Quick change PCRs were performer in according to the protocol proposed by Stratagene for the kit (QuickChange® Site-Directed Mutagenesis Kit).

1-Reaction:

- 5 µl of 10× reaction buffer
- 50 ng of dsDNA template
- 125 ng of oligonucleotide primer #1
- 125 ng of oligonucleotide primer #2
- 1 µl of dNTP mix
- ddH2O to a final volume of 50 µl
- Then add 1µl of *PfuTurbo* DNA polymerase (2.5 U/µl)

2-PCR

Segment	Cycles	Temperature	Time
1	1	95°C	30"
2	18	95°C	30"
		55°C	1'
		68°C	10'

3-Digestion of the parental DNA and Bacterial Transformation

- Add 1µl of the *Dpn* I restriction enzyme (10 U/µl) directly to each amplification and immediately incubate each reaction at 37°C for 1 hour
- Transfer 1 and 10 µl of the *Dpn* I-treated DNA from each sample to separate aliquots of the supercompetent cells 50µl.
- Swirl the transformation reactions gently to mix and incubate the reactions on ice for 30'.

- Heat pulse the transformation reactions for 45 seconds at 42°C and then
- Place the reactions on ice for 2' (n*ote: This heat pulse has been optimized for transformation in 14-ml BD Falcon polypropylene round-bottom tubes).*

4 couples of primers were used:

a. Ser131Glu

Ser131Glu1° for:

5'-gagagatggatgaaagcttggccaacctcg-3'

Ser131Glu1° rev:

5'-ctcatcttcttcgaggttggccaagctttc-3'

b. Ser131Ala

Ser131Ala1° for:

5'-gatggatgaaagcttggccaacctcgcagaagatgag-3'

Ser131Ala1° rev:

5'-ctcatcttctgcgaggttggccaagctttcatccatc-3'

c. Ser137Glu

Ser137Glu2° for:

5'-ggccaacctctcagaagatgagtattatga-3'

Ser137Glu2° rev:

5'-ctctcttcttcttcataatactcatcttct-3'

d. Ser137Ala

Ser137Ala2° for:

5'-ggccaacctctcagaagatgagtattatgcagaagaagagag-3'

Ser137Ala2° rev:

5'-ctctcttcttctgcataatactcatcttctgagaggttggcc-3'

Quick change PCRs failed anytime, and an alternative strategy has been performed by molecular cloning.

The mutagenic cloning were performed by a first mutagenic step through PCR, and then by the transfer (restriction and ligation) of the mutations in the final vector pTP6_Ko-FLAG/LSD1.

Mutagenic PCRs

Segment	Cycles	Temperature	Time
1	1	95°C	30 seconds
2	25	95°C	30"
		53°C	30"
		72°C	60"
3	1	72°C	5'

Primers for the mutation Ser131Glu:

Ser131Glu1° for:

5'-gagagatggatgaaagcttggccaacctcg-3'

LSD1Exon8rev

5'-tttctctttaggaacagcttg-3'

Primer for the mutation Ser131Ala:

Ser131Ala1° for:

5'-gatggatgaaagcttggccaacctcgcagaagatgag-3'

LSD1Exon8rev

5'-tttctctttaggaacagcttg-3'

High fidelity Fusion Polymerase (NEB Cat. No M0530L) and 5 ng of the vectors pTP6_Ko-FLAG/LSD1wt was used in each reaction.

About 1µg of PCR products were obtained by gel extraction (QIAquick Gel Extraction Kit Cat. No: 28704) from the reaction Ser131Ala and Ser131Glu.

DNAs were restricted by the *HINDIII endonuclease* (NEB Cat. No R0104L) (1Unit) in Buffer3 (NEB) for 2 hours at 37°C, the purified fragment was obtained and ligated by T4 ligase (NEB Cat. No M0202L) into the *HINDIII* pre-digested vector pGEMt-EASY LSD1 at 16°C O/N.

Then, the mutated gene was cutted by the *BSPEI* and *AGEI* endonucleases, producing a fragment containing either by the mutation Ser131Ala or Ser131Glu. These fragments (purified by gel extractions) were ligated into two vectors pTP6_Ko-FLAG/LSD1 (digested with the same enzymes). The complete sequencing of the mutated genes (S131E and S131A) confirmed the mutations.

43. Transfection of HEK293T cells

Two day before, $1.5x10^6$ HEK293T were seeded in 10 cm dish. The exogenous DNA represented by 5µg of the eukaryotic vectors pTP6_Ko-FLAG/LSD1wt, pTP6_Ko-FLAG/LSD1Ser131Ala, and pTP6_Ko-FLAG/LSD1Ser131Glu were linearized by the restriction enzyme ScaI (NEB Cat. No R0122L) in Buffer3 (NEB) O/N at 37°C.

After this stage, each DNA has been incubated with 10 µl of transfection reagent FuGENE6 (ROCHE Cat. No 11815091001) at r.t. for 5' and then with 500 µl of OptiMEM medium without FBS for 25'.

Each mix was added to the dish (confluency 60-80%). The culture was incubated for 24 hours, at 37°C, 5% CO_2, and then the transfection medium was replaced by fresh medium.

Selection of transfected cells was carried out by three treatments of puromycin (Sigma Aldrich Cat. No F8833); the treatments were carried out by increasing concentrations (1 day 0.1 µg/ml, 2 days 0.3 µg/ml, 2 days 1 µg/ml) .

The expression of the exogenous LSD1 was detected by WB against the N-terminal Flag (*ϟDYKDDDDKϟ*) and by another epitope. Stable expression was assumed after 10 day, starting from the DNA transfection.

44. mRNAs extraction and Real time PCR

Approximately 400 µl of cellular pellet, obtained by scraping and centrifugation (250g, 5', 25 °C) were dissolved in 1 ml Trizol (GibcoBRL/Life Technologies). Then, 0.2 ml of chloroform was added and a briefly mixing was done. The suspension was centrifuged at 15 000x*g* for 10' at 4°C. The upper phase (solvent: chloroform) was recovered. RNA precipitation is performed by the addition of an equal amount of isopropanol 100%, incubation in ice and centrifugation allow to observe a little pellet on the bottom of the eppendorf. The pellet was washed by 750 ul of Ethanol/DEPC water 3:1 (Ethanol 75%), centrifugated, recovered and dried at room temperature in top-less eppendorf. Finally, the air dried pellet was dissolved in 50 µl of DEPC water.

RNA was quantify by NanoDrop technology (NanoDrop 1000 Spectro-photometer Thermofisher scientific) and stored at -80°C.

44A. mRNAs reverse-transcription

1 ug of mRNA of each sample or treatment was converted to cDNA by reverse-transcription in according to proposed protocol. (Cloned AMV first strand synthesis kit-Invitrogen Life technology).

44B. Quantification by Realtime PCR

mRNA levels were quantified by real-time PCR using SYBR Green and are represented relative to *GAPDH* (glyceraldehyde 3-phosphate dehydrogenase) expression. For a direct comparison of the cell lines, mRNA levels are divided to the amount of the specific mRNA in the control cell (value = 1), thus each value is a ratio.

Each reaction contains 0,1 µl of cDNA, 1 µl of forward primer (10 µM), 1 µl of reverse primer (10 µM), 10 µl of Sybr-green master mix (Life technology) and 7.9 µl of H_2O.

The sequences of oligonucleotides used for quantitative PCR (qPCR) are listed below:

BMP2-F	5′-CCAACACTGTGCGCAGCTT-3′
BMP2-R	5′-CCCACTCGTTTCTGGTAGTTCTTC-3′
PAX6-F	5′-GCTTCACCATGGCAAATAACC-3′
PAX6-R	5′-GGCAGCATGCAGGAGTATGA-3′
FOX2-F	5′-CTGAAGCCGGAACACCACTAC-3′
FOX2-R	5′-CGAGGACATGAGGTTGTTGATG-3′
RCO2-F	5'-TCCCTGACGAGTGGACAGTAGAG-3'
RCO2-R	5'-TGCCATGGAAGCCAAA-3'
ZNF1-F	5'-TGCTGTCAAAGTTGTGTCAGTGA-3'
ZNF1-R	5'-CCTCCTTCAGGAAGCTTGGA-3'
CK2B-F	5'-ACTGTGAGAACCAGCCAATGC-3'
CK2B-R	5'-ATGGCTTCACCTGGGATGTC-3'
GAP-F	5'-CCAGCCGAGCCACATCGCT-3'
GAP-R	5'-ATGAGCCCAGCCTTCTCCAT-3'

45. Nuclear and cytoplasmic subfractionation

The buffer 10 mM HEPES pH 7.9, 1.5 mM $MgCl_2$, 10 mM KCl, 0.5 mM DTT, 0.01% NP40 (500µl) was added to a large petri dish (125cm^2) on ice and a thorough scraping was performed. Cells have been incubated in ice for 10' and then centrifuged at 4°C at 3000 rpm for 10'. The supernatant was the cytoplasmatic fraction. The pellet was resuspended in 500 µl of RIPA buffer and homogenized by Dounce. After 30' of incubation, the mix was centrifuged at 18000xg for 20' at 4°C. The clear extract has been considered as the nuclear extract.

46. Immunoprecipitation

500 µg of protein lysates in RIPA buffer (PBS buffer 1X, 0.5% Na-Deoxicolate, 1% NP40, 0.1% SDS, Protease inhibitor Cocktail - EDTA free Roche mini) were incubated for 4 h at 4°C in agitation, then 15µl of anti-FLAG Ig beads/PBS1:1 (Sigma Aldrich A2220) were added to the mix. The binding has been performed for 30' at 4°C by agitation.

Beads were collected by centrifugation at 1000xg for 3' at 4°C, while the surnatant were placed in a new tube.

Beads were washed 3 times in 1 ml of PBS (5' rocking agitation) and then spun down by centrifugation at 1000xg for 3' at 4°C.

The final pellet of beads was suspended in non-reducing Laemmli buffer and subjected in SDS-PAGE to separate proteins. Heating at 95°C for 5' of the pellet allowed the complete rescuing of the immunoprecipitated proteins.

Finally, WBs were performed to detect co-immunoprecipitates proteins.

Supplementary materials

S1. Expression and purification of recombinant CK2α subunit and its mutated forms Δ1-336 and CK2α-4E

- CK2α-Δ1-336

Theorical MW (Protparam prediction): 40 KDa (≈)

Theorical pI: 7.0

The induction and the purification of CK2α-Δ1-336 were done and a good yield of purification has been reached by Heparin Anionic Exchanger, in the figure 39 are reported all the steps of the purification.

Fig. 39 Purification of CK2α-Δ1-336

In this coomassie stained SDS-PAGE, they are reported all the steps of the purification. The white arrows show the final result of the purification of CK2α-Δ1-336.

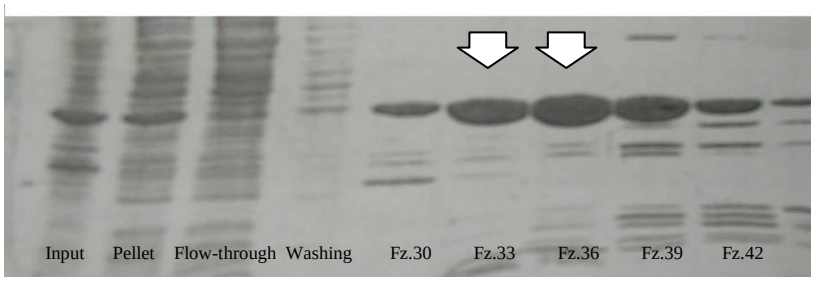

The fractions 33-36 have been dialyzed with a semi-permeable membrane in 25mM Tris-HCl buffer pH 7.5, Glycerol 50%.

3 ml of CK2α-Δ1-336 at concentration of 2.35mg/ml has been obtained.

- CK2α-wt

Theorical MW (Protparam prediction): 45 KDa (≈)

Theorical pI: 7.3

CK2α-wt purification is reported in the following image (Fig. 40), furthermore the induction and the purification by Heparin Anionic Exchanger are observable.

Fig. 40 Purification of CK2α-wt

In this coomassie stained SDS-PAGE, they are reported several steps of the purification. The white arrows show the intermediate of purification of CK2α-wt.

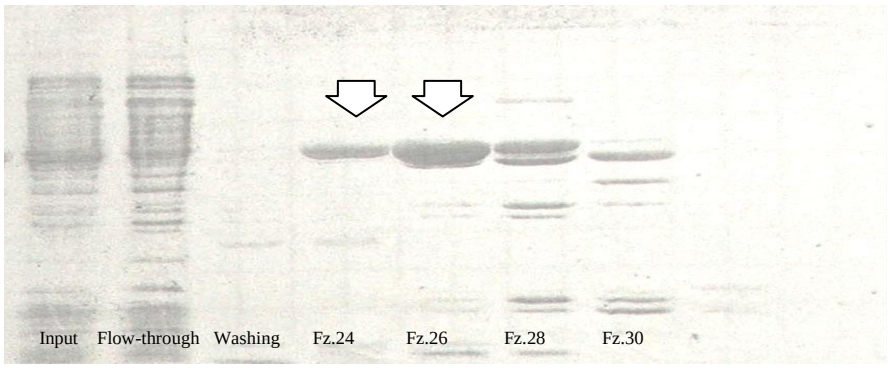

The fractions 24-26 have been loaded in the G75 superdex 26/60 a size exclusion chromatographic column to separate CK2α-wt from other undesirable proteins. In the figure 41 is reported the final fractionation of CK2α-wt. The undesired and spontaneous degradation of CK2α-wt (fractions >84) is also observable. Size exclusion allowed to enrich the full-length protein and discard the degradation product 1-330(≈), unfortunately during this process a big amount of CK2α-wt were lost. The yield of the process was less than 50%.

Fig. 41 Purification of CK2α-wt

In these two coomassie stained SDS-PAGEs, they are reported several steps of the purification. The white arrows show final result of the purification of CK2α-wt.

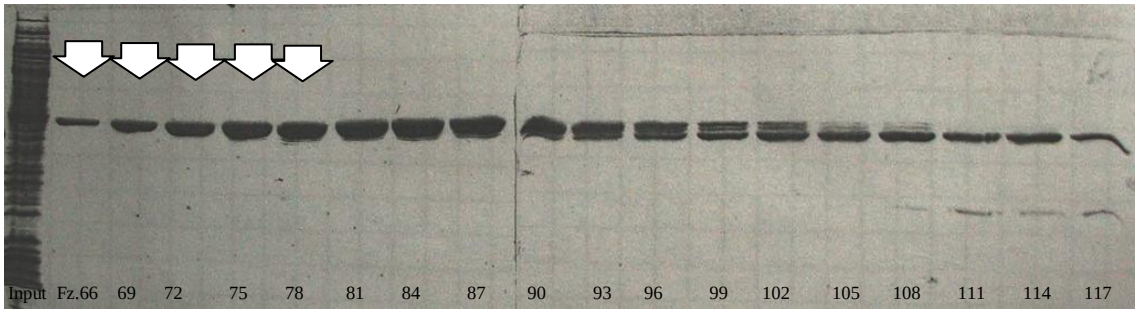

The fractions 66-78 have been concentrated by Amicon membrane (Cut-off 10 KDa and 0.2 ml of CK2α-wt at concentration 10 mg/ml has been obtained.

- CK2α-4E

Theorical MW (Protparam prediction): 45 KDa
(Observed: 50 KDa)

Theorical pI: 7.3

CK2α-4E protein was kindly provided by Dr. Lolli G. Expression and purification were performed, following a protocol quite similar respect to CK2α-wt. CK2α-4E is a tetra mutant form of CK2α with the four substitutions, Thr344Glu, Thr360Glu, Ser360 and Ser370Glu.
In the image (Fig. 42) are reported the final results of the three purifications (CK2α-wt, CK2α4E and CK2α-Δ1-336) analyzed by SDS-PAGE (commassie stained).

Fig. 42 Summary of the three forms of CK2α obtained

In this coomassie stained SDS-PAGE, purified forms of CK2α: Wt, mutant 4E, c-terminal truncated 1-336 form, respectively lane 1, 2 and 3.

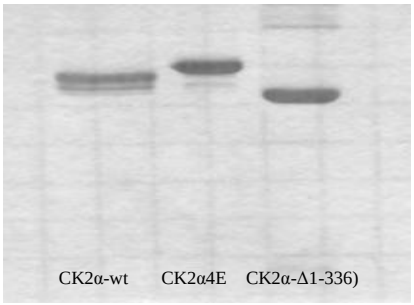

In the first lane is reported the commassie staining of CK2α-wt and an undesired and spontaneous degradation, probably the ratio between full-length forms vs. degraded form is 90%. Also CK2α4E undergoes to a spontaneous degradation, but in this case, it seems a little percentage. The third lane represents CK2α-Δ1-336. It is the stable form of CK2 and it has a very clear profile. The three enzymes have good and comparable yield of purity.

S2. Stimulatory effect of Poly-L-lysine in CK2α autophosphorylation

To better understand the CK2α-4E autophosphorylation in presence of CK2β and in particular to shed light on the role of CK2 α-β interaction in this process, we performed an experiment of stimulation by Poly-L-lysine (Fig. 43).

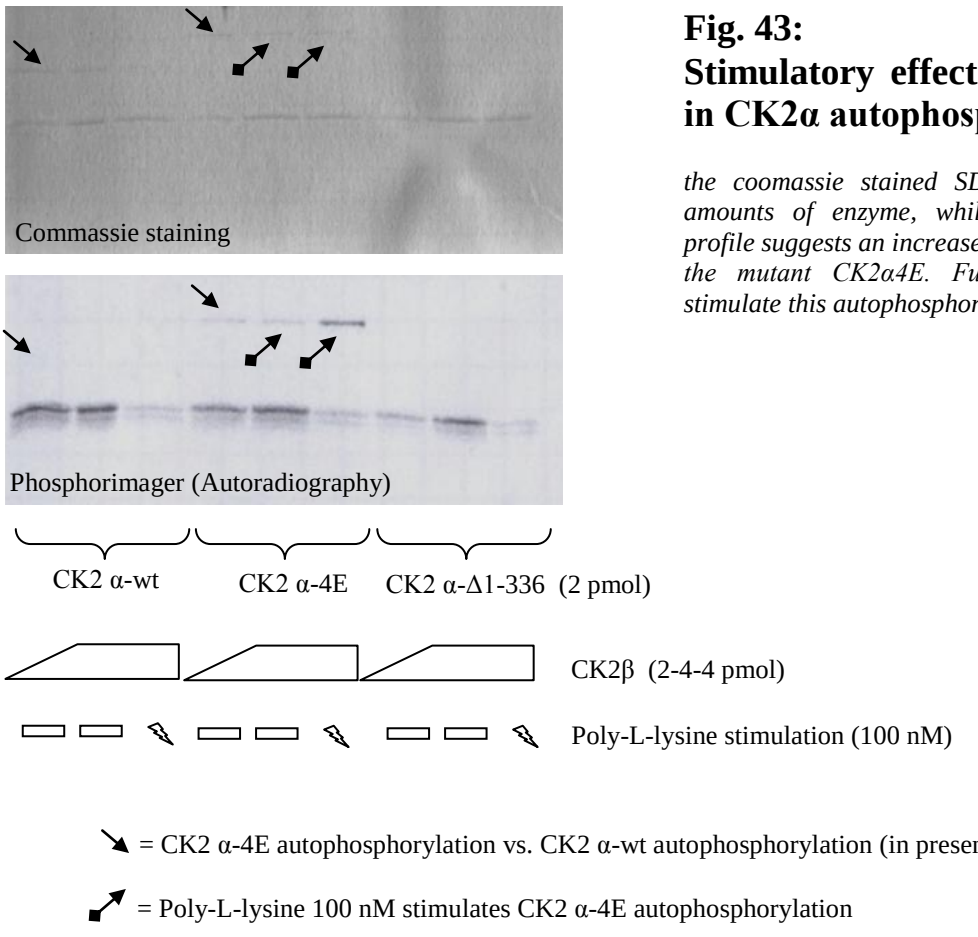

Fig. 43:
Stimulatory effect of Poly-L-lysine in CK2α autophosphorylation

the coomassie stained SDS-PAGE shows similar amounts of enzyme, while the autoradiographic profile suggests an increased autophosphorylation in the mutant CK2α4E. Furthermore poly-L-lysine stimulate this autophosphorylation.

100 nM poly-L-lysine stimulates significatively CK2α-4E autophosphorylation, while it represses CK2β autophosphorylation.
Strong basic proteins (e.g. histone proteins) might exert a similar effect

on the autophosphorylation, further suggesting the occurrence of Ser357 autophosphorylation *in vivo*. Indeed, CK2 phosphorylation by Cyclin dependent kinase 1 (Cdk1) leads to the accumulation of CK2 in the mitotic spindle, subsequently CK2 conjugated to histone particles generates an "hot spot" of activity due to the interaction.

In summary, the mutant CK2α-4E (or the phosphorylated CK2α *in vivo*) gains a good putative autophosphorylation site. The Ser357 could be quickly phosphorylated when supported by the mutated residues (or phospho-residues) and by the high concentration of histone proteins.

S3: Mass spectrometry characterization of the CK2 phosphorylation profiles

2D separation of a total soluble cellular extracts derived from human neuroblastoma cells (SK-N-BE) phosphorylated by either CK2α4E or CK2αwt reveals many phosphorylated spots. Nine radio labeled spots were excided and analyzed by mass spectrometry. The image discloses the position (Fig. 44) of the spots and the table (Tab. S3) the identity of the phosphorylated proteins.

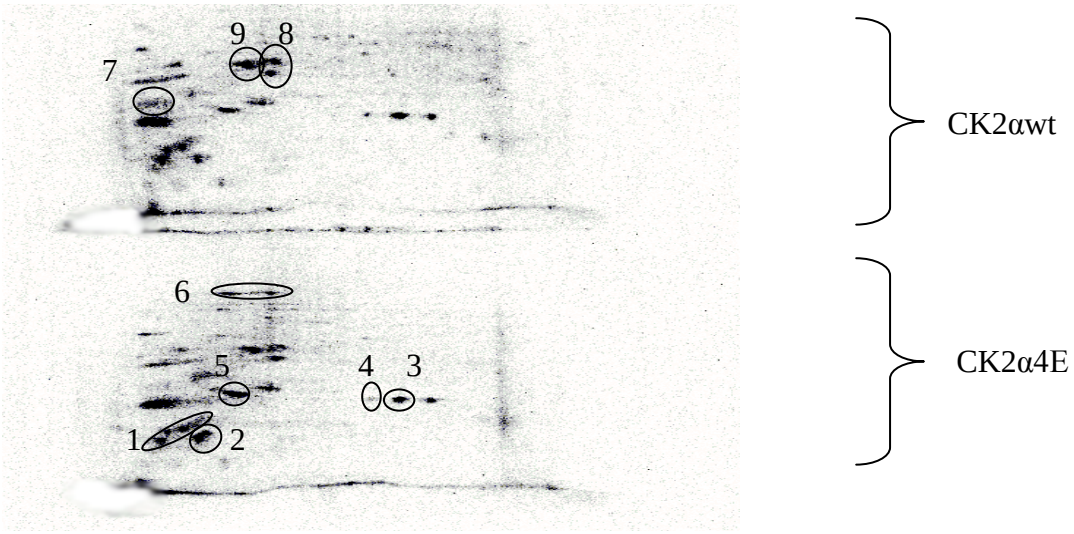

SPOT 01 prot_acc	prot_desc	score	mass	matches
GBLP_BOVIN	Guanine nucleotide-binding protein subunit beta-2-like 1 OS=Bos taurus GN=GNB2L1 PE=2 SV=3	510	35623	30
ETFA_HUMAN	Electron transfer flavoprotein subunit alpha, mitochondrial OS=Homo sapiens GN=ETFA PE=1 SV=1	330	35484	11
SFRS1_BOVIN	Splicing factor, arginine/serine-rich 1 OS=Bos taurus GN=SFRS1 PE=2 SV=1	238	27870	10
RS3_BOVIN	40S ribosomal protein S3 OS=Bos taurus GN=RPS3 PE=2 SV=1	227	26885	9
EFTS_HUMAN	Elongation factor Ts, mitochondrial OS=Homo sapiens GN=TSFM PE=1 SV=2	225	35794	10
ARPC2_BOVIN	Actin-related protein 2/3 complex subunit 2 OS=Bos taurus GN=ARPC2 PE=1 SV=1	195	34470	8
CDK1_BOVIN	Cell division protein kinase 1 OS=Bos taurus GN=CDK1 PE=2 SV=2	192	34075	9
PIPNB_BOVIN	Phosphatidylinositol transfer protein beta isoform OS=Bos taurus GN=PITPNB PE=1 SV=3	143	31874	4
ESTD_HUMAN	S-formylglutathione hydrolase OS=Homo sapiens GN=ESD PE=1 SV=2	141	32082	9
P5CR1_HUMAN	Pyrroline-5-carboxylate reductase 1, mitochondrial OS=Homo sapiens GN=PYCR1 PE=1 SV=2	139	33624	6
CASP3_HUMAN	Caspase-3 OS=Homo sapiens GN=CASP3 PE=1 SV=2	131	32156	5
ISOC1_BOVIN	Isochorismatase domain-containing protein 1 OS=Bos taurus GN=ISOC1 PE=2 SV=1	128	32450	4
RM01_HUMAN	39S ribosomal protein L1, mitochondrial OS=Homo sapiens GN=MRPL1 PE=1 SV=2	119	37170	6
GNPI1_HUMAN	Glucosamine-6-phosphate isomerase 1 OS=Homo sapiens GN=GNPDA1 PE=1 SV=1	117	32861	5

VDAC1_BOVIN	Voltage-dependent anion-selective channel protein 1 OS=Bos taurus GN=VDAC1 PE=1 SV=3	107	30864	4
VATE1_BOVIN	V-type proton ATPase subunit E 1 OS=Bos taurus GN=ATP6V1E1 PE=2 SV=1	102	26194	4
TRYP_PIG	Trypsin OS=Sus scrofa PE=1 SV=1	102	25246	7
HCDH_HUMAN	Hydroxyacyl-coenzyme A dehydrogenase, mitochondrial OS=Homo sapiens GN=HADH PE=1 SV=2	93	34327	4
SFR2B_HUMAN	Splicing factor, arginine/serine-rich 2B OS=Homo sapiens GN=SFRS2B PE=1 SV=1	82	32410	3
PHB2_HUMAN	Prohibitin-2 OS=Homo sapiens GN=PHB2 PE=1 SV=2	74	33276	2
VDAC2_BOVIN	Voltage-dependent anion-selective channel protein 2 OS=Bos taurus GN=VDAC2 PE=2 SV=2	69	32239	3
DECR_HUMAN	2,4-dienoyl-CoA reductase, mitochondrial OS=Homo sapiens GN=DECR1 PE=1 SV=1	65	36400	2
TATD1_HUMAN	Putative deoxyribonuclease TATDN1 OS=Homo sapiens GN=TATDN1 PE=1 SV=2	54	34290	2

SPOT 02

prot_acc	prot_desc	score	mass	matches
PSA1_HUMAN	Proteasome subunit alpha type-1 OS=Homo sapiens GN=PSMA1 PE=1 SV=1	466	29892	31
SFRS1_BOVIN	Splicing factor, arginine/serine-rich 1 OS=Bos taurus GN=SFRS1 PE=2 SV=1	288	27870	11
PGES2_HUMAN	Prostaglandin E synthase 2 OS=Homo sapiens GN=PTGES2 PE=1 SV=1	191	42130	7
NIT2_HUMAN	Omega-amidase NIT2 OS=Homo sapiens GN=NIT2 PE=1 SV=1	175	31086	7
CDK1_BOVIN	Cell division protein kinase 1 OS=Bos taurus GN=CDK1 PE=2 SV=2	163	34075	6
PROSC_HUMAN	Proline synthase co-transcribed bacterial homolog protein OS=Homo sapiens GN=PROSC PE=1 SV=1	149	30680	7
PSA4_BOVIN	Proteasome subunit alpha type-4 OS=Bos taurus GN=PSMA4 PE=1 SV=1	148	29820	8
PNPH_HUMAN	Purine nucleoside phosphorylase OS=Homo sapiens GN=PNP PE=1 SV=2	143	32381	8
EXOS6_HUMAN	Exosome complex exonuclease MTR3 OS=Homo sapiens GN=EXOSC6 PE=1 SV=1	135	28573	6
SFRS2_BOVIN	Splicing factor, arginine/serine-rich 2 OS=Bos taurus GN=SFRS2 PE=2 SV=3	133	25461	6
VATE1_BOVIN	V-type proton ATPase subunit E 1 OS=Bos taurus GN=ATP6V1E1 PE=2 SV=1	123	26194	4
TRYP_PIG	Trypsin OS=Sus scrofa PE=1 SV=1	111	25246	9
UCK2_HUMAN	Uridine-cytidine kinase 2 OS=Homo sapiens GN=UCK2 PE=1 SV=1	91	29494	4
SFRS7_BOVIN	Splicing factor, arginine/serine-rich 7 OS=Bos taurus GN=SFRS7 PE=2 SV=1	84	27209	3
RS3_BOVIN	40S ribosomal protein S3 OS=Bos taurus GN=RPS3 PE=2 SV=1	77	26885	2
CDK5_BOVIN	Cell division protein kinase 5 OS=Bos taurus GN=CDK5 PE=1 SV=2	71	33836	2
IF4H_HUMAN	Eukaryotic translation initiation factor 4H OS=Homo sapiens GN=EIF4H PE=1 SV=5	65	27439	2
ECH1_HUMAN	Delta(3,5)-Delta(2,4)-dienoyl-CoA isomerase, mitochondrial OS=Homo sapiens GN=ECH1 PE=1 SV=2	63	36220	2
EI2BA_HUMAN	Translation initiation factor eIF-2B subunit alpha OS=Homo sapiens GN=EIF2B1 PE=1 SV=1	62	34046	2
K1C9_CANFA	Keratin, type I cytoskeletal 9 OS=Canis familiaris GN=KRT9 PE=3 SV=1	58	77161	2

SPOT 03

prot_acc	prot_desc	score	mass	matches
IF2A_HUMAN	Eukaryotic translation initiation factor 2 subunit 1 OS=Homo sapiens GN=EIF2S1 PE=1 SV=3	473	36445	26
PURB_HUMAN	Transcriptional activator protein Pur-beta OS=Homo sapiens GN=PURB PE=1 SV=3	318	33434	11
UCHL5_HUMAN	Ubiquitin carboxyl-terminal hydrolase isozyme L5 OS=Homo sapiens GN=UCHL5 PE=1 SV=3	314	37938	16
TCAL4_HUMAN	Transcription elongation factor A protein-like 4 OS=Homo sapiens GN=TCEAL4 PE=1 SV=2	259	24774	9
SEC13_HUMAN	Protein SEC13 homolog OS=Homo sapiens GN=SEC13 PE=1 SV=3	255	36157	12
TRYP_PIG	Trypsin OS=Sus scrofa PE=1 SV=1	159	25246	11
NMI_HUMAN	N-myc-interactor OS=Homo sapiens GN=NMI PE=1 SV=2	131	35248	6
FPPS_HUMAN	Farnesyl pyrophosphate synthase OS=Homo sapiens GN=FDPS PE=1 SV=4	118	48884	5
TBA1A_CRIGR	Tubulin alpha-1A chain OS=Cricetulus griseus GN=TUBA1A PE=2 SV=1	91	50956	3
KCD12_HUMAN	BTB/POZ domain-containing protein KCTD12 OS=Homo sapiens GN=KCTD12 PE=1 SV=1	88	36034	3
HNRPC_HUMAN	Heterogeneous nuclear ribonucleoproteins C1/C2 OS=Homo sapiens GN=HNRNPC PE=1 SV=4	85	33721	4
CE051_HUMAN	UPF0600 protein C5orf51 OS=Homo sapiens GN=C5orf51 PE=1 SV=1	80	34380	3
PP2AB_BOVIN	Serine/threonine-protein phosphatase 2A catalytic subunit beta isoform OS=Bos taurus GN=PPP2CB PE=2 SV=1	66	36249	3

SPOT 04

prot_acc	prot_desc	score	mass	matches
GLRX3_HUMAN	Glutaredoxin-3 OS=Homo sapiens GN=GLRX3 PE=1 SV=2	363	37763	20
K2C1_HUMAN	Keratin, type II cytoskeletal 1 OS=Homo sapiens GN=KRT1 PE=1 SV=6	302	66212	12
UCHL5_HUMAN	Ubiquitin carboxyl-terminal hydrolase isozyme L5 OS=Homo sapiens GN=UCHL5 PE=1 SV=3	302	37938	13
PURB_HUMAN	Transcriptional activator protein Pur-beta OS=Homo sapiens GN=PURB PE=1 SV=3	270	33434	9
ODBB_HUMAN	2-oxoisovalerate dehydrogenase subunit beta, mitochondrial OS=Homo sapiens GN=BCKDHB PE=1 SV=2	221	43947	9
CRK_HUMAN	Adapter molecule crk OS=Homo sapiens GN=CRK PE=1 SV=2	206	33881	8
DPH5_HUMAN	Diphthine synthase OS=Homo sapiens GN=DPH5 PE=1 SV=2	171	32057	9
SNAG_BOVIN	Gamma-soluble NSF attachment protein OS=Bos taurus GN=NAPG PE=1 SV=3	170	35041	7
K1C9_HUMAN	Keratin, type I cytoskeletal 9 OS=Homo sapiens GN=KRT9 PE=1 SV=3	164	62311	6
TRYP_PIG	Trypsin OS=Sus scrofa PE=1 SV=1	106	25246	10

SPOT 05

prot_acc	prot_desc	score	mass	matches
MTNA_HUMAN	Methylthioribose-1-phosphate isomerase OS=Homo sapiens GN=MRI1 PE=1 SV=1	345	39552	14
RFC2_HUMAN	Replication factor C subunit 2 OS=Homo sapiens GN=RFC2 PE=1 SV=3	284	39700	11
TADBP_HUMAN	TAR DNA-binding protein 43 OS=Homo sapiens GN=TARDBP PE=1 SV=1	202	45138	8
VTA1_BOVIN	Vacuolar protein sorting-associated protein VTA1 homolog OS=Bos taurus GN=VTA1 PE=2 SV=1	182	34279	13
HNRPK_BOVIN	Heterogeneous nuclear ribonucleoprotein K OS=Bos taurus GN=HNRNPK PE=2 SV=1	162	51343	6
UBCP1_BOVIN	Ubiquitin-like domain-containing CTD phosphatase 1 OS=Bos taurus GN=UBLCP1 PE=2 SV=1	162	36852	8
ROAA_MOUSE	Heterogeneous nuclear ribonucleoprotein A/B OS=Mus musculus GN=Hnrnpab PE=1 SV=1	157	30954	6
AS3MT_HUMAN	Arsenite methyltransferase OS=Homo sapiens GN=AS3MT PE=1 SV=3	124	42716	6
TRYP_PIG	Trypsin OS=Sus scrofa PE=1 SV=1	108	25246	9
ILEU_HUMAN	Leukocyte elastase inhibitor OS=Homo sapiens GN=SERPINB1 PE=1 SV=1	101	42857	3
PTPA_BOVIN	Serine/threonine-protein phosphatase 2A activator OS=Bos taurus GN=PPP2R4 PE=2 SV=1	54	37285	2

SPOT 06

prot_acc	prot_desc	score	mass	matches
GANAB_HUMAN	Neutral alpha-glucosidase AB OS=Homo sapiens GN=GANAB PE=1 SV=3	816	107375	46
HGS_HUMAN	Hepatocyte growth factor-regulated tyrosine kinase substrate OS=Homo sapiens GN=HGS PE=1 SV=1	511	86848	21
K2C1_HUMAN	Keratin, type II cytoskeletal 1 OS=Homo sapiens GN=KRT1 PE=1 SV=6	458	66212	18
KDM1A_HUMAN	Lysine-specific histone demethylase 1A OS=Homo sapiens GN=KDM1A PE=1 SV=2	314	93484	13
K1C10_HUMAN	Keratin, type I cytoskeletal 10 OS=Homo sapiens GN=KRT10 PE=1 SV=6	254	59076	10
HS74L_HUMAN	Heat shock 70 kDa protein 4L OS=Homo sapiens GN=HSPA4L PE=1 SV=2	251	95705	8
ALBU_BOVIN	Serum albumin OS=Bos taurus GN=ALB PE=1 SV=4	198	71735	8
TRYP_PIG	Trypsin OS=Sus scrofa PE=1 SV=1	169	25246	12
OGDHL_HUMAN	2-oxoglutarate dehydrogenase-like, mitochondrial OS=Homo sapiens GN=OGDHL PE=2 SV=3	99	115474	4

SPOT 07

prot_acc	prot_desc	score	mass	matches
ALDOA_HUMAN	Fructose-bisphosphate aldolase A OS=Homo sapiens GN=ALDOA PE=1 SV=2	611	39964	39
PGK1_HUMAN	Phosphoglycerate kinase 1 OS=Homo sapiens GN=PGK1 PE=1 SV=3	457	45083	33
THIL_HUMAN	Acetyl-CoA acetyltransferase, mitochondrial OS=Homo sapiens GN=ACAT1 PE=1 SV=1	359	45526	15
AATM_HUMAN	Aspartate aminotransferase, mitochondrial OS=Homo sapiens GN=GOT2 PE=1 SV=2	215	47943	10
PCBP1_BOVIN	Poly(rC)-binding protein 1 OS=Bos taurus GN=PCBP1 PE=2 SV=1	206	38113	7
HNRPD_HUMAN	Heterogeneous nuclear ribonucleoprotein D0 OS=Homo sapiens GN=HNRNPD PE=1 SV=1	140	38623	7

CSK21_BOVIN	Casein kinase II subunit alpha OS=Bos taurus GN=CSNK2A1 PE=1 SV=1	129	45257	7
SEPT9_HUMAN	Septin-9 OS=Homo sapiens GN=SEPT9 PE=1 SV=2	112	65716	6
DHSO_HUMAN	Sorbitol dehydrogenase OS=Homo sapiens GN=SORD PE=1 SV=4	104	39081	6
TRYP_PIG	Trypsin OS=Sus scrofa PE=1 SV=1	96	25246	9
AATC_HUMAN	Aspartate aminotransferase, cytoplasmic OS=Homo sapiens GN=GOT1 PE=1 SV=3	95	46503	3
SERC_HUMAN	Phosphoserine aminotransferase OS=Homo sapiens GN=PSAT1 PE=1 SV=2	95	40894	3
RM37_HUMAN	39S ribosomal protein L37, mitochondrial OS=Homo sapiens GN=MRPL37 PE=1 SV=2	84	48726	2
EF1A1_BOVIN	Elongation factor 1-alpha 1 OS=Bos taurus GN=EEF1A1 PE=2 SV=1	84	50535	3
K1C10_CANFA	Keratin, type I cytoskeletal 10 OS=Canis familiaris GN=KRT10 PE=2 SV=1	72	57889	2
TOM40_BOVIN	Mitochondrial import receptor subunit TOM40 homolog OS=Bos taurus GN=TOMM40 PE=2 SV=1	60	38127	3
PRS10_BOVIN	26S protease regulatory subunit 10B OS=Bos taurus GN=PSMC6 PE=2 SV=1	58	44401	2

SPOT 08

prot_acc	prot_desc	score	mass	matches
PDIA3_CERAE	Protein disulfide-isomerase A3 OS=Cercopithecus aethiops GN=PDIA3 PE=2 SV=1	786	57241	41
SYHC_HUMAN	Histidyl-tRNA synthetase, cytoplasmic OS=Homo sapiens GN=HARS PE=1 SV=2	735	58085	27
AINX_HUMAN	Alpha-internexin OS=Homo sapiens GN=INA PE=1 SV=2	393	55570	17
HNRPK_BOVIN	Heterogeneous nuclear ribonucleoprotein K OS=Bos taurus GN=HNRNPK PE=2 SV=1	378	51343	17
VATB2_BOVIN	V-type proton ATPase subunit B, brain isoform OS=Bos taurus GN=ATP6V1B2 PE=1 SV=3	370	56967	15
ARP3_BOVIN	Actin-related protein 3 OS=Bos taurus GN=ACTR3 PE=1 SV=3	293	47909	15
PEPD_HUMAN	Xaa-Pro dipeptidase OS=Homo sapiens GN=PEPD PE=1 SV=3	256	55507	10
ODO2_HUMAN	Dihydrolipoyllysine-residue succinyltransferase component of 2-oxoglutarate dehydrogenase complex, mitochondrial OS=Homo sapiens GN=DLST PE=1 SV=3	239	49125	12
AL9A1_HUMAN	4-trimethylaminobutyraldehyde dehydrogenase OS=Homo sapiens GN=ALDH9A1 PE=1 SV=3	235	54904	7
K2C1_HUMAN	Keratin, type II cytoskeletal 1 OS=Homo sapiens GN=KRT1 PE=1 SV=6	185	66212	8
P20D2_HUMAN	Peptidase M20 domain-containing protein 2 OS=Homo sapiens GN=PM20D2 PE=1 SV=2	159	48172	6
GOPC_HUMAN	Golgi-associated PDZ and coiled-coil motif-containing protein OS=Homo sapiens GN=GOPC PE=1 SV=1	147	50986	6
TRYP_PIG	Trypsin OS=Sus scrofa PE=1 SV=1	145	25246	9
NFM_BOVIN	Neurofilament medium polypeptide OS=Bos taurus GN=NEFM PE=1 SV=3	139	103219	7
S10AB_HUMAN	Protein S100-A11 OS=Homo sapiens GN=S100A11 PE=1 SV=2	118	11875	5
NFM_PIG	Neurofilament medium polypeptide (Fragment) OS=Sus scrofa GN=NEFM PE=1 SV=2	105	52096	5
FAD1_HUMAN	FAD synthase OS=Homo sapiens GN=FLAD1 PE=1 SV=1	100	66148	4

SPOT 09

prot_acc	prot_desc	score	mass	matches
PDIA3_CERAE	Protein disulfide-isomerase A3 OS=Cercopithecus aethiops GN=PDIA3 PE=2 SV=1	1193	57241	98
HNRPK_BOVIN	Heterogeneous nuclear ribonucleoprotein K OS=Bos taurus GN=HNRNPK PE=2 SV=1	521	51343	30
SNX4_HUMAN	Sorting nexin-4 OS=Homo sapiens GN=SNX4 PE=1 SV=1	266	52231	10
PEPD_HUMAN	Xaa-Pro dipeptidase OS=Homo sapiens GN=PEPD PE=1 SV=3	259	55507	10
LDHB_HUMAN	L-lactate dehydrogenase B chain OS=Homo sapiens GN=LDHB PE=1 SV=2	238	36970	10
GOPC_HUMAN	Golgi-associated PDZ and coiled-coil motif-containing protein OS=Homo sapiens GN=GOPC PE=1 SV=1	237	50986	10
K2C1_HUMAN	Keratin, type II cytoskeletal 1 OS=Homo sapiens GN=KRT1 PE=1 SV=6	200	66212	8
MSTO1_HUMAN	Protein misato homolog 1 OS=Homo sapiens GN=MSTO1 PE=1 SV=1	190	62933	7
PP2BA_BOVIN	Serine/threonine-protein phosphatase 2B catalytic subunit alpha isoform OS=Bos taurus GN=PPP3CA PE=1 SV=1	178	59487	7
DPYL2_HUMAN	Dihydropyrimidinase-related protein 2 OS=Homo sapiens GN=DPYSL2 PE=1 SV=1	168	62823	6
GPKOW_HUMAN	G patch domain and KOW motifs-containing protein OS=Homo sapiens GN=GPKOW PE=1 SV=2	130	52481	5
TRYP_PIG	Trypsin OS=Sus scrofa PE=1 SV=1	122	25246	11
K22E_HUMAN	Keratin, type II cytoskeletal 2 epidermal OS=Homo sapiens GN=KRT2 PE=1 SV=2	95	65748	3
PRS4_HUMAN	26S protease regulatory subunit 4 OS=Homo sapiens GN=PSMC1 PE=1 SV=1	54	49367	2

S4. Expression and purification of recombinant human LSD1

Theorical MW (Protparam prediction): 94 KDa (observed by SDSPAGE ≈120KDa)
Theorical pI: 6.0

LSD1 purification is reported in the figure 45, furthermore the induction and the purification by His-trap GE column is observable.

Fig. 45 Purification of LSD1

In this coomassie stained SDS-PAGE, they are reported the first step of the purification. The white arrows show the intermediate of purification of LSD1. The input represents the extracted proteins, sonicated and centrifugated loaded in the column (lane 1 starting from left), while the other lanes are the fractions obtained by His trap GE column.

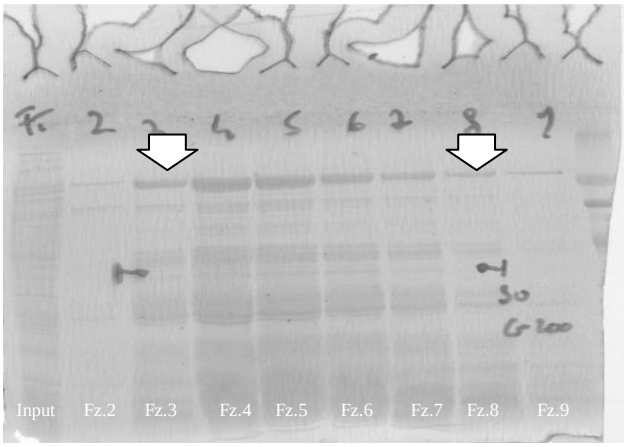

The fractions 2-8 have been loaded in the G200 superdex 26/60 a size

exclusion chromatographic column to separate LSD1 from other undesirable proteins. In the figure 46 is reported the final fractionation of LSD1.

Fig. 46 Purification of LSD1

In these two coomassie stained SDS-PAGEs, there are the fraction obtained by the gel-exclusion. The white arrows show final result of the purification of LSD1; a single band has been obtained.

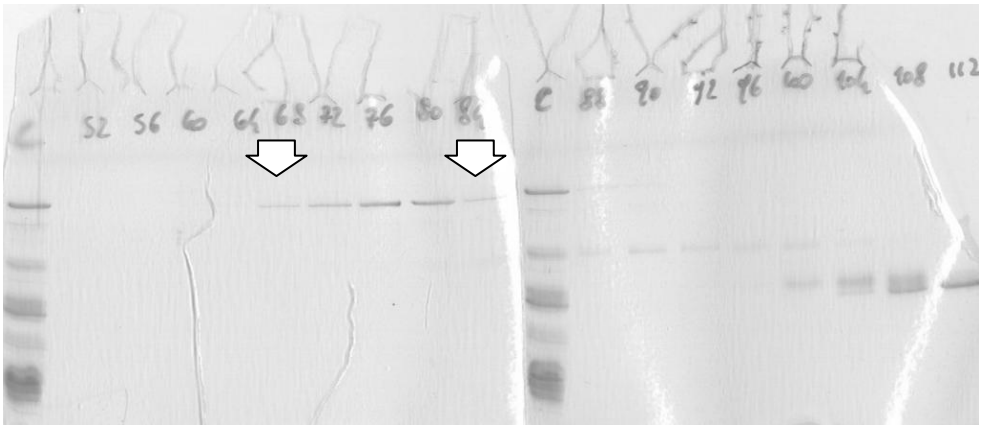

The fractions 68-84 have been concentrated by Amicon membrane (Cut-off 10 KDa.

1 ml of recombinant LSD1 at concentration 0.9 mg/ml has been obtained.

S.5 Phosphorylation of CK2α by Proline directed Kinases

In our hypothesis, the phosphorylation of CK2 by Cdk1 starts the pathway; in this section we disclose that also other kinases are able to phosphorylate the C-terminus CK2α.

In the image (Fig.47), we provide evidence about the phosphorylation in the C-terminal segment of CK2α-wt (AA 336-391) and also in the N-terminal kinase domain (AA 1-336) by Homeodomain Interacting Protein-Kinase 2 (HIPK2), a proline directed kinase.

Furthermore the experiment discloses the opposite reaction, the phosphorylation of HIPK2 by CK2.

CK2α-Δ1-336 a C-terminal truncated form of CK2α appears as a bad substrate in comparison to CK2α-wt, suggesting that the bigger amount of phosphates are linked to the C-terminal domain of the full length protein (Fig. 47).

Hence, HIPK2 is able to phosphorylate CK2α, as well as, Cdk1.

The phosphorylation of CK2α by HIPK2 suggests the "activation" of CK2α in the whole cell cycle, while Cdk1 is activated only during the early mitosis.

HIPK2 is activated during the apoptosis [87], and now CK2 might be correlated to the DNA condensation in the peculiar half-moon appearance during the early stages of the apoptosis.

Fig. 47**: C-terminal phosphorylation of CK2α by HIPK2**

In this autoradiography are reported the phosphorylation of HIPK2 by CK2α (lane 3 vs.lane4) and the phosphorylation of CK2α by HIPK2. CK2α-Δ1-336 a C-terminal truncated form of CK2α appears as a bad substrate in comparison to CK2α-wt; the N-terminal section 1-336 is phosphorylated by HIPK2, but the bigger amount of phosphates are linked to the C-terminal domain of the full length protein (lane 2 vs.lane 4).

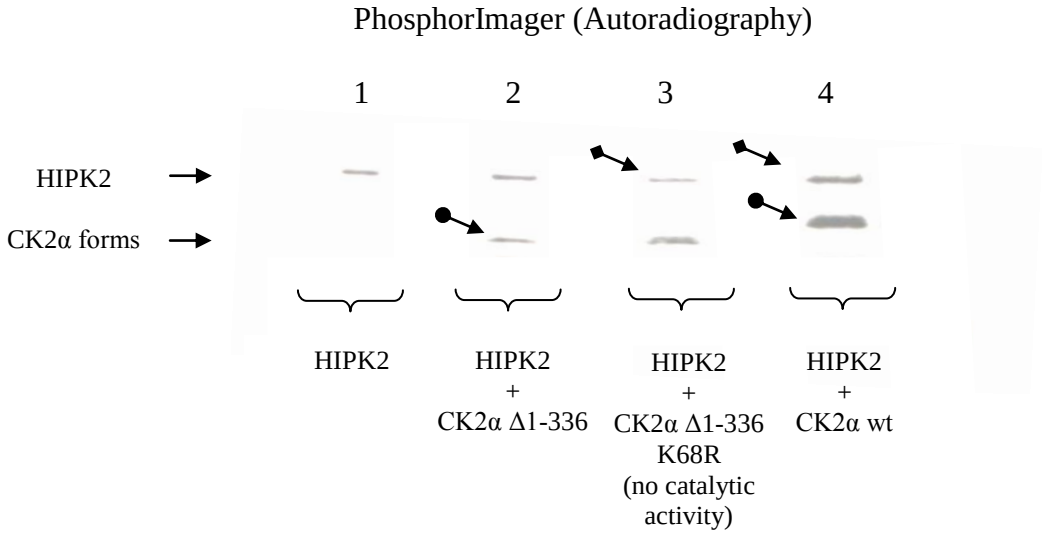

References

1. Manning G, Whyte DB, Martinez R, Hunter T, Sudarsanam S: The protein kinase complement of the human genome. Science 2002, 298:1912-1934.
2. Olsen JV, Blagoev B, Gnad F, Macek B, Kumar C, Mortensen P, Mann M: Global, in vivo, and site-specific phosphorylation dynamics in signaling networks. Cell 2006, 127:635-648.
3. Hanks SK, Hunter T: Protein kinases 6. The eukaryotic protein kinase superfamily: kinase (catalytic) domain structure and classification. Faseb J 1995, 9:576-596.
4. Meggio F, Pinna LA: One-thousand-and-one substrates of protein kinase CK2? Faseb J 2003, 17:349-368.
5. Burnett G, Kennedy E: The enzymatic phosphorylation of proteins. J Biol Chem 1954211(2) 969-80.
6. Ruzzene M, Di Maira G, Tosoni K, Pinna LA: Assessment of CK2 constitutive activity in cancer cells. Methods Enzymol 2009484:495-514.
7. Pinna LA: Protein kinase CK2: a challenge to canons. J Cell Sci 2002, 115:3873-3878.
8. Niefind K, Putter M, Guerra B, Issinger OG, Schomburg D: GTP plus water mimic ATP in the active site of protein kinase CK2. Nat Struct Biol 1999, 6:1100-1103.
9. Sarno S, Ghisellini P, Pinna LA: Unique activation mechanism of protein kinase CK2. The N-terminal segment is essential for constitutive activity of the catalytic subunit but not of the holoenzyme. J Biol Chem 2002, 277:22509 -22514.
10. Sarno S, Vaglio P, Meggio F, Issinger OG, Pinna LA: Protein kinase CK2 mutants defective in substrate recognition. Purification and kinetic analysis. J Biol Chem 1996, 271:10595-10601.
11. Jeffrey PD, Russo AA, Polyak K, Gibbs E, Hurwitz J, Massague J, Pavletich NP: Mechanism of CDK activation revealed by the structure of a cyclinA-CDK2 complex. Nature 1995, 376:313-320.
12. Dobrowolska G, Meggio F, Marin O, Lozeman FJ, Li D, Pinna LA, Krebs EG: Substrate recognition by casein kinase-II: the role of histidine-160. FEBS Lett 1994, 355:237-241.
13. Meggio F, Marin O, Pinna LA: Substrate specificity of protein kinase CK2. Cell Mol Biol Res 1994, 40:401-409.
14. Salvi M, Sarno S, Cesaro L, Nakamura H, Pinna LA: Extraordinary pleiotropy of protein kinase CK2 revealed by weblogo phosphoproteome analysis. Biochim Biophys Acta 2009, 1793:847-859.
15. Cohen P: Protein kinases--the major drug targets of the twenty-first century? Nat Rev Drug Discov 2002, 1:309-315.
16. Sarno S, Pinna LA: Protein kinase CK2 as a druggable target. Mol Biosyst 2008, 4:889-894.
17. Cozza G, Pinna LA, Moro S: Kinase Ck2 inhibition: AN update. Curr Med Chem 2012.
18. Sarno S, Papinutto E, Franchin C, Bain J, Elliott M, Meggio F, Kazimierczuk Z, Orzeszko A, Zanotti G, Battistutta R, Pinna LA: ATP site-directed inhibitors of protein kinase CK2: an update. Curr Top Med Chem 2011, 11:1340-1351.
19. Siddiqui-Jain A, Drygin D, Streiner N, Chua P, Pierre F, O'Brien SE, Bliesath J, Omori M, Huser N, Ho C, et al: CX-4945, an orally bioavailable selective inhibitor of protein kinase CK2, inhibits prosurvival and angiogenic signaling and exhibits antitumor efficacy. Cancer Res 2010, 70:10288-10298.
20. Wang H, Davis A, Yu S, Ahmed K: Response of cancer cells to molecular interruption of the CK2 signal. Mol Cell Biochem 2001, 227:167-174.
21. Chen S, Guttridge DC, You Z, Zhang Z, Fribley A, Mayo MW, Kitajewski J, Wang CY: Wnt-1 signaling inhibits apoptosis by activating beta-catenin/T cell factor-mediated transcription. J Cell Biol 2001, 152:87-96.
22. Song DH, Dominguez I, Mizuno J, Kaut M, Mohr SC, Seldin DC: CK2 phosphorylation of the armadillo repeat region of beta-catenin potentiates Wnt signaling. J Biol Chem 2003, 278:24018-24025.
23. Bernatik O, Ganji RS, Dijksterhuis JP, Konik P, Cervenka I, Polonio T, Krejci P, Schulte G, Bryja V: Sequential activation and inactivation of Dishevelled in the Wnt/beta-catenin pathway by casein kinases. J Biol Chem 2011, 286:10396-10410.
24. Di Maira G, Salvi M, Arrigoni G, Marin O, Sarno S, Brustolon F, Pinna LA, Ruzzene M: Protein kinase CK2 phosphorylates and upregulates Akt/PKB. Cell Death Differ 2005, 12:668-677.
25. Torres J, Rodriguez J, Myers MP, Valiente M, Graves JD, Tonks NK, Pulido R: Phosphorylation-regulated cleavage of the tumor suppressor PTEN by caspase-3: implications for the control of protein stability and PTEN-protein interactions. J Biol Chem 2003, 278:30652-30660.
26. Barroga CF, Stevenson JK, Schwarz EM, Verma IM: Constitutive phosphorylation of I kappa B alpha by casein kinase II. Proc Natl Acad Sci U S A 1995, 92:7637-7641.
27. Bren GD, Pennington KN, Paya CV: PKC-zeta-associated CK2 participates in the turnover of free IkappaBalpha. J Mol Biol 2000, 297:1245-1258.
28. Trembley J, Chen Z, Unger G, Slaton J, Kren B, Van Waes C, Ahmed K: Emergence of protein kinase CK2 as a key target in cancer therapy. Biofactors 2010, 17:349-368.
29. Guerra B, Issinger OG: Protein kinase CK2 and its role in cellular proliferation, development and pathology. Electrophoresis 1999, 20:391-408.
30. Messenger MM, Saulnier RB, Gilchrist AD, Diamond P, Gorbsky GJ, Litchfield DW: Interactions between protein kinase CK2 and Pin1. Evidence for phosphorylation-dependent interactions. J Biol Chem 2002, 277:23054-23064.
31. Bosc D, Slominski E, Sichler C, Litchfield D: Phosphorylation of casein kinase II by p34cdc2. Identification of phosphorylation sites using phosphorylation site mutants in vitro. J Biol Chem 1995.
32. Alvarado-Diaz CP, Tapia JC, Antonelli M, Moreno RD: Differential localization of alpha' and beta subunits of

protein kinase CK2 during rat spermatogenesis. Cell Tissue Res 2009, 338:139-149.
33. Dominguez I, Degano IR, Chea K, Cha J, Toselli P, Seldin DC: CK2alpha is essential for embryonic morphogenesis. Mol Cell Biochem 2011, 356:209-216.
34. Escalier D, Silvius D, Xu X: Spermatogenesis of mice lacking CK2alpha': failure of germ cell survival and characteristic modifications of the spermatid nucleus. Mol Reprod Dev 2003, 66:190-201.
35. St-Denis NA, Derksen DR, Litchfield DW: Evidence for regulation of mitotic progression through temporal phosphorylation and dephosphorylation of CK2alpha. Mol Cell Biol 2009, 29:2068-2081.
36. St-Denis NA, Bailey ML, Parker EL, Vilk G, Litchfield DW: Localization of phosphorylated CK2alpha to the mitotic spindle requires the peptidyl-prolyl isomerase Pin1. J Cell Sci 2011, 124:2341-2348.
37. Eom GH, Cho YK, Ko JH, Shin S, Choe N, Kim Y, Joung H, Kim HS, Nam KI, Kee HJ, Kook H: Casein kinase-2alpha1 induces hypertrophic response by phosphorylation of histone deacetylase 2 S394 and its activation in the heart. Circulation 2011, 123:2392-2403.
38. Shi X, Seldin DC, Garry DJ: Foxk1 recruits the Sds3 complex and represses gene expression in myogenic progenitors. Biochem J 2012, 446:349-357.
39. Kornberg RD, Thomas JO: Chromatin structure; oligomers of the histones. Science 1974, 184:865-868.
40. Luger K, Mader AW, Richmond RK, Sargent DF, Richmond TJ: Crystal structure of the nucleosome core particle at 2.8 A resolution. Nature 1997, 389:251-260.
41. Henikoff S: Nucleosome destabilization in the epigenetic regulation of gene expression. Nat Rev Genet 2008, 9:15-26.
42. Strahl BD, Allis CD: The language of covalent histone modifications. Nature 2000, 403:41-45.
43. Jenuwein T, Allis CD: Translating the histone code. Science 2001, 293:1074-1080.
44. Fischle W, Wang Y, Allis CD: Histone and chromatin cross-talk. Curr Opin Cell Biol 2003, 15:172-183.
45. Waterborg JH: Dynamics of histone acetylation in vivo. A function for acetylation turnover? Biochem Cell Biol 2002, 80:363-378.
46. Peserico A, Simone C: Physical and functional HAT/HDAC interplay regulates protein acetylation balance. J Biomed Biotechnol 2010, 2011:371832.
47. Bannister AJ, Kouzarides T: Reversing histone methylation. Nature 2005, 436:1103-1106.
48. Dormann HL, Tseng BS, Allis CD, Funabiki H, Fischle W: Dynamic regulation of effector protein binding to histone modifications: the biology of HP1 switching. Cell Cycle 2006, 5:2842-2851.
49. Shi Y, Lan F, Matson C, Mulligan P, Whetstine JR, Cole PA, Casero RA, Shi Y: Histone demethylation mediated by the nuclear amine oxidase homolog LSD1. Cell 2004, 119:941-953.
50. Trewick SC, McLaughlin PJ, Allshire RC: Methylation: lost in hydroxylation? EMBO Rep 2005, 6:315-320.
51. Waterborg JH: Dynamic methylation of alfalfa histone H3. J Biol Chem 1993, 268:4918-4921.
52. Shi Y, Whetstine JR: Dynamic regulation of histone lysine methylation by demethylases. Mol Cell 2007, 25:1-14.
53. Dhalluin C, Carlson JE, Zeng L, He C, Aggarwal AK, Zhou MM: Structure and ligand of a histone acetyltransferase bromodomain. Nature 1999, 399:491-496.
54. Rosenfeld JA, Wang Z, Schones DE, Zhao K, DeSalle R, Zhang MQ: Determination of enriched histone modifications in non-genic portions of the human genome. BMC Genomics 2009, 10:143.
55. Black JC, Whetstine JR: Chromatin landscape: methylation beyond transcription. Epigenetics 2011, 6:9-15.
56. Guelen L, Pagie L, Brasset E, Meuleman W, Faza MB, Talhout W, Eussen BH, de Klein A, Wessels L, de Laat W, van Steensel B: Domain organization of human chromosomes revealed by mapping of nuclear lamina interactions. Nature 2008, 453:948-951.
57. Mikkelsen TS, Ku M, Jaffe DB, Issac B, Lieberman E, Giannoukos G, Alvarez P, Brockman W, Kim TK, Koche RP, et al: Genome-wide maps of chromatin state in pluripotent and lineage-committed cells. Nature 2007, 448:553-560.
58. Pauler FM, Sloane MA, Huang R, Regha K, Koerner MV, Tamir I, Sommer A, Aszodi A, Jenuwein T, Barlow DP: H3K27me3 forms BLOCs over silent genes and intergenic regions and specifies a histone banding pattern on a mouse autosomal chromosome. Genome Res 2009, 19:221-233.
59. Braig M, Lee S, Loddenkemper C, Rudolph C, Peters AH, Schlegelberger B, Stein H, Dorken B, Jenuwein T, Schmitt CA: Oncogene-induced senescence as an initial barrier in lymphoma development. Nature 2005, 436:660-665.
60. Hayashi MT, Takahashi TS, Nakagawa T, Nakayama J, Masukata H: The heterochromatin protein Swi6/HP1 activates replication origins at the pericentromeric region and silent mating-type locus. Nat cell biol 2009, 11:357–362.
61. Regha K, Sloane MA, Huang R, Pauler FM, Warczok KE, Melikant B, Radolf M, Martens JH, Schotta G, Jenuwein T, Barlow DP: Active and repressive chromatin are interspersed without spreading in an imprinted gene cluster in the mammalian genome. Mol Cell 2007, 27:353-366.
62. Chen ES, Zhang K, Nicolas E, Cam HP, Zofall M, Grewal SI: Cell cycle control of centromeric repeat transcription and heterochromatin assembly. Nature 2008, 451:734-737.
63. Quivy JP, Gerard A, Cook AJ, Roche D, Almouzni G: The HP1-p150/CAF-1 interaction is required for pericentric heterochromatin replication and S-phase progression in mouse cells. Nat Struct Mol Biol 2008, 15:972-979.
64. Cimbora DM, Schubeler D, Reik A, Hamilton J, Francastel C, Epner EM, Groudine M: Long-distance control of origin choice and replication timing in the human beta-globin locus are independent of the locus control region. Mol Cell Biol 2000, 20:5581-5591.
65. Briggs SD, Bryk M, Strahl BD, Cheung WL, Davie JK, Dent SY, Winston F, Allis CD: Histone H3 lysine 4 methylation is mediated by Set1 and required for cell growth and rDNA silencing in Saccharomyces cerevisiae.

Genes Dev 2001, 15:3286-3295.
66. Grewal SI, Jia S: Heterochromatin revisited. Nat Rev Genet 2007, 8:35-46.
67. Wang Z, Zang C, Rosenfeld JA, Schones DE, Barski A, Cuddapah S, Cui K, Roh TY, Peng W, Zhang MQ, Zhao K: Combinatorial patterns of histone acetylations and methylations in the human genome. Nat Genet 2008, 40:897-903.
68. Lopez-Rubio JJ, Gontijo AM, Nunes MC, Issar N, Hernandez Rivas R, Scherf A: 5' flanking region of var genes nucleate histone modification patterns linked to phenotypic inheritance of virulence traits in malaria parasites. Mol Microbiol 2007, 66:1296-1305.
69. Shuang L, Wenjuan B, Hong J, Bo L, Lin Z, Hongchang Z, Ji L, Jing L, Xingzhi X: LSD1 is required for chromosome segregation during mitosis. European Journal of Cell Biology 2010, Volume 89, Issue 7, July 2010, Pages 557–563.
70. Bergmann JH, Rodriguez MG, Martins NM, Kimura H, Kelly DA, Masumoto H, Larionov V, Jansen LE, Earnshaw WC: Epigenetic engineering shows H3K4me2 is required for HJURP targeting and CENP-A assembly on a synthetic human kinetochore. Embo J 2011, 30:328-340.
71. Karaman MW, Herrgard S, Treiber DK, Gallant P, Atteridge CE, Campbell BT, Chan KW, Ciceri P, Davis MI, Edeen PT, et al: A quantitative analysis of kinase inhibitor selectivity. Nat Biotechnol 2008, 26:127-132.
72. Metzger E, Wissmann M, Yin N, Muller JM, Schneider R, Peters AH, Gunther T, Buettner R, Schule R: LSD1 demethylates repressive histone marks to promote androgen-receptor-dependent transcription. Nature 2005, 437:436-439.
73. Metzger E, Imhof A, Patel D, Kahl P, Hoffmeyer K, Friedrichs N, Muller JM, Greschik H, Kirfel J, Ji S, et al: Phosphorylation of histone H3T6 by PKCbeta(I) controls demethylation at histone H3K4. Nature 2010, 464:792-796.
74. Forneris F, Binda C, Adamo A, Battaglioli E, Mattevi A: Structural basis of LSD1-CoREST selectivity in histone H3 recognition. J Biol Chem 2007, 282:20070-20074.
75. Justin N, De Marco V, Aasland R, Gamblin SJ: Reading, writing and editing methylated lysines on histone tails: new insights from recent structural studies. Curr Opin Struct Biol 2010, 20:730-738.
76. Lee MG, Wynder C, Bochar DA, Hakimi MA, Cooch N, Shiekhattar R: Functional interplay between histone demethylase and deacetylase enzymes. Mol Cell Biol 2006, 26:6395-6402.
77. Shi YJ, Matson C, Lan F, Iwase S, Baba T, Shi Y: Regulation of LSD1 histone demethylase activity by its associated factors. Mol Cell 2005, 19:857-864.
78. Shi X, Potvin B, Huang T, Hilgard P, Spray DC, Suadicani SO, Wolkoff AW, Stanley P, Stockert RJ: A novel casein kinase 2 alpha-subunit regulates membrane protein traffic in the human hepatoma cell line HuH-7. J Biol Chem 2001, 276:2075-2082.
79. Dephoure N, Zhou C, Villen J, Beausoleil SA, Bakalarski CE, Elledge SJ, Gygi SP: A quantitative atlas of mitotic phosphorylation. Proc Natl Acad Sci U S A 2008, 105:10762-10767.
80. Romero-Oliva F, Jacob G, Allende JE: Dual effect of lysine-rich polypeptides on the activity of protein kinase CK2. J Cell Biochem 2003, 89:348-355.
81. Gocke CB, Yu H, Kang J: Systematic identification and analysis of mammalian small ubiquitin-like modifier substrates. J Biol Chem 2005, 280:5004-5012.
82. Adamo A, Sese B, Boue S, Castano J, Paramonov I, Barrero MJ, Izpisua Belmonte JC: LSD1 regulates the balance between self-renewal and differentiation in human embryonic stem cells. Nat Cell Biol 2011, 13:652-659.
83. Gocke C, Yu H: ZNF198 Stabilizes the LSD1–CoREST–HDAC1 Complex on Chromatin through Its MYM-Type Zinc Fingers. PLoS ONE 2008, 3(9): e3255. .
84. Tontsch S, Zach O, Bauer HC: Identification and localization of M-CoREST (1A13), a mouse homologue of the human transcriptional co-repressor CoREST, in the developing mouse CNS. Mech Dev 2001, 108:165-169.
85. Wang Y, Zhang H, Chen Y, Sun Y, Yang F, Yu W, Liang J, Sun L, Yang X, Shi L, et al: LSD1 is a subunit of the NuRD complex and targets the metastasis programs in breast cancer. Cell 2009, 138:660-672.
86. Shi YJ, Matson C, Lan F, Iwase S, Baba T, Shi Y: Regulation of LSD1 histone demethylase activity by its associated factors. Mol Cell 2005, 19:857-864.
87. Hofmann TG, Stollberg N, Schmitz ML, Will H: HIPK2 regulates transforming growth factor-beta-induced c-Jun NH(2)-terminal kinase activation and apoptosis in human hepatoma cells. Cancer Res 2003, 63:8271-8277.